AN ABSTRACT OF THE THESIS OF

Ralph Edward Miller for the degree Doctor of Philosophy
(Name of student) (Degree)

in Chemistry presented on November 22, 1974
(Major department) (Date)

Title: The Rotational Motion of Molecules in Crystalline Solids

Redacted for privacy

Abstract approved:
Professor J. C. Decius

Theoretical studies and experimental results are presented for the rotational motion of molecules in crystalline solids.

The group theory is solved for molecules of any symmetry matrix isolated at a site in a crystal field of any symmetry. As the potential barrier to rotation of the molecule relative to the host crystal is raised, certain symmetry operations become decreasingly "feasible" in the sense of Longuet-Higgins. Using correlation methods the symmetry species of the rotational states are determined from the free rotation limit to any of the librational limits. Examples of linear, symmetric, spherical, and asymmetric rotors are given. From the symmetry of states and the dipole and polarizability tensors, selection rules are applied to predict spectra in the infrared and Raman effect. Comparisons with experimental data are made whenever possible and good agreement with hindered rotor models is obtained for CH_3 and NH_3 in argon matrices.

New Raman studies are reported for methane isolated in noble gas matrices and the low temperature crystal phases of neat methane which give additional support to the evidence for rotation and the James-Keenan model for the lowest temperature phase of neat CH_4.

The Rotational Motion of Molecules in Crystalline Solids

by

Ralph Edward Miller

A THESIS

submitted to

Oregon State University

in partial fulfillment of
the requirements for the
degree of

Doctor of Philosophy

Commencement June 1975

APPROVED:

Redacted for privacy

Professor of Chemistry
in charge of major

Redacted for privacy

Chairman of Department of Chemistry

Redacted for privacy

Dean of Graduate School

Date thesis is presented November 22, 1974

Typed by Carol Miller for Ralph E. Miller

ACKNOWLEDGEMENTS

I want to express my sincere thanks to Dr. J. C. Decius for all his help and guidance during my studying at Oregon State. I want to also thank Dr. J. W. Nibler for his aid in doing the experiments and Dr. H. H. Wickman for helping in the liquid helium experiments. I particularly want to thank Dr. Lou Allamandola, Mr. Larry Frederickson, Mr. Mike Lesiecki, Mr. Larry Morgan, and Mr. Hossein Rojhantalab for their help in running the experiments. I am very indebted to my wife, Carol, for typing this thesis and for her help and encouragement during our stay in Corvallis.

I am grateful to the National Science Foundation and the Department of Chemistry for providing financial support for my graduate studies.

TABLE OF CONTENTS

LIST OF FIGURES

LIST OF TABLES

THE ROTATIONAL MOTION OF MOLECULES IN CRYSTALLINE SOLIDS

I. INTRODUCTION

There have been a number of quantum mechanical calculations of molecular rotation in crystal fields beginning with Pauling (112) in 1930. Since then there have been relatively few molecules found to exhibit rotational motion in solids. Most examples of rotation have been for molecules isolated in a noble gas crystal, although rotation has also been found to occur in molecular crystals. If molecules are not able to rotate, they can undergo small oscillations or librations about an equilibrium position which corresponds to a minimum in the potential with respect to rotation. Intermediate to the extremes of rotation and libration is the situation where tunneling occurs between equivalent potential minima. There are fewer known examples where tunneling is important than for rotation so most molecules in solids by far are thought to just librate. In this work we will focus our attention on the questions of rotation and tunneling. The tunneling problem is particularly suited to the methods of group theory and this will be a major topic.

The experimental methods used to study rotational motion have usually been infrared studies of vibrational bands and far-infrared spectra of rotational transitions. Other methods which have been used are microwave, inelastic neutron scattering, analysis of electronic absorption bands, paramagnetic resonance,

and the Raman effect. The Raman effect would provide a good comparison with infrared studies because of possible coincidences on the one hand and differences in vibration-rotation selection rules on the other. Previous Raman studies, however, have not been very useful due to a lack of resolution.

In the present study we will first review the previous work dealing with rotation of molecules in solids. This includes a number of theoretical treatments and many experimental results. Then the group theory is solved for a matrix isolated molecule of any symmetry at a site in a crystal field of any symmetry. To the extent that intermolecular coupling is not important, the group theory is also applicable to molecular crystals. As the potential barrier to rotation of the molecule relative to the host crystal is raised, certain symmetry operations become decreasingly "feasible" in the sense of Longuet-Higgins (93). Using correlation methods (161) the symmetry species of the rotational states can be determined from the free rotation limit to any of the librational limits. The rotational energy levels may be determined qualitatively for all cases and quantitatively near a high barrier limit where tunneling between equivalent potential minima is important. From the symmetry of states and the dipole and polarizability tensors, selection rules may be applied to predict spectra in the infrared and Raman effect. In order to examine various aspects of this theoretical work a series of experiments were performed using the Raman effect to complement other existing work. The molecule under study is methane and certain deuterated

methanes, both in the neat crystalline form and matrix isolated in the noble gas crystals. From this experimental work certain conclusions may be made regarding the rotational motion of methane in crystalline solids and the crystal structure of methane. Comparisons between theory and experimental results are also made for other molecules which are believed to exhibit rotational motion.

II. LITERATURE REVIEW

Previous studies concerning rotation in solids started with theoretical efforts for diatomic molecules. These were followed by experimental results which were interpreted at first in terms of rotational motion, but many of these conclusions have since been proven to be incorrect. More recent theoretical work has solved the problem of a spherical rotor and the effect of translation has been added to this and previous work. The experimental studies have shown that rotational motion of molecules in noble gas matrices does occur for various hydrides. In addition, impurity ions in alkali halides show evidence of hindered rotation, the solid hydrogens exhibit nearly free rotation, and low temperature phases in both CH_4 and CD_4 give experimental results indicating rotation.

A. Theoretical Studies

Pauling (112) developed a two-dimensional model for rotation of diatomics in molecular crystals in 1930. He used a potential given by $V = V_o (1-\cos 2\theta)$. This model assumes a cylindrical potential due to the crystal. Rough criteria for determining rotational motion and oscillational motion are given and phase transitions in crystals are discussed in terms of the motion changing from oscillational to rotational.

Stern (147) solved the problem of an X_2 molecule in a cylindrical field. He included the ϕ dependence in his solutions and made a correlation diagram from the free rotor limit to the high barrier limit.

Devonshire (35) found the energy levels of an XY molecule in an octahedral field. He used the first non-constant term in the spherical harmonics which has octahedral symmetry and this has degree four. The solutions are found by assuming the wave functions to be linear combinations of spherical harmonics.

Cundy (33) followed the procedure of Devonshire and solved the problem of an XY molecule in a tetrahedral field. He used a spherical harmonic of degree three for a potential function.

In 1951 Nagamiya (104) found the rotational energy levels assuming a high barrier for molecules of T_d and C_{3V} symmetries in tetrahedral and trigonal fields. This study was in connection with the zero-point entropies of CH_4, CD_4, and CH_3D. He also found the degeneracy of the levels for octahedral fields.

In order to support the interpretation of rotation in solids, Armstrong (3, 4) and Flygare (43) gave alternative solutions for a linear molecule. These papers related the barrier to rotation with interactions between the guest molecule and host crystal.

Friedmann and Kimel (48-51) developed the rotation-translation coupling model (RTC) for diatomic molecules. They assumed rotation about a center of interaction which in general will couple translational motion with rotation. For unsymmetrical molecules such as the hydrogen halides, the center of interaction is nearer the hydrogen than the center of mass. This model also assumes a spherical potential due to the crystal field.

In 1966 Sauer (133) improved the Devonshire calculation by increasing the basis set from functions up to $\ell = 7$ to $\ell = 12$. This

increased size of the secular determinant was beyond the machine solution capabilities that Devonshire had.

Quite recently, Jacobi (74, 75) and Schnepp (75) have determined the wave functions and energy levels for both the rotational and librational cases of an X_2 molecule (and linear XY_2) at a site having the symmetry S_6. The rotational wave functions are spherical harmonics and the librational wave functions are harmonic oscillator-like variational functions. The molecules under study were o-H_2, N_2, and CO_2.

King (86, 87) and Hornig (87) treated the cases of either tetrahedral or octahedral molecules in an octahedral field. They calculated the rotational energy levels using wave functions which are symmetry-adapted linear combinations of spherical-top functions. The potential functions included both degree four and degree six terms.

Soon after the work of King and Hornig, the effect of translation was added by Friedmann, Shalom, and Kimel (52). Since the center of mass and center of interaction coincide for a tetrahedral molecule, this effect would be expected to be smaller than for XY diatomics.

Nishiyama (107, 108) and Yamamoto (108) have added the Coriolis effect to the problem of a tetrahedral molecule in an octahedral field. They used potential functions which were predicted by Yasuda (165) assuming additivity of pairwise potentials. These calculations were done for CH_4 and CD_4 in the noble gas matrices. Kataoka, Okada, and Yamamoto (80) have made similar calculations

for the lowest temperature phase of CH_4. These results will be discussed in considerable detail in Chapter V.

Smith (146) followed the procedure of King and Hornig and solved the rotational problem for a tetrahedral molecule in a tetrahedral field. The potential function used has degree three which is the first non-constant term having the appropriate symmetry.

In a paper based on part of the present study, Miller and Decius (98) presented the general group theory solution for matrix isolated molecules. This earlier work will be expanded in Chapter III.

B. Experimental Studies

The noble gas crystals have been widely used in matrix experiments, including Ne, Ar, Kr, and Xe. All of these form face-centered cubic crystals (36, 70, 118, 163) although it has been shown that certain diatomic molecules stabilize hexagonal packing for Ar (9). It is thought that a small molecule which has been substituted for a noble gas atom may undergo rotational motion if their sizes are comparable since a substitutional cavity is nearly spherical in nature. If a molecule occupies a vacancy in a face-centered cubic lattice of atoms, it is at a site having octahedral symmetry. So, the crystal field theories of Devonshire (35) for diatomic molecules, and King and Hornig (87) for tetrahedral molecules are appropriate. Other molecules have been compared to free rotors.

1. Matrix Isolated Molecules

Although most of the evidence for rotation in matrices has been from vibration-rotation bands, the first evidence of rotation in a matrix was from EPR work on the NH_2 radical in Ar (44). McConnell (97) interpreted the observed intensities in terms of the splitting of rotational levels and the conversion of para-NH_2 to the ground state ortho molecules. Robinson (130, 131) and McCarty (130) interpreted the structure in the electronic band of NH_2 in Ar at $4.2^{\circ}K$ in terms of nearly free rotation. Milligan and Jacox (100) attribute structure in the bending mode of NH_2 in Ar to rotation.

Catalano and Milligan (22) reported structure in the ν_2 bands of H_2O, D_2O, and HDO in Ar, Kr, and Xe. This was followed by the work of Glasel (53), and Redington and Milligan (126, 127). Robinson (128) looked at the far-infrared spectra of H_2O in Ne, Ar, Kr, and Xe. In a study of nuclear spin conversion, Hopkins, Curl, and Pitzer (69) examined the time dependence of H_2O in Ar for the ν_2 and ν_3 bands. All of this work points to rotational motion of H_2O in the noble gas matrices, but the assignments and spectra did not always agree from one study to another.

Milligan, Hexter and Dressler (99) studied NH_3 in N_2 and Ar and assigned features in both matrices to rotation and inversion of NH_3. Pimentel, Bulanin, and Van Thiel (115) interpreted all the bands in N_2 as due to nonrotating monomers, dimers, and trimers. Hopkins, Curl, and Pitzer (69) looked at the time dependence of ν_2 in Ar and found only two lines with a clear time dependence.

The vibration-rotation spectra of hydrogen halides in noble gas matrices have been the object of numerous investigations. Schoen, Mann, Knobler, and White (138) first reported HCl in Ar and later Mann, Acquista, and White (95) extended the study to include HCl, DCl, HBr, and DBr in Ar and Kr. Bowers and Flygare (14) reported spectra for HCl, DCl, HBr, DBr, and HI in Ar, Kr, and Xe. Bowers, Kerley, and Flygare (15) added work on HF in Ne, Ar, Kr, and Xe. Keyser and Robinson (84, 85) examined HCl and DCl in Kr and Xe. Verstegen, Goldring, Kimel, and Katz (154) also studied HCl in Ar, Kr, and Xe. Most of this work was reported about the same time. Other studies on HCl and HBr have been made by Kwok (91), Shurvell

and Harvey (144), and Brunel and Peyron (17). Barnes, Hallam, and Scrimshaw (8), and Davies and Hallam (34) have found the vibration-translation line for HCl and DCl in Ar which is predicted by the RTC theory. Robinson and co-workers (96, 129, 155) have observed HF and DF in Ne, Ar, Kr, and Xe in both the far-infrared and mid-infrared regions, and also HCl in Ar and Kr in the far-infrared. Barnes, Davies, Hallam, Scrimshaw, Hayward and Milward (7) have found rotational transitions for HCl and DCl in Ar. Rotation-translation coupling theories have generally been used to interpret the spectra of the hydrogen halides. Mason, Von Holle, and Robinson (96) have explained their results on HF and DF by considering perturbations to the rotational potential function. The crystal field theory of Devonshire (35) has not been successful in explaining the spectra of hydrogen halides because the translational motion cannot be ignored.

The infrared spectra of methyl radicals in Ar have been recorded by Milligan and Jacox (101). They observe structure in the ν_2 band of CH_3 which is interpreted as due to rotational degrees of freedom, but not nearly free rotation.

Cabana, Savitsky, and Hornig (20) studied the infrared spectra of CH_4 and CD_4 in Ar, Kr, and Xe. They found structure in the ν_3 and ν_4 bands which they interpreted as due to rotation using King's model (86). Chamberland, Belzile, and Cabana (23) repeated some of the previous work and found that there were some lines which they did not observe and they attributed these to the spray deposition of samples. Frayer and Ewing (46, 47) studied the ν_3 and ν_4

infrared spectra of CH_4 in Ar in connection with nuclear-spin conversion. They found time dependent intensity changes consistent with nuclear-spin conversion. Cabana, Anderson, and Savoie (21) reported the Raman spectrum of CH_4 in Kr. They were not able to resolve structure in the ν_3 band, but observed a much broader feature than in the infrared. Hopkins, Curl, and Pitzer (69) looked at the infrared spectra of CH_3D in Ar, Kr, and Xe. They observed intensity changes which are consistent with nuclear-spin conversion and rotational splittings.

Many of the molecules discussed in this section will be examined further after the group theory has been presented in Chapter III. Finding the splitting of the ground librational state near the librator limit is quite easy for most cases and the hindered rotor spectra can be predicted and compared to the reported spectra. This is especially significant for molecules of symmetry C_{2V} (H_2O, NH_2), C_{3V} (NH_3, CH_3D), and D_{3h} (CH_3) since extended calculations have not been done for these symmetries in an octahedral crystal field.

While convincing evidence has been found for rotation of molecules in noble gas matrices, the picture with nitrogen as a matrix is quite different (116). There have been splittings observed in the vibrational bands of molecules in nitrogen (61, 62, 63, 99), but these have usually been due to dimers or higher aggregates (7, 8, 81, 82, 115, 149) and in any case, not to rotational motion.

2. Alkali Halide Impurities

The alkali halides make a convenient host for studying either cation or anion impurities. A substituted impurity ion will be at an octahedral site for either NaCl-type or CsCl-type crystals, although the environment in the two types will be different. Again the theories of Devonshire (35), and King and Hornig (87) will be appropriate for diatomic and tetrahedral ions, respectively.

The CN^- ion in alkali halides was first studied by Maki and Decius (94), and Price, Sherman, and Wilkinson (122, 123). The broad vibrational fundamental was later interpreted (32, 42, 105, 140, 141) in terms of rotational motion of the ion using the Devonshire model (35). The potential minima for the CN^- ion have been found to be along <100> and <110> directions for NaCl-type and CsCl-type lattices (140), respectively.

The rotational motion of OH^- and OD^- in NaCl-type lattices has been studied extensively by Klein and co-workers in both the infrared and Raman effect (24, 41, 88, 113, 114, 156). They have looked at the vibrational fundamental and also the librational mode and compared their results with the Devonshire model. The potential minima have been found to be along <100> directions (77, 90, 158). The splittings in the ground librational state due to tunneling between equivalent minima have been determined to be of the order of .2 cm^{-1} (16, 40).

The application of the Devonshire model to these studies is complicated by local distortions of the lattice (142) and displacement

of the center of mass from the lattice point (92). The coupling of translational and librational motions presents an additional problem (83).

The spectra of the NH_4^+ ion in NaCl-type lattices was reported by Vedder and Hornig (153) and the fine structure in the vibrational bands was interpreted as due to rotational motion. They determined that the motion was much different from free rotation. This was about the time of King's work (86) and detailed comparisons with his model were not possible. These results will be discussed further in Chapter III.

The vibrational spectra of the NO_2^- ion in potassium halides have been examined by Narayanamurti, Seward, and Pohl (106) and interpreted using a hindered rotor model. They determined the potential minima to occur when the C_2 axis of the ion is along a ⟨110⟩ direction of a crystal. Their calculations will be compared to the solution for a C_{2V} molecule in an octahedral field in Chapter III. The rotational motion of NO_2^- in $NaNO_2$ has been studied by van der Elsken and co-workers (157) and the barriers to rotation have been found to be quite high.

3. Molecular Crystals

The solid hydrogens are the only examples of molecular crystals which exhibit nearly free rotation. Para-hydrogen and ortho-deuterium have a hexagonal close-packing structure (109, 124, 150, 151) at lowest temperatures and ortho-hydrogen and para-deuterium are face-centered cubic (59) at lowest temperatures. This difference in

the structure is reflected in the spectra. The nearly free rotation in the solids is best illustrated by the splitting in the rotational bands. The Raman rotational spectrum of para-hydrogen has been observed by Bhatnagar, Allin, and Welsh (11), and recently the Raman rotational spectra of both ortho- and para-hydrogen has been reported by Prior and Allin (124) in a mixture cointaining 94 per cent ortho. A very extensive theoretical treatment for para-hydrogen has been carried out by Van Kranendonk and Karl (151).

Rotation in solid methane was first suggested by Pauling (112). Early thermodynamic work by Clusius and co-workers (26, 27, 28, 45, 89) established two phases in solid CH_4 and three in CD_4. Further heat capacity work has been done by Colwell, Gill, and Morrison (29-31). Recent birefringence studies by Ballik, Gannon, and Morrison (5, 6) have shown that there are three phases of CH_4, but that the transition from phase II $\longrightarrow$ III is quite complex and that under conditions when equilibrium is reached, phase II exists only between 18 to 20°K. X-ray data has established that the carbon atoms form essentially a face-centered cubic lattice in all phases of CH_4 and CD_4 (56, 58, 102, 103, 136, 137). James and Keenan (76) predicted that phase II of CH_4 (22.2-27.1°K) would have 3/4 ordered molecules and 1/4 rotating molecules. This structure was confirmed by the neutron diffraction studies of Press (120), who determined the space group to be O_h^6 (Fm3c) with six ordered molecules at D_{2d} sites and two disordered molecules at 0 sites. Press determined phase I of CD_4 to be disordered with respect to molecular orientations. Phase III of CD_4 has been found to be

tetragonal by neutron diffraction (121), X-ray (13), and birefringence studies (6), but the exact structure has not been determined. The lowest temperature phase of CH_4 has also shown evidence of rotation while phase I appears to be disordered like CD_4. The complications surrounding phase II of CH_4 mean that studies of CH_4 have been done in phases I and III. The heat capacity of CH_4 showed a thermal anomaly at 8°K (29, 30). Subsequent NMR experiments have shown that nuclear-spin conversion does occur (64, 132, 162). Kataoka, Okada, and Yamamoto (80) have made an extended James-Keenan calculation for phase III CH_4 and can explain the zero-point entropy (30), NMR experiments (64, 132, 162), far-infrared absorption (135), and inelastic neutron scattering (37, 60, 78) with a structure similar to phase II of CH_4. The infrared experiments by Chapados and Cabana (25) have added to the evidence for rotation. They assign the spectra of phase II CD_4 and phase III CH_4 (~9°K) in terms of both ordered molecules and rotating molecules and agree with the structure determined by Press. Early Raman studies (2) are consistent with this interpretation for phase II CD_4 and phase III CH_4. The far-infrared spectra of Savoie and Fournier (135) agree with the two expected lattice modes in phase II CD_4 and phase III CH_4. The band shape studies by Ewing (39) of CH_4 and CD_4 in the liquid and phase I suggest there is rotational motion in phase I. The conclusions are that phase I of CH_4 and CD_4 is disordered and the molecules undergo some sort of rotational motion (38, 54, 55, 119, 145, 148), phase II of CD_4 and phase III of CH_4 have the structure predicted by James and

Keenan, phase III of CD_4 is not understood very well yet, and little is known about phase II of CH_4. The conclusions about phase III CH_4 will be examined further in Chapter V.

III. GROUP THEORY AND APPLICATIONS TO MOLECULAR ROTATION IN CRYSTALLINE SOLIDS

A. Group Theory

Our approach to the problem of rotating molecules in crystal fields uses the methods of group theory developed by Longuet-Higgins (93). This method uses the fact that the Hamiltonian is invariant to permutations of the positions and spins of any set of identical nuclei, an inversion of the positions of all particles in the center of mass, and the product of such a permutation and an inversion. Let P stand for a permutation, E for the identity, E* for the inversion of all particles, and P* for the product PE* = E*P. These are the fundamental symmetry operations and it will be shown how they are related to the conventional rotation and reflection operations. An important part of this method is to determine which operations are feasible and which are not. In the symmetry group for ammonia, E* is feasible because the inversion occurs with a frequency which is not negligible compared with the resolution of the spectroscopic data. In the symmetry group for methane, however, E* is not feasible because inversion occurs at a frequency which is too small. The symmetry group, then, is the set of all feasible operations. One point to be made is that if there are any operations of the type P* in a group, then there are equal numbers of starred and unstarred operations. The group will have a subgroup of permutations and a coset of permutation-inversions.

It is most important to relate the permutation operations with

point group operations and rotations. A permutation or permutation-inversion for a rigid molecule is equivalent to a point group operation on the internal coordinates followed by a bodily rotation of the molecule about an axis through the center of mass. We can write this as $P(r) = Q[r_e + R(\rho)]$ where R is a point group operation, Q is a rotation, r_e is the 3N dimensional vector describing the equilibrium positions of the atoms, ρ is the corresponding displacement vector, and $r = r_e + \rho$. Once the one to one mapping between P and R is established it is clear that the group $\{R\}$ is isomorphic to the group $\{P\}$. For linear molecules the mapping from $\{R\}$ to $\{P\}$ is a homomorphism. The symmetries of the dipole (μ) and polarizability (α) tensors are most easily determined from the point group operations. The operation R which is associated with each P or P* will determine the symmetries of translation and rotation and therefore the symmetries of μ and α.

The group $\{Q\}$ is important in classifying the rotational states since it consists of bodily rotations of the molecule. The group $\{Q\}$ is isomorphic to the permutation group unless the molecule possesses a center of symmetry in which case $\{Q\}$ is isomorphic to the subgroup of $\{P\}$ which is just the permutations. The reason for this is that the rotation in $\{Q\}$ corresponding to the i operation is C_1, the identity. So, in this case, both an operation of the type P and P* will map to the same operation in $\{Q\}$.

The permutation group has many advantages over the point group. The algebraic properties of a group are much easier to study using permutations. The nuclear spin symmetries are found directly from

permutation operations. On the other hand, transformations of internal coordinates are much easier using point groups, the rotational properties are determined from the $\{Q\}$ groups, so a knowledge of the relationship between these groups is a very important asset.

The cycle structure of P or P* is important in relating the operations P, Q, and R. For any P, R is a rotation and Q is a rotation in the opposite sense of R. P will be one or more cycles of length n and the corresponding rotations will be $\pm 360^{\circ}/n$ (cycles of length one will not be written). For any P*, R is a reflection or rotation and reflection, and Q is the product of rotations associated with a reflection and rotation. For any reflection, Q is a rotation of 180° about an axis perpendicular to the plane. For a rotation and reflection Q is the product of C_n^{-1} and C_2 where both rotations are about the same axis. If a molecule is planar, then E* is a feasible operation and is associated with σ_h. The cycle structure of P* is not in general as simple as that of P. If P* consists of two cycles, R could be any reflection plane or inversion. If P* has the longest cycle of length six, then R could either be S_3 or S_6. The cycle structure of P* may include smaller cycles for different sets of nuclei. The associated elements of P, Q, and R are summarized in Table I.

The difference between the inversion operation i for a molecule with a center of symmetry, and the parity operation E* which is an inversion of all particles through the center of mass is worthy of an explanation, especially with the term inversion being used for both. The i operation acts on the displacements and inverts the displacements

TABLE I. CORRESPONDENCE BETWEEN PERMUTATIONS P, PERMUTATION-INVERSIONS P*, RIGID ROTATIONS Q, AND POINT GROUP OPERATIONS R.

P	Q	R	P*	Q	R
E	C_1	C_1	E*	C_2	σ_h, σ_v(linear)
two cycles	C_2	C_2	two cycles*	C_2	$\sigma_h, \sigma_v, \sigma_d$
three cycles	C_3^{-1}	C_3	two cycles*	$C_2 \times C_2 = C_1$	i
four cycles	C_4^{-1}	C_4	(six) three cycles*	$C_3^{-1} \times C_2 = C_6$	S_3
six cycles	C_6^{-1}	C_6	four cycles*	$C_4^{-1} \times C_2 = C_4$	S_4
			six cycles*	$C_6^{-1} \times C_2 = C_3$	S_6

TABLE II. CORRESPONDENCE BETWEEN INTERNAL COORDINATE $\{R\}$ GROUPS AND RIGID ROTATION $\{Q\}$ GROUPS.

	$\{R\}$	$\{Q\}$	$\{R\}$	$\{Q\}$	
	C_n	C_n	S_{2n}	C_{2n}	n even
	C_i	C_1	S_{2n}	C_n	n odd
	C_s	C_2	D_{nh}	D_n	n even
	D_n	D_n	D_{nh}	D_{2n}	n odd
	C_{nv}	D_n	D_{nd}	D_{2n}	n even
n even	C_{nh}	C_n	D_{nd}	D_n	n odd
n odd	C_{nh}	C_{2n}	T, T_h	T	
			T_d, O, O_h	O	

through the center of the molecule. The i operation is defined with respect to the body-fixed axes of the molecule. The E* operation inverts the space-fixed coordinates of the molecule. It is equivalent to a reflection of the displacements through the plane of the molecule followed by a bodily rotation of all particles through 180° about an axis perpendicular to the plane. The effect of parity on the displacements of the molecule is determined by the behavior with respect to σ_h. The parity operation is still meaningful for molecules without a molecular plane of symmetry in connection with rotational levels as shown by Oka (110).

The correspondence between the groups $\{R\}$ and $\{Q\}$ can now be made for the 32 crystallographic point groups, keeping in mind the isomorphism between $\{R\}$ and $\{P\}$. If a group contains the symmetry operation i, then it is a direct product of a rotational group with the group C_i, and since the element in $\{Q\}$ for both E and i is C_1, then the group $\{Q\}$ is isomorphic to this rotational group. The correspondence between $\{R\}$ and $\{Q\}$ is summarized in Table II.

Let us assume that a guest molecule has the symmetry of the point group $\bar{M}$ (for molecule) and it occupies a site in a host crystal which has the symmetry of the point group S (for site) in the absence of the guest molecule. Operations in $\bar{M}$ are related to the molecule and body-fixed axes while operations in S are related to the crystal and space-fixed axes. The point groups $\bar{M}$ and S can be divided into the corresponding permutation subgroups plus the cosets of permutation-inversions. These are denoted as follows:

$\bar{M} = \bar{M}(P) + \bar{M}(P^*)$ and $S = S(P) + S(P^*)$. If $\bar{M}$ or S happened to be a purely rotational group, then there would be no operations of the type P*. The elements of a group which are appropriate for a guest molecule in a host crystal consist of products of operations in S(P) with operations in $\bar{M}(P)$ and operations in S(P*) with operations in $\bar{M}(P^*)$. The operations are combined in this way because an inversion includes all particles, not just the molecule or the crystal alone. Operations in $\bar{M}$ and S commute since the operands in $\bar{M}$ are atoms of the molecule and the operands in S are atoms of the crystal.

The precise meaning of operations in $\bar{M}$ and operations in S will be illustrated through an example (Figure 1). Let us consider a molecule such as methane in a cubic crystal field with the four atoms numbered $\bar{1}$ to $\bar{4}$ and the eight corners numbered 1 to 8. For simplicity the atoms are oriented in the corners of the cube. The operation $E(\overline{123})$ permutes the atoms as shown. It is equivalent to a C_3 operation on the internal coordinates followed by a C_3^{-1} rotation of the entire molecule. The operator $(123)(587)\bar{E}$ could be interpreted as a C_3^{-1} rotation of the crystal but instead we fix the crystal to the space-fixed axes and define $(123)(587)\bar{E}$ to be a C_3 rotation of the molecule about space-fixed axes. We are assuming that the atoms in the crystal are stationary. The effect of the operation $(123)(587)(\overline{123})$ is a C_3^{-1} rotation of the molecule about the axis corresponding to the $\bar{4}$ bond and then a C_3 rotation of the molecule about the axis through corners 4 and 6 of the cube. The displacements of the molecule relative to the body-fixed axes

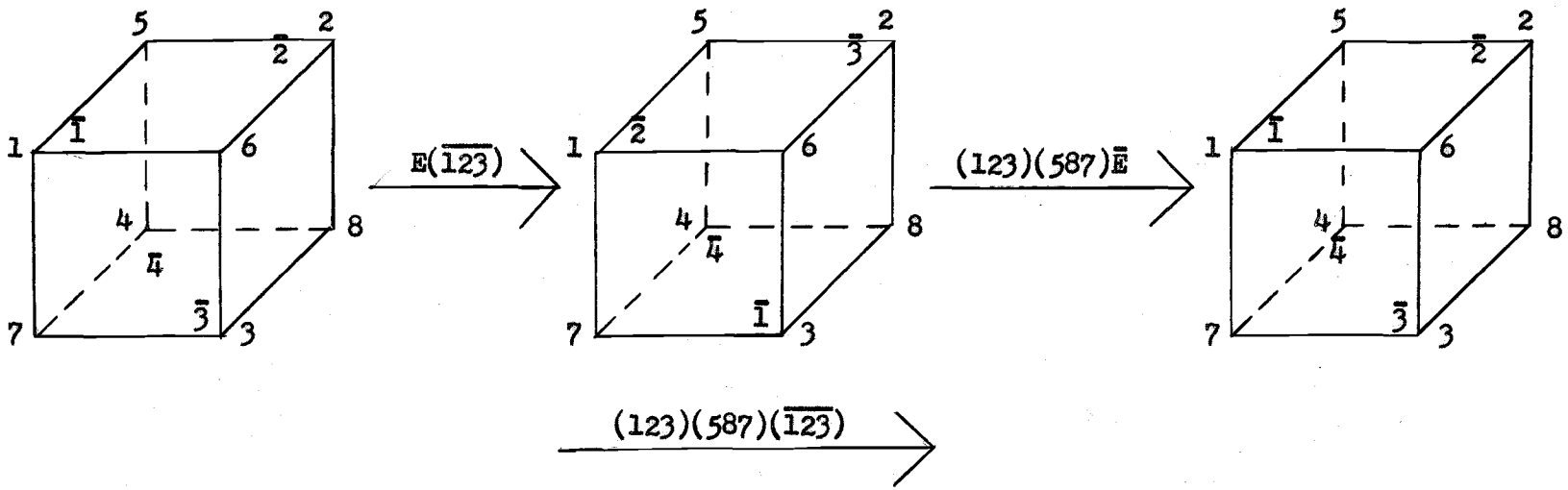

Figure 1. Illustration of operations for a tetrahedral molecule ($\bar{T}_d$) in a cubic crystal field (O_h).

are transformed by a C_3 operation ($E(\overline{123})$) and the displacements of the molecule relative to the space-fixed axes are also transformed by a C_3 operation ($(123)(587)\bar{E}$). Similarly an operation such as $(34)(58)^*(\overline{34})^*$ can be interpreted as a σ_d operation on the displacements of the molecule relative to both the body-fixed and space-fixed axes while keeping the crystal fixed in space. Therefore, μ and α for internal transitions are determined by the operations in $\bar{M}$, and μ and α for overall transitions, rotational or librational, including vibrational, are determined by the operations in S.

The appropriate group depends in general on the freedom of the molecule to rotate with respect to the crystal. The largest possible group is the product of all operations of S(P) with $\bar{M}(P)$ and of all S(P*) with $\bar{M}(P^*)$. This group will be denoted by $G = (S,\bar{M}) = S(P)\,\bar{M}(P) + S(P^*)\,\bar{M}(P^*)$. Some operations in G become less feasible as the barrier to rotation increases and at the high barrier or librator limit, rotation of the molecule with respect to the crystal is not feasible. We will be using the correlation between the free rotation group G and some high barrier subgroup $\bar{\bar{H}}$, and the rotational energy levels will be given as a function of the barrier height in general. If both S and $\bar{M}$ are rotational groups, the order of G is $g = sm$ where g, s, and m represent the order of their respective groups. If either S or $\bar{M}$ is not a rotational group, then $g = sm/2$ since half of all combinations between the groups would involve P's with P*'s and these are not allowed. At a limit of no rotation the appropriate subgroup $\bar{\bar{H}}$ is isomorphic to a common subgroup of S and $\bar{M}$. $\bar{\bar{H}}$ is isomorphic to the greatest common subgroup of S and $\bar{M}$

if the molecule is oriented to the crystal in the highest symmetry possible. An operation in $\bar{\bar{H}}$ consists of the product of an operation in S with an operation in $\bar{M}$ so that there is no rotation of the molecule relative to the crystal when the molecule is at an equilibrium position. The librational states in $\bar{\bar{H}}$ have a degeneracy which is increased by the factor g/h (h is the order of $\bar{\bar{H}}$) and this factor is also the number of equivalent minima in the potential with respect to rotation. In certain cases there may be significant groups which lie in between the limits for G and $\bar{\bar{H}}$. For instance, some of the relative rotations may be feasible but not all. In this case the group would be a subgroup of $G = (S, \bar{M})$, but the problem would be essentially no different than that for G and $\bar{\bar{H}}$.

We would like to be able to write G as a direct product of groups so that the character table may be obtained from known character tables of smaller groups. The problem in general is that G is not simply S x $\bar{M}$ because P operations from S do not combine with P* operations from $\bar{M}$ and vice versa.

If either S or $\bar{M}$ is a rotational group then G is a direct product. Let $\bar{M}$ be a rotational group, then $G = 'S'(P) \times '\bar{M}'$ where $'S'(P) \cong S(P)$ and $'\bar{M}' \cong \bar{M}$ ($\cong$ means is isomorphic to). Operations in $'\bar{M}'$ are products of E in S with an operation in $\bar{M}$ and operations in $'S'(P)$ are products of $\bar{E}$ in $\bar{M}$ with an operation in S(P). It is clear that every operation in $'\bar{M}'$ commutes with every operation in $'S'(P)$ since in both cases the commutation is with the identity, either E or $\bar{E}$. The character table is then found from the character tables of the groups S(P) and $\bar{M}$. The symmetry species of G are

written as the product of those in S(P) and $\bar{M}$.

If neither S nor $\bar{M}$ is a rotational group and either S or $\bar{M}$ is a direct product group (with $\{E,\sigma_h\}$ or $\{E,i\}$) then G is a direct product. Let $\bar{M}$ be a direct product group, say $\bar{M} = \bar{M}(P) \times \{\bar{E},\bar{I}\}$. In the permutation notation $\bar{I}$ would be the appropriate permutation-inversion. Then $G = 'S' \times '\bar{M}'(P)$ where $'S' \cong S$ and $'\bar{M}'(P) \cong \bar{M}(P)$. Operations in $'\bar{M}'(P)$ are products of E in S with an operation in $\bar{M}(P)$, operations in $'S'(P)$ are products of $\bar{E}$ in $\bar{M}$ with an operation in S(P), and operations in $'S'(P^*)$ are products of $\bar{I}$ in $\bar{M}$ with an operation in $S(P^*)$. In this case commutation also depends on $\bar{I}$ commuting with every element in $\bar{M}(P)$. The fact that $\bar{I}$ commutes with everything in $\bar{M}(P)$ is evident from the assumption that $\bar{M}$ is a direct product of $\bar{M}(P)$ with $\{\bar{E},\bar{I}\}$. The character table can now be found from those of S and $\bar{M}(P)$ and the symmetry species are products of those in S and $\bar{M}(P)$.

It is possible in some cases to have G equal to two direct products if, for example, S and $\bar{M}$ were both direct product groups. This difference amounts to different labeling of the symmetry species of G, but no changes other than that.

In the 32 crystallographic point groups there are only six which are neither rotational groups nor direct product groups. These are S_4, C_{3v}, C_{4v}, C_{6v}, D_{2d}, and T_d. Unless both the molecular symmetry and crystal site symmetry appear in this set of six groups, the group G will be a direct product. This leaves relatively few groups to consider which have a more complicated character table. These special cases can be solved rather easily, sometimes by

inspection, but better methods are using Clifford theory or induction of characters from subgroups (12). The symmetry species for these groups can no longer be labeled in terms of direct products of symmetry species of the familiar point groups.

B. The Linear Rotor

The preceding discussion will become more understandable by looking at a number of examples. The simplest case to start with is a diatomic molecule in various crystal fields. The group for an XY molecule consists of just $\bar{E}$ and $\bar{E}^*$. The C_∞^ϕ rotations do not move the molecule relative to the crystal so for this problem they are mapped into the identity. All of the σ_v planes have an operation in $\{Q\}$ which is a C_2 rotation perpendicular to the plane and all these rotations interchange X and Y. All the σ_v planes then are mapped to the same permutation-inversion and it is $\bar{E}^*$, the parity operator. For an X_2 molecule there is the additional symmetry of the identical nuclei and by the same reasoning as before the symmetry operations appropriate for motion of the molecule relative to the crystal are $\bar{E}$, $(\overline{12})$, $\bar{E}^*$, and $(\overline{12})^*$. The associated point group operations are the ∞C_2 with $(\overline{12})$ and i and S_∞^ϕ with $(\overline{12})^*$. Thus there is a homomorphism from $\bar{C}_{\infty v}$ onto $\{\bar{E},\bar{E}^*\}$ and $\bar{D}_{\infty h}$ onto $\{\bar{E},(\overline{12}),\bar{E}^*,(\overline{12})^*\}$.

The group G can always be written as the direct product 'S' x '$\bar{M}$'(P). '$\bar{M}$'(P) is $\{E\bar{E}\}$ or $\{E\bar{E},E(\overline{12})\}$ for the XY and X_2 cases, respectively. So, for the XY molecule $G \cong S$ and the symmetry species are those of S. For the X_2 molecule G = 'S' x $\{E\bar{E},E(\overline{12})\}$ so the symmetry species are those of S with the additional label of s or a which means symmetric or antisymmetric to the operation $E(\overline{12})$; thus there are twice as many symmetry species in G as in S.

The examples for diatomic molecules are appropriate for linear

molecules as long as they remain linear. Bunker (18, 19) and Papousek (18) have used the Longuet-Higgins approach to linear molecules and determined an extended permutation group which is isomorphic to the point group. The use of this extended group makes it possible to treat the molecule when it is nonlinear as well, for instance, the vibrational bending mode. The linear XY_2 molecule will be treated by itself at the end of this section.

1. XY and X_2 Molecules in a D_{3h} Field

The first example will treat the XY and X_2 molecules in a crystal field having the symmetry D_{3h}. The groups $\{P\}$, $\{R\}$, and $\{Q\}$ are listed for D_{3h} in Table III.

TABLE III. THE PERMUTATION GROUP $\{P\}$, THE POINT GROUP $\{R\}$, AND THE ROTATION GROUP $\{Q\}$ FOR THE GROUP D_{3h}.

$$D_{3h}\ \{P\} = \{E,(123),(132),(12),(13),(23),E^*,(123)^*,(132)^*,(12)^*,(13)^*,(23)^*\}$$

$$\{R\} = \{E,C_3,C_3^{-1},\ C_2^{I},C_2^{II},C_2^{III},\sigma_h,S_3,S_3^{-1},\sigma_v^{I},\sigma_v^{II},\sigma_v^{III}\}$$

$$\{Q\} = \{C_1,C_3^{-1},C_3,C_2^{'I},C_2^{'II},C_2^{'III},C_2,C_6,C_6^{-1},C_2^{"I},C_2^{"II},C_2^{"III}\}$$

The group G is $'D_{3h}'$ for the XY molecule and $'D_{3h}' \times '\bar{C}_2'$ for the X_2 molecule. The character table for $G = (D_{3h}, \bar{D}_{\infty h})$ is given in Table IV. The character table for $G = (D_{3h}, \bar{C}_{\infty v})$ is found in the first six rows and columns, and the symbol s is dropped from the symmetry species. In order to determine $\bar{\bar{H}}$ it is necessary to examine the Q operations. We will assume that at the librator limit the equilibrium position of either molecule is along the threefold axis of

TABLE IV. THE CHARACTER TABLE FOR $(D_{3h}, \bar{D}_{h})$ AND CORRELATION TO THE GROUP $\bar{\bar{D}}_{3h}$.

$(D_{3h}, \bar{D}_{\infty h})$	$\bar{\bar{E}}$	$2(123)\bar{\bar{E}}$	$3(12)\bar{\bar{E}}$	$E^*\bar{\bar{E}}^*$	$2(123)^*\bar{\bar{E}}^*$	$3(12)^*\bar{\bar{E}}^*$	$E(\overline{12})$	$2(123)(\overline{12})$	$3(12)(\overline{12})$	$E^*(\overline{12})^*$	$2(123)^*(\overline{12})^*$	$3(12)^*(\overline{12})^*$	$\bar{\bar{D}}_{3h}$
sA_1'	1	1	1	1	1	1	1	1	1	1	1	1	A_1'
sA_2'	1	1	-1	1	1	-1	1	1	-1	1	1	-1	A_2'
sE'	2	-1	0	2	-1	0	2	-1	0	2	-1	0	E'
sA_1''	1	1	1	-1	-1	-1	1	1	1	-1	-1	-1	A_1''
sA_2''	1	1	-1	-1	-1	1	1	1	-1	-1	-1	1	A_2''
sE_1''	2	-1	0	-2	1	0	2	-1	0	-2	1	0	E''
aA_1'	1	1	1	1	1	1	-1	-1	-1	-1	-1	-1	A_2''
aA_2'	1	1	-1	1	1	-1	-1	-1	1	-1	-1	1	A_1''
aE'	2	-1	0	2	-1	0	-2	1	0	-2	1	0	E''
aA_1''	1	1	1	-1	-1	-1	-1	-1	-1	1	1	1	A_2'
aA_2''	1	1	-1	-1	-1	1	-1	-1	1	1	1	-1	A_1'
aE''	2	-1	0	-2	1	0	-2	1	0	2	-1	0	E'

the crystal. The XY molecule is included in the X_2 case so only the X_2 molecule will be treated now. The operations in $\{Q\}$ for the X_2 molecule are $\bar{C}_1$ for $\bar{E}$ and $(\overline{12})^*$, and $\bar{C}_2$ for $(\overline{12})$ and $\bar{E}^*$. Operations from D_{3h} which have rotations in $\{Q\}$ parallel to the threefold axis can combine with $\bar{E}$ and $(\overline{12})^*$, and operations which have 180° rotations in $\{Q\}$ perpendicular to the threefold axis can combine with $(\overline{12})$ and $\bar{E}^*$. The group $\bar{\bar{H}} = \bar{\bar{D}}_{3h}$ consists of the following 12 operations: $\{E\bar{E},(123)\bar{E},(132)\bar{E},(12)(\overline{12}),(13)(\overline{12}),(23)(\overline{12}),E^*(\overline{12})^*,(123)^*(\overline{12})^*,(132)^*(\overline{12})^*,(12)^*\bar{E}^*,(13)^*\bar{E}^*,(23)^*\bar{E}^*\}$. The point is that these operations in $\bar{\bar{D}}_{3h}$ do not rotate the molecule relative to the crystal when the molecule is positioned along the threefold axis of the crystal. For the XY molecule simply remove operations with $(\overline{12})$ and $(\overline{12})^*$, and this gives $\bar{\bar{H}} = \bar{\bar{C}}_{3V} = \{E\bar{E},(123)\bar{E},(132)\bar{E},(12)^*\bar{E}^*,(13)^*\bar{E}^*,(23)^*\bar{E}^*\}$. Comparing the orders of the groups we see that for the X_2 molecule $g = 24$, $h = 12$ and for the XY molecule $g = 12$, $h = 6$; so in both cases there are two equivalent potential minima. Also note that the greatest common subgroup of D_{3h} and $D_{\infty h}$ is D_{3h}, and of D_{3h} and $C_{\infty V}$ is C_{3V}.

Appropriate manipulation of the character table in Table IV then shows that the correlation of symmetry species takes the form

XY: $\bar{\bar{H}} = \bar{\bar{C}}_{3V}$	$G = (D_{3h}, \bar{\bar{C}}_{\infty V})$
A_1	$A_1' + A_2''$
A_2	$A_2' + A_1''$
E	$E' + E''$

X_2:	$\bar{\bar{H}} = \bar{\bar{D}}_{3h}$	$G = (D_{3h}, \bar{\bar{D}}_{\infty h})$
	A_1'	$sA_1' + aA_2''$
	A_2'	$sA_2' + sA_1''$
	E'	$sE' + aE''$
	A_1''	$sA_1'' + aA_2'$
	A_2''	$sA_2'' + aA_1'$
	E''	$sE'' + aE'$

This is seen to be very similar to the standard correlation between C_{3V} and D_{3h}, the difference being in the s and a labels. Knowing the correlation from $\bar{\bar{C}}_{3V}$ to $(D_{3h}, \bar{\bar{C}}_{\infty V})$ which is the same as C_{3V} to D_{3h}, one finds the correlation from $\bar{\bar{D}}_{3h}$ to $(D_{3h}, \bar{\bar{D}}_{\infty h})$ by the route $\bar{\bar{D}}_{3h} \longrightarrow \bar{\bar{C}}_{3V} \longrightarrow (D_{3h}, \bar{\bar{C}}_{\infty V}) \longrightarrow (D_{3h}, \bar{\bar{D}}_{\infty h})$. For example, A_1'' in $\bar{\bar{D}}_{3h}$ goes to A_2 in $\bar{\bar{C}}_{3V}$ which goes to $A_2' + A_1''$ in $(D_{3h}, \bar{\bar{C}}_{\infty V})$ and this goes to $sA_1'' + aA_2'$, the s modifying the symmetry species in $\bar{\bar{D}}_{3h}$.

The selection rules require knowledge of the μ and α symmetries in external coordinates which are for XY

$$\Gamma(\mu) = A_2'' + E' \qquad \Gamma(\alpha) = 2A_1' + E' + E'',$$

and for X_2

$$\Gamma(\mu) = sA_2'' + sE' \qquad \Gamma(\alpha) = 2sA_1' + sE' + sE''.$$

For the XY molecule the symmetry of the librational states in $\bar{\bar{C}}_{3V}$ is A_1 for the ground state and E for the first excited state. Near the high barrier limit one finds from correlation that the A_1 state is split into $A_1' + A_2''$ components and the E state split into $E' + E''$ components. Thus the selection rules for the infrared allow two librator transitions ($A_1' \longrightarrow E'$, $A_2'' \longrightarrow E''$) and all four possible transitions are allowed in the Raman effect.

For the X_2 case, the selection rules obviously impose the additional restrictions on initial and final states, s $\leftrightarrow$ s and a $\leftrightarrow$ a, but s $\not\leftrightarrow$ a. Since the A_1' ground state in $\bar{\bar{D}}_{3h}$ is $sA_1' + aA_2''$ in G, and the first excited librator state is E'' in $\bar{\bar{D}}_{3h}$ or $sE'' + aE'$ in G, no infrared transition is allowed, and only a doublet ($sA_1' \longrightarrow sE''$, $aA_2'' \longrightarrow aE'$) may appear in the Raman effect.

Physically this amounts to saying that ortho and para forms of X_2 may have slightly different librator frequencies. Ortho molecules have nuclear spin symmetry sA_1' and para molecules have nuclear spin symmetry aA_1'. The overall wave function is s for bosons and a for fermions so if the vibronic state is s, then ortho (para) molecules must be in s(a) rotational states for X a boson, and a(s) rotational states for X a fermion. Zero spin nuclei would only populate a or s states and would yield a librator Raman singlet.

The energy correlation diagram from the free rotor limit to the librator limit is shown in Figure 2 for the X_2 molecule. The same diagram holds for the XY molecule if the s and a labels are dropped for G and the ' and " labels are dropped for $\bar{\bar{H}}$. It is interesting to note that each level of $\bar{\bar{D}}_{3h}$ provides accommodations for both an s and an a state, i.e., for both ortho and para spin modifications.

Examples of a system with this symmetry are para-hydrogen, ortho-deuterium and HD in these crystals. The crystals are hexagonal close-packed (109, 124, 150, 151) and have a site of symmetry D_{3h}. Hydrogen is nearly a free rotor so the splitting of states near the

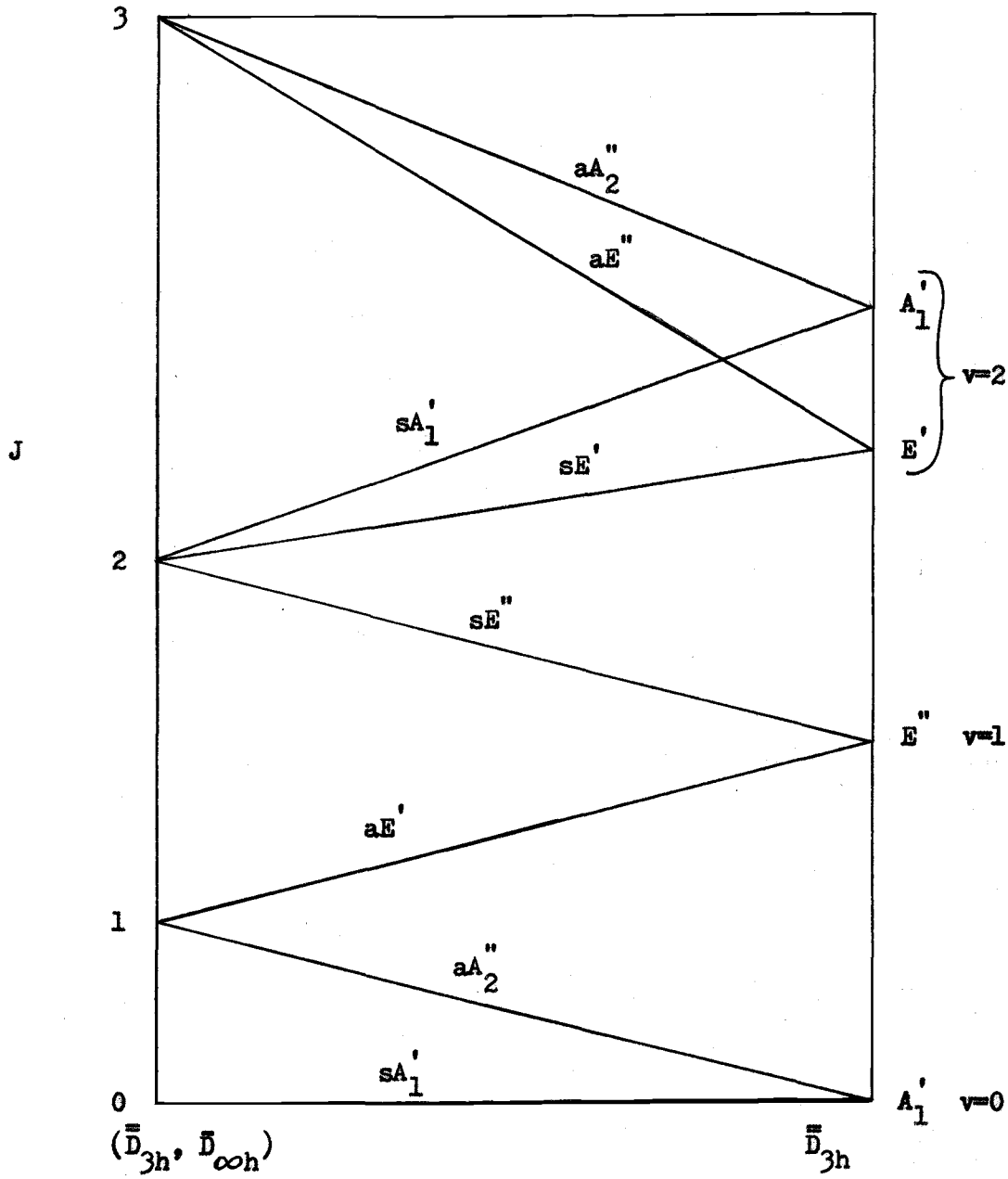

Figure 2. Correlation of rotational energy levels for an X_2 molecule from the $(D_{3h}, D_{\infty h})$ free rotor limit to the D_{3h} libator limit.

rotational limit is appropriate. The $J = 0 \longrightarrow J = 2$ transition for para-hydrogen shows a triplet in the Raman effect corresponding to the transitions $sA_1' \longrightarrow sE''$, sE', sA_1' (11, 124, 151).

2. XY and X_2 Molecules in an S_6 Field

For an XY molecule $G = {}^{\prime}S_6^{\prime}$ and for X_2, $G = {}^{\prime}S_6^{\prime} \times {}^{\prime}\bar{C}_2^{\prime}$. Assuming the equilibrium position of the molecule at the librator limit to be along the threefold axis of the crystal one finds $\bar{\bar{H}} = \bar{\bar{C}}_3$ for the XY case and $\bar{\bar{H}} = \bar{\bar{S}}_6$ for X_2.

The correlation of the symmetry species for the groups and the symmetry of μ and α in G is as follows:

XY	$\bar{\bar{H}} = \bar{\bar{C}}_3$	$G = (S_6, \bar{C}_{\infty v})$
	A	$A_g + A_u$
	E	$E_g + E_u$
	$\Gamma(\mu) = A_u + E_u$	$\Gamma(\alpha) = 2A_g + 2E_g$
X_2	$\bar{\bar{H}} = \bar{\bar{S}}_6$	$G = (S_6, \bar{D}_{\infty h})$
	A_g	$sA_g + aA_u$
	E_g	$sE_g + aE_u$
	A_u	$sA_u + aA_g$
	E_u	$sE_u + aE_g$
	$\Gamma(\mu) = sA_u + sE_u$	$\Gamma(\alpha) = 2sA_g + 2sE_g$

For the XY molecule the symmetry of the librational states in $\bar{\bar{C}}_3$ is A for the ground state and E for the first excited state. Near the high barrier limit the A state splits into $A_g + A_u$ components and the E state into $E_g + E_u$. Now there are two infrared active librator transitions and two Raman active transitions. For

the X_2 molecule, the activity is again a Raman doublet ($sA_g \rightarrow sE_g$, $aA_u \rightarrow aE_u$).

The energy correlation diagram for the X_2 molecule is shown in Figure 3. In this example the rotational states combine either s with g, or a with u. This is a consequence of having a center of symmetry, i, for both the molecule and the crystal. The $\{Q\}$ group for G has the order g/2. The diagram can also be used for the XY molecule if the s and a labels are dropped for G and the g label for $\bar{\bar{H}}$.

Examples of an S_6 site are found in the cubic close-packed crystals of ortho-hydrogen (59), para-deuterium (59), and CO_2 (163). Again ortho-hydrogen and para-deuterium are nearly free rotors. Since the nuclear spin is zero for ^{16}O, then only the s rotational states are occupied for CO_2 and any tunnel splitting disappears because of the spin restrictions.

Jacobi and Schnepp (75) point out the symmetric and antisymmetric states of both the free rotor and high barrier limits. If all the nuclear spins are of the same symmetry then either s or a states may be occupied but not both, and the spectra would be expected to be sharp. If there is disorder in the nuclear spins, then there will be a splitting of states although it may indeed be small.

3. XY Molecules in O_h and T_d Fields

The rotational energies of an XY molecule in an O_h and T_d field have been found for certain potential functions (33, 35).

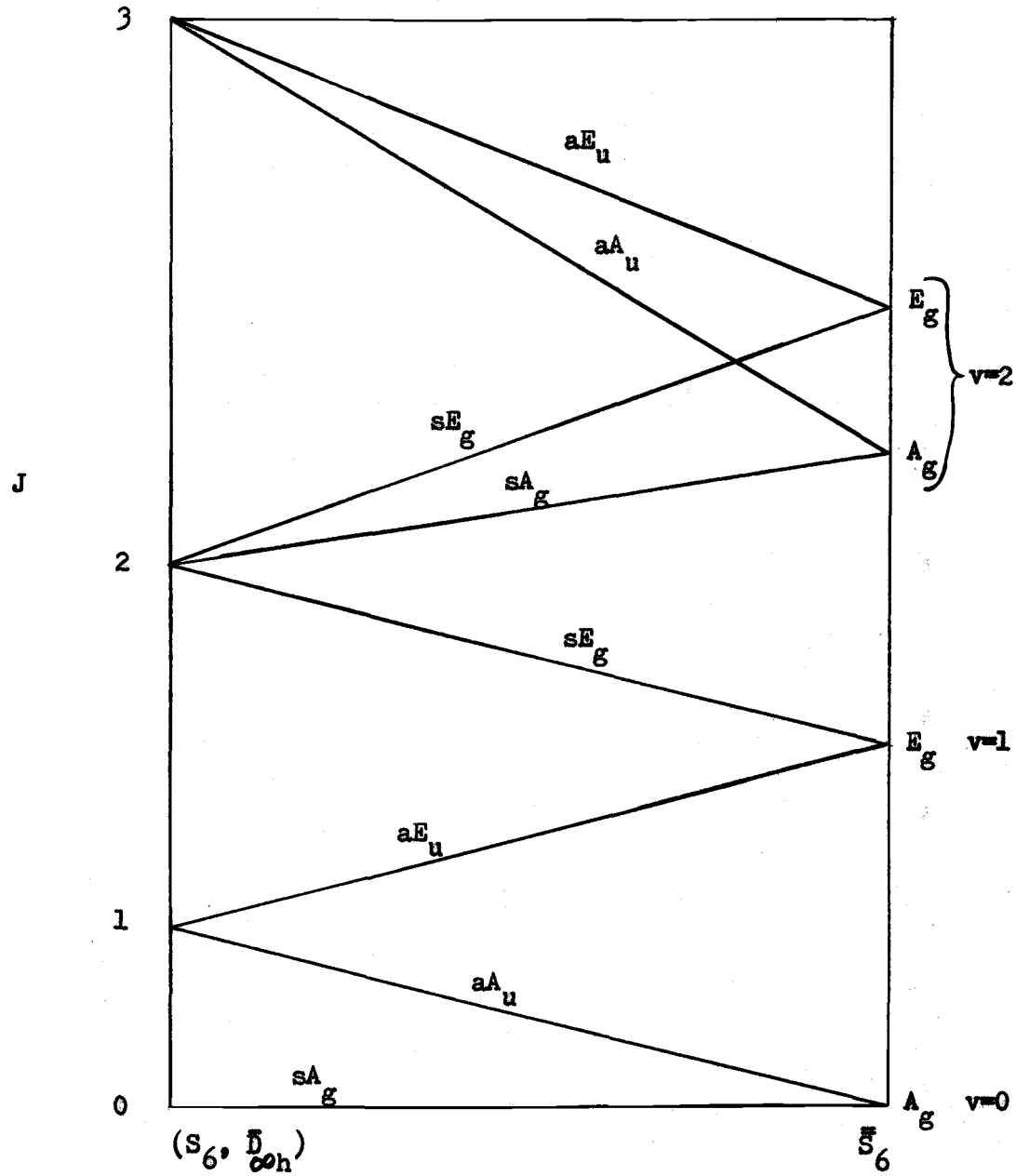

Figure 3. Correlation of rotational energy levels for an X_2 molecule from the $(S_6, D_{\infty h})$ free rotor limit to the S_6 librator limit.

We want to examine these problems using symmetry to point out features which are correct for all potential functions having the appropriate symmetry.

An XY molecule in an O_h field most likely has a potential minimum along a Cartesian axis (⟨100⟩) or a body diagonal (⟨111⟩). In both cases $G \cong O_h$ and if the minimum is along a Cartesian axis $\bar{\bar{H}} = \bar{\bar{C}}_{4V}$, while $\bar{\bar{H}} = \bar{\bar{C}}_{3V}$ if the minimum is along a body diagonal. The correlation between groups is the standard one for C_{4V} and C_{3V} with O_h. The first three librator states in $\bar{\bar{C}}_{4V}$ are A_1, E, and $A_1 + B_2 + B_1$; while the first three in $\bar{\bar{C}}_{3V}$ are A_1, E, and $A_1 + E$. Devonshire's diagram (35) has the $\bar{\bar{C}}_{4V}$ limit to the right, and the $\bar{\bar{C}}_{3V}$ limit to the left. This is the format used in Figure 4. The states in G which make up a state in $\bar{\bar{H}}$ are found from correlation. As an example in $\bar{\bar{C}}_{4V}$, $A_1 \longrightarrow A_{1g} + F_{1u} + E_g$, $E \longrightarrow F_{2g} + F_{1u} + F_{2u} + F_{1g}$, etc. The symmetry of μ is F_{1u} and of α is $A_{1g} + E_g + F_{2g}$ so selection rules may be applied near either limit to predict the spectra.

An XY molecule in a T_d field could have a potential minimum along a threefold or twofold axis of the crystal. Again $G \cong T_d$ and if the minimum is along a threefold axis $\bar{\bar{H}} = \bar{\bar{C}}_{3V}$, while $\bar{\bar{H}} = \bar{\bar{C}}_{2V}$ if the minimum is along a twofold axis. Cundy's work (33) was for the minimum corresponding to $\bar{\bar{H}} = \bar{\bar{C}}_{3V}$. The first three librator states in $\bar{\bar{C}}_{3V}$ are A_1, E, and $A_1 + E$; and in $\bar{\bar{C}}_{2V}$ they are A_1, $B_1 + B_2$, and $2A_1 + A_2$. From the correlation between groups the symmetries of states in G forming the states in $\bar{\bar{H}}$ can be determined. Figure 5 shows the rotational energy levels for both limits, while the potential function

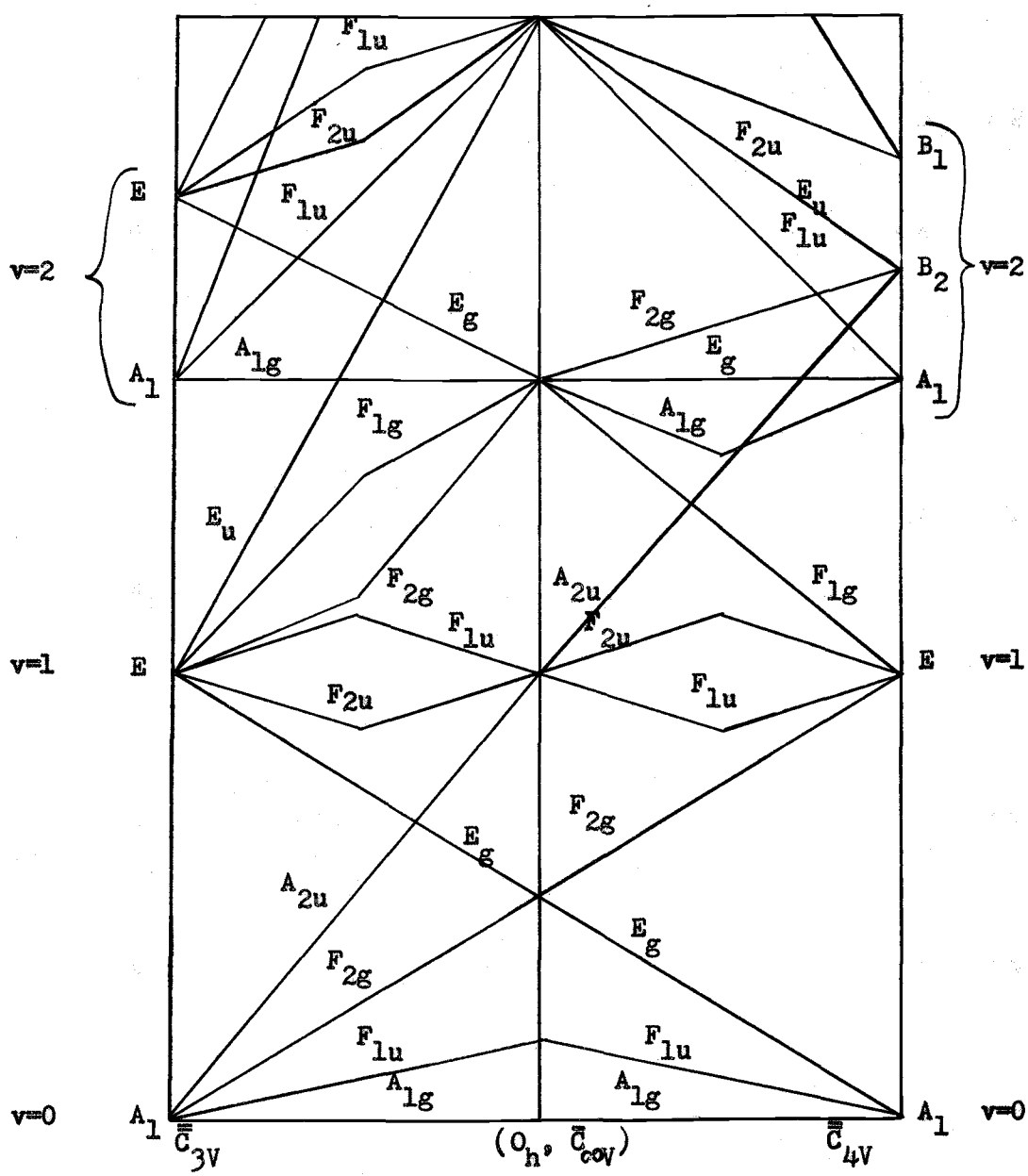

Figure 4. Correlation of rotational energy levels for an XY molecule from the $(O_h, \bar{C}_{\infty v})$ free rotor limit to the $\bar{\bar{C}}_{3V}$ and $\bar{\bar{C}}_{4V}$ librator limits.

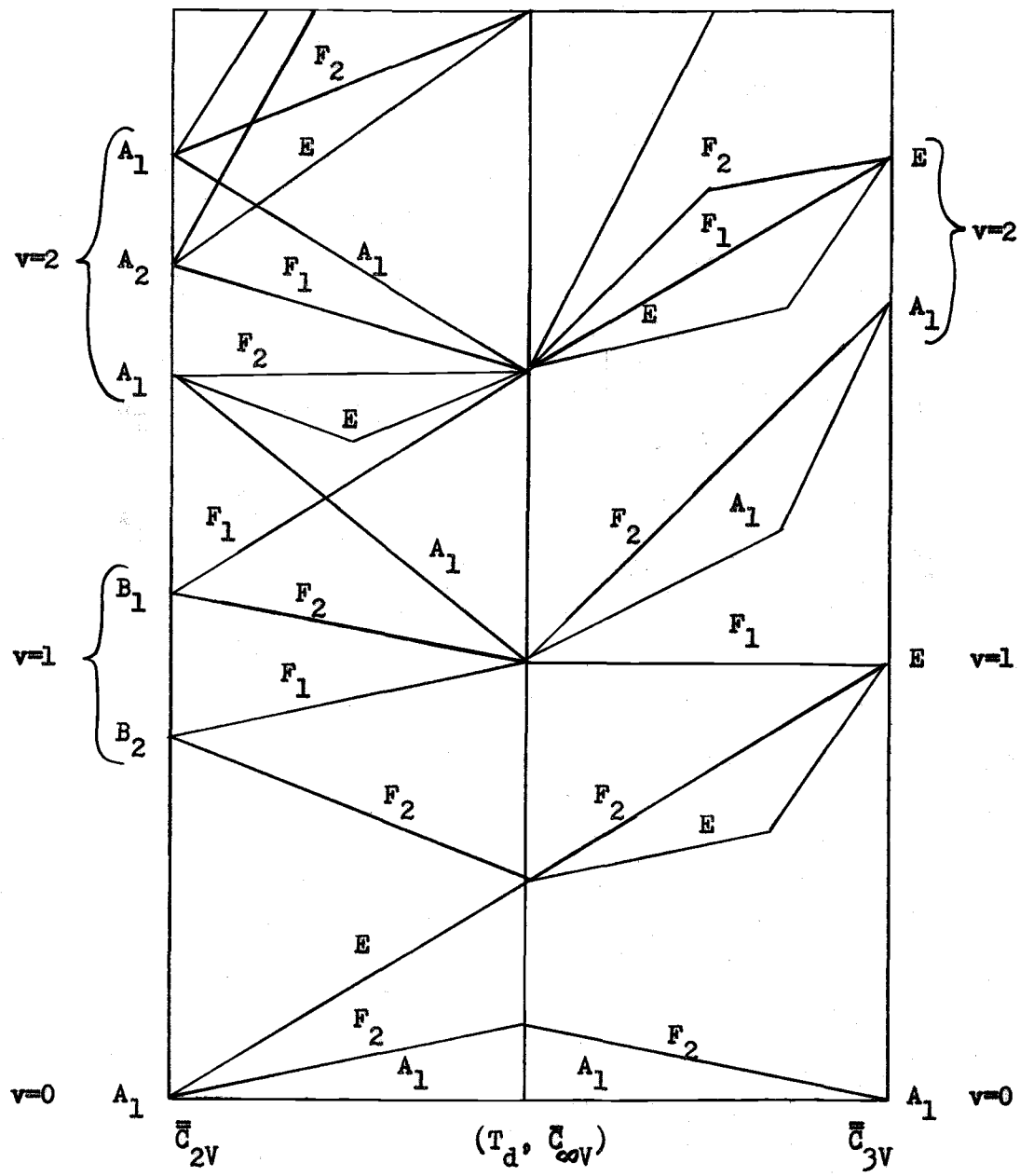

Figure 5. Correlation of rotational energy levels for an XY molecule from the $(T_d, C_{\infty V})$ free rotor limit to the C_{2V} and C_{3V} librator limits.

that Cundy used was appropriate only toward $\bar{\bar{H}} = \bar{\bar{C}}_{3V}$. However, Cundy's diagram has a crossing of T_2 ($=F_2$) levels from J=4 and J=5 which is symmetry forbidden; presumably this should be an avoided crossing. The spectra may be determined by noting that $\Gamma(\mu) = F_2$ and $\Gamma(\alpha) = A_1 + E + F_2$.

Examples which are appropriate for O_h symmetry are linear ions in a salt crystal and diatomic molecules in noble gas matrices. A number of these examples were discussed in Chapter II.

4. High Barrier Solution for an XY Molecule in an O_h Field

The problem of an XY molecule in an octahedral field has been solved for an $\ell=4$ spherical harmonic potential function using spherical harmonic wave functions (35, 133). When there is no potential barrier the spherical harmonics are the exact solutions to the problem. At the high barrier limit, one would expect the solutions to be harmonic oscillator functions. Some of the general features of the Hamiltonian for this problem have been discussed independently by Shore (143), and Sauer, Schirmer, and Schneider (134). Sauer et. al. have a correlation diagram from the free rotor limit to the $\bar{\bar{C}}_{4V}$ librator limit for the ground and first excited librator states. Both of these papers gave the ground state librator wave functions of the appropriate symmetry. In this study we have assumed harmonic oscillator solutions for a Hamiltonian with both $\ell=4$ and $\ell=6$ spherical harmonic potential functions. Using linear combinations of these solutions, the symmetrized wave functions for both the ground and first excited librator states are

found and their respective energies near the high barrier limit.

The Hamiltonian is

$$H = \frac{-\hbar^2}{2I}\left(\frac{\partial^2}{\partial\theta^2} + \cot\theta\,\frac{\partial}{\partial\theta} + \frac{1}{\sin^2\theta}\,\frac{\partial^2}{\partial\phi^2}\right) + \frac{V_o}{2}\left(c_4V_4 + c_6V_6\right)$$

where $V_4 = 1 + 6\cos^2\theta - 7\cos^4\theta - \sin^4\theta\cos 4\phi$,

$V_6 = 1 - 5\cos^2\theta + 15\cos^4\theta - 11\cos^6\theta + \sin^4\theta\cos 4\phi$

$(11\cos^2\theta - 1)$, $c_4 + c_6 = 1$, V_o is the barrier height, and I is the moment of inertia for the XY molecule. We will assume that $\overline{\overline{H}} = \overline{\overline{C}}_{4V}$ so that there are six minima in the Cartesian directions. This will restrict the values for c_4 and c_6 to the extent that the lowest minima must be in Cartesian directions. At the high barrier limit for $\theta \approx \pi/2$, $\phi \approx 0$, the Hamiltonian has the form $H = -\frac{\hbar^2}{2I}\left(\frac{\partial^2}{\partial\gamma^2} + \frac{\partial^2}{\partial\phi^2} + 4V_o\gamma^2 + 4V_o\phi^2\right)$ where $\gamma = \theta - \pi/2$. The eigenfunctions for this Hamiltonian are two-dimensional harmonic oscillator wave functions of the form

$$N_\phi N_\gamma H_\phi H_\gamma \exp(-\alpha\phi^2/2)\exp(-\alpha\gamma^2/2),$$

where $\alpha = 2\sqrt{\tilde{V}_o\tilde{B}}$, $\tilde{V}_o = \frac{V_o}{hc}$, $\tilde{B} = \frac{h}{8\pi^2 cI}$, N_ϕ and N_γ are normalization constants and H_ϕ and H_γ are Hermite polynomials. The energy is $\frac{E}{hc} = (n+1)\tilde{\nu}_L$ where $\tilde{\nu}_L = 4\sqrt{\tilde{V}_o\tilde{B}}$ and $n = n_\phi + n_\gamma$. The wave functions at the minimum corresponding to the +x axis will be labeled $\psi_{xn_\phi n_\gamma}$ so that

$$\psi_{xoo} = N_{xoo}\exp(-\alpha(\phi^2+\gamma^2)/2),$$

$$\psi_{xol} = N_{xol}\exp(-\alpha(\phi^2+\gamma^2)/2),$$

and $$\psi_{xl0} = N_{xl0}\,\phi\exp(-\alpha(\phi^2+\gamma^2)/2).$$

The wave functions have been chosen to be real and the normalization

is such that $\int(\psi_{xn_\phi n_\gamma})^2 \, d\Omega = 1$, where $d\Omega = d\phi \cos\gamma \, d\gamma$. The limits of integration are $-\pi/4$ to $\pi/4$ for both ϕ and γ and when α is sufficiently large for the harmonic oscillator approximation to be appropriate, then the integrand is negligible at $\pm\pi/4$ so the limits can be extended to $\pm\infty$. An important integral formula from which many others can be derived is

$$I = \int_{-\infty}^{\infty} e^{-ax^2} \cos bx dx = \left(\frac{\pi}{a}\right)^{\frac{1}{2}} e^{-b^2/4a}$$

After normalization we have

$$\psi_{xoo} = \left(\frac{\alpha \exp(\frac{1}{4\alpha})}{\pi}\right)^{\frac{1}{2}} \exp\left(-\alpha(\phi^2+\gamma^2)/2\right)$$

$$\psi_{xol} = \left(\frac{4\alpha^3 \exp(\frac{1}{4\alpha})}{\pi(2\alpha-1)}\right)^{\frac{1}{2}} \gamma \exp\left(-\alpha(\phi^2+\gamma^2)/2\right)$$

and $$\psi_{xl0} = \left(\frac{2\alpha^2 \exp(\frac{1}{4\alpha})}{\pi}\right)^{\frac{1}{2}} \phi \exp\left(-\alpha(\phi^2+\gamma^2)/2\right)$$

The wave functions along the y axis would be identical except for the substitution $\phi - \pi/2$ for ϕ.

The problem now is to find the wave functions of the correct symmetry for the v=0 and v=1 librator states near the $\bar{C}_{4V}$ limit, and then the energies of these states. The linear combination is found using a method devised by Wigner (159, 161), which can be written as

$$\psi_n^{(\Gamma)} = N \sum_P \chi_P^{(\Gamma)} \, P\psi_{xn_\phi n_\gamma}$$

where $\chi_P^{(\Gamma)}$ is the character for the operation P of the Γ symmetry species, $P\psi_{xn_\phi n_\gamma}$ is the transformed wave function and the sum is over all P in the group. This gives the following wave functions:

$$\psi^{A}_{o}{}_{1g} = \frac{1}{\sqrt{6}} (\psi_{xoo} + \psi_{\bar{x}oo} + \psi_{yoo} + \psi_{\bar{y}oo} + \psi_{zoo} + \psi_{\bar{z}oo})$$

$$\psi^{E}_{o}{}_{g} = \frac{1}{\sqrt{12}} (2\psi_{xoo} + 2\psi_{\bar{x}oo} - \psi_{yoo} + \psi_{\bar{y}oo} + \psi_{zoo} + \psi_{\bar{z}oo})$$

$$\psi^{F}_{o}{}_{1u} = \frac{1}{\sqrt{2}} (\psi_{xoo} - \psi_{\bar{x}oo})$$

$$\psi^{F}_{1}{}_{2g} = \frac{1}{2} (\psi_{xlo} + \psi_{\bar{x}lo} - \psi_{ylo} - \psi_{\bar{y}lo})$$

$$\psi^{F}_{1}{}_{1g} = \frac{1}{2} (\psi_{xlo} + \psi_{\bar{x}lo} + \psi_{ylo} + \psi_{\bar{y}lo})$$

$$\psi^{F}_{1}{}_{1u} = \frac{1}{2} (\psi_{xol} + \psi_{\bar{x}ol} + \psi_{yol} + \psi_{\bar{y}ol})$$

$$\psi^{F}_{1}{}_{2u} = \frac{1}{2} (\psi_{xol} + \psi_{\bar{x}ol} - \psi_{yol} - \psi_{\bar{y}ol})$$

The energy of each state is found by assuming that only significant overlap occurs between the four nearest minima. The Hamiltonian in the γ, ϕ coordinates is

$$H = \frac{-\hbar^2}{2I} \left(\frac{\partial^2}{\partial\gamma^2} - \tan\gamma \frac{\partial}{\partial\gamma} + \frac{1}{\cos^2\gamma} \frac{\partial^2}{\partial\phi^2}\right) + \frac{V_o}{2} (C_4V_4 + C_6V_6).$$

We assume that the integrals involving any two minima separated by a 90° rotation are the same. With these assumptions the energies are the following:

$$E^{A}_{o}{}_{1g} = \frac{\langle \psi^{A}_{o}{}_{1g} / H / \psi^{A}_{o}{}_{1g} \rangle}{\langle \psi^{A}_{o}{}_{1g} / \psi^{A}_{o}{}_{1g} \rangle} = \frac{\alpha_o + 4\beta_o}{1 + 4\epsilon_o} = \alpha_o + 4\beta_o - 4\epsilon_o\alpha_o$$

$$E^{F}_{o}{}_{1u} = \alpha_o$$

$$E^{E}_{o}{}_{g} = \alpha_o - 2\beta_o + 2\epsilon_o\alpha_o$$

where $\alpha_o = \langle \psi_{xoo} / H / \psi_{xoo} \rangle$, $\beta_o = \langle \psi_{yoo} / H / \psi_{xoo} \rangle$

and $\epsilon_o = \langle \psi_{yoo} / \psi_{xoo} \rangle$. The denominator is expanded as $\frac{1}{1 \pm x} = 1 \mp x$ since $x \ll 1$.

Similarly $E_1^F 2g = \alpha_g - 2\beta_g + 2\epsilon_g \alpha_g$

$E_1^F 1g = \alpha_g + 2\beta_g - 2\epsilon_g \alpha_g$

where $\alpha_g = \langle \psi_{xlo} / H / \psi_{xlo} \rangle$, $\beta_g = \langle \psi_{ylo} / H / \psi_{xlo} \rangle$

and $\epsilon_g = \langle \psi_{ylo} / \psi_{xlo} \rangle$;

and $E_1^F 1u = \alpha_u + 2\beta_u - 2\epsilon_u \alpha_u$

$E_1^F 2u = \alpha_u - 2\beta_u + 2\epsilon_u \alpha_u$

where $\alpha_u = \langle \psi_{xol} / H / \psi_{xol} \rangle$, $\beta_u = \langle \psi_{yol} / H / \psi_{xol} \rangle$

and $\epsilon_u = \langle \psi_{yol} / \psi_{xol} \rangle$.

The values of all the integrals and expressions for the energies are summarized in the Appendix.

The parameter c_6 which determines the amount of the V_6 term may be varied and the energy levels can then be found for a given value of c_6 as a function of α. This is most conveniently done using GROPE (Graphical Representation of Parameterized Expressions) and a typical plot of energy levels versus α is shown in Figure 6.

The energy of the v = 1 levels is something less than $2\tilde{\nu}_L = 16\ \tilde{V}_o/\alpha$. We see then that α must be about 16 for the v = 1 levels to be below the potential barrier. The actual value of α

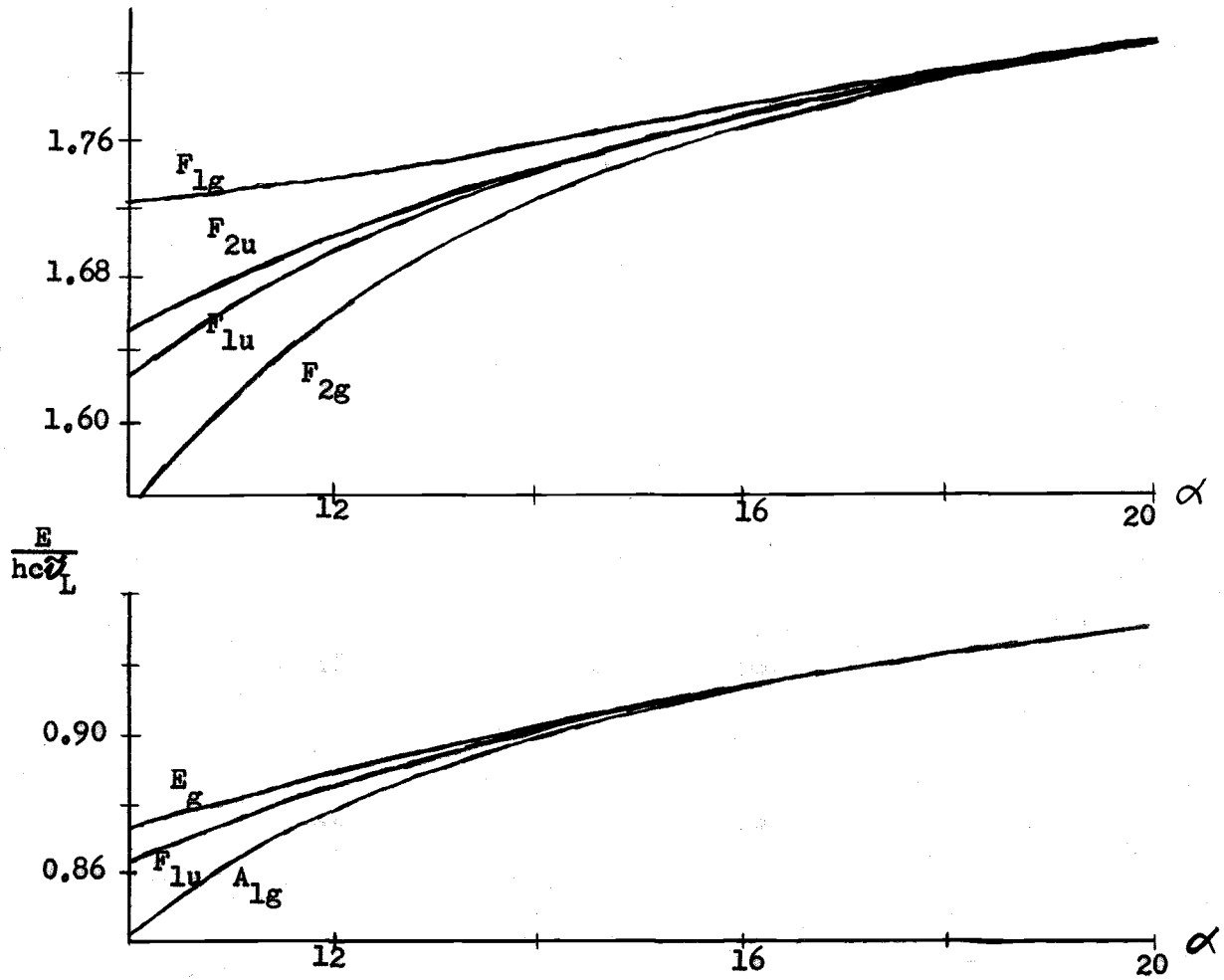

Figure 6. The v=0 and v=1 librator levels near the $\bar{\bar{C}}_{4V}$ high barrier limit for (O_h, $\bar{C}_{\infty V}$) using harmonic oscillator wave functions ($C_4 = 1$, $C_6 = 0$).

may be obtained from a graph of the v = 1 levels and $V_o = \alpha\tilde{\nu}_1/8$. The harmonic oscillator approximation for the v = 1 levels will begin to be valid for $\alpha \approx 16$ and will become better as α increases. This same discussion is relevant for the v = 0 levels and $\alpha \approx 8$ but the range of α has been from 10 to 26 so that the approximation is valid for the v = 0 levels.

The neglecting of the next nearest neighbor contributions can be seen to be small since the exponential factor is $\exp(-\alpha\pi^2/4)$ compared to $(-\alpha\pi^2/16)$. For $\alpha = 16$ this is about 10^{-17} compared to 10^{-4}. The approximation for the limits of integration can also be seen to be valid. For the overlap integral of the wave functions ψ_{xoo} and ψ_{yoo}, the substitution $\delta = \phi - \pi/4$ is made and then after integrating over γ we have

$$\langle \psi_{yoo} / \psi_{xoo} \rangle = \left(\frac{\alpha}{\pi}\right)^{\frac{1}{2}} \int_{-\pi/4}^{\pi/4} \exp\left(-\alpha\left(\delta^2 + \pi^2/16\right)\right) d\delta$$

and the integrand is found to be $\exp(-\alpha\pi^2/8)$ at the limits of integration. For $\alpha = 16$, $\exp(-\alpha\pi^2/8)$ is $\sim 10^{-9}$ which is negligible compared to the value of the integral of $\sim 10^{-4}$. So $\pm\pi/4$ can be replaced by $\pm\infty$ and we assume that $\langle \psi_{yoo} / \psi_{xoo} \rangle = \exp(-\alpha\pi^2/16)$.

This method is seen to be complementary to the method used by Devonshire (35). While the energies near the free rotor limit cannot be found, those near the high barrier limit can be found more easily.

5. Linear XY_2 Molecules in an O_h Field

The extended permutation group for $\bar{D}_{\infty h}$ (18, 19) is used for

the molecule so it is more convenient to write $G = {}'O' \times {}'D_{\infty h}'$ and retain the symmetry species of the molecule. The difference between linear molecules and diatomics can be illustrated by looking at $G = (O_h, \bar{D}_{\infty h})$ and $\bar{\bar{H}} = \bar{\bar{D}}_{4h}$ (Figure 7). The correlation from $\bar{\bar{D}}_{4h}$ to $(O_h, \bar{D}_{\infty h})$ for the ground librator state is the following for states including $\bar{\Delta}$ terms:

$$A_{1g} \longrightarrow A_1\bar{\bar{\Sigma}}_g^+ + F_1\bar{\bar{\Sigma}}_g^- + F_1\bar{\Pi}_g + E\bar{\bar{\Sigma}}_g^+ + F_2\bar{\Pi}_g + E\bar{\Delta}_g + F_2\bar{\Delta}_g.$$

Also, $\Gamma(\mu) = F_1\bar{\bar{\Sigma}}_u^-$ and $\Gamma(\alpha) = A_1\bar{\bar{\Sigma}}_g^+ + E\bar{\bar{\Sigma}}_g^+ + F_2\bar{\bar{\Sigma}}_g^+$.

The symmetry requirements for the various wave functions are more difficult to recognize using the notation from $\bar{D}_{\infty h}$. If Y is a boson the overall wave function must be symmetric to $(\overline{12})$ ($\Gamma\bar{\bar{\Sigma}}_g^+$ or $\Gamma\bar{\bar{\Sigma}}_u^-$ where Γ is any symmetry species from O). Similarly if Y is a fermion the overall wave function is $\Gamma\bar{\bar{\Sigma}}_g^-$ or $\Gamma\bar{\bar{\Sigma}}_u^+$. The nuclear spin symmetries are $A_1\bar{\bar{\Sigma}}_g^+$ (ortho) and $A_1\bar{\bar{\Sigma}}_u^+$ (para). Assuming a vibronic state of symmetry $A_1\bar{\bar{\Sigma}}_g^+$, then ortho (para) molecules must be in $\bar{\bar{\Sigma}}_g^+$ or $\bar{\bar{\Sigma}}_u^-$ ($\bar{\bar{\Sigma}}_g^-$ or $\bar{\bar{\Sigma}}_u^+$) rotational states for Y a boson, and $\bar{\bar{\Sigma}}_g^-$ or $\bar{\bar{\Sigma}}_u^+$ ($\bar{\bar{\Sigma}}_g^+$ or $\bar{\bar{\Sigma}}_u^-$) rotational states for Y a fermion. In this example there is a center of symmetry in both O_h and $\bar{D}_{\infty h}$, so the rotational states have only g symmetry.

In discussing the possible types of transitions which can occur, it is convenient to distinguish between two classes of transitions involving the librational modes. In the first category we have those for which the librational quantum number, which becomes an oscillator quantum number in the high barrier limit, does not change, but in which a transition between levels for a

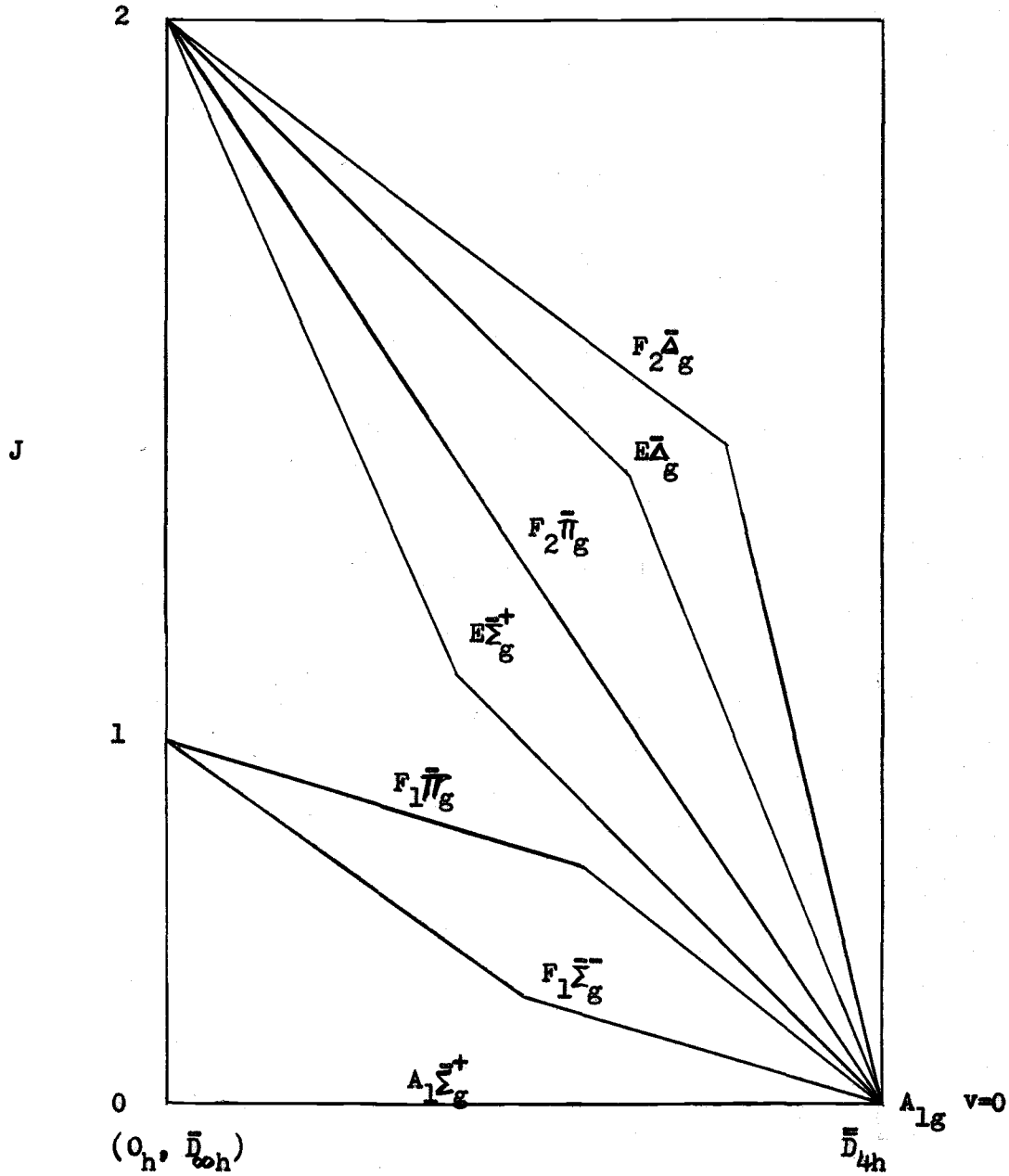

Figure 7. Correlation of rotational energy levels for a linear rotor from the $(O_h, \bar{D}_{\infty h})$ free rotor limit to the $\bar{\bar{D}}_{4h}$ librator limit.

single librational state split by tunneling does occur. One could speak of these as tunneling transitions (24), but for convenience, we propose to describe such transitions as "orientation" transitions. In the second category, there are changes in the librational quantum numbers: these will be described simply as "librational" transitions. Thus we may speak about pure orientation, pure libration, vibration-orientation, or vibration-libration transitions, reserving the latter two terms for cases in which an internal vibration undergoes a transition simultaneously with changes in the rotational states.

The vibration-orientation transitions are listed in Table V for ν_1 (Raman) and ν_2 and ν_3 (infrared). The linear motions involve only the Σ_g^+ levels and could be understood from the diatomic examples. The non-linear ν_2 fundamental involves the Π_g rotational levels. The Coriolis effect is ignored for this case.

TABLE V. ALLOWED VIBRATION-ORIENTATION TRANSITIONS BETWEEN LIBRATIONAL STATES FOR A LINEAR XY_2 MOLECULE IN AN OCTAHEDRAL FIELD NEAR THE $\bar{\bar{D}}_{4h}$ HIGH BARRIER LIMIT.

A. $\nu_1(A_1\bar{\bar{\Sigma}}_g^+)$ Raman transitions

$A_1\bar{\bar{\Sigma}}_g^+ \longrightarrow A_1\bar{\bar{\Sigma}}_g^+,\ E\bar{\bar{\Sigma}}_g^+$

$F_1\bar{\bar{\Sigma}}_g^- \longrightarrow F_1\bar{\bar{\Sigma}}_g^-$

$E\bar{\bar{\Sigma}}_g^+ \longrightarrow A_1\bar{\bar{\Sigma}}_g^+,\ E\bar{\bar{\Sigma}}_g^+$

B. $\nu_2(A_1\bar{\bar{\Pi}}_u)$ Infrared transitions

$A_1\bar{\bar{\Sigma}}_g^+ \longrightarrow F_1\bar{\bar{\Pi}}_g$

$F_1\bar{\bar{\Sigma}}_g^- \longrightarrow F_1\bar{\bar{\Pi}}_g,\ F_2\bar{\bar{\Pi}}_g$

$E\bar{\bar{\Sigma}}_g^+ \longrightarrow F_1\bar{\bar{\Pi}}_g,\ F_2\bar{\bar{\Pi}}_g$

C. $\nu_3(A_1\bar{\bar{\Sigma}}_u^+)$ Infrared transitions

$A_1\bar{\bar{\Sigma}}_g^+ \longrightarrow F_1\bar{\bar{\Sigma}}_g^-$

$F_1\bar{\bar{\Sigma}}_g^- \longrightarrow A_1\bar{\bar{\Sigma}}_g^+,\ E\bar{\bar{\Sigma}}_g^+$

$E\bar{\bar{\Sigma}}_g^+ \longrightarrow F_1\bar{\bar{\Sigma}}_g^-$

C. The Symmetric Rotor

1. A $\bar{C}_{3V}$ Molecule in a C_3 Field

For this example $\bar{M} = \bar{C}_{3V}$, $S = C_3$ and since S is a rotational group, then $G = 'S' \times '\bar{M}'(P) = 'C_3' \times '\bar{C}_3'$. The greatest common subgroup of C_{3V} and C_3 is C_3 so at the librator limit we assume $\bar{\bar{H}} = \bar{\bar{C}}_3$. If we let $S = \{E, (123), (132)\}$ and $\bar{M}(P) = \{\bar{E}, (\overline{123}), (\overline{132})\}$ then $\bar{\bar{H}} = \{E\bar{E}, (123)(\overline{123}), (132)(\overline{132})\}$. The character table and correlation between G and $\bar{\bar{H}}$ is given in Table VI. For convenience we let $E = E_+ + E_-$, $E_o = E_+\bar{E}_- + E_-\bar{E}_+$, and $E_2 = E_+\bar{E}_+ + E_-\bar{E}_-$.

The first excited librator states are of symmetry A + E in the group $\bar{\bar{C}}_3$. At the free rotor limit the wave functions are labeled by JKM. The appropriate symmetry is A or $\bar{A}$ if M or K is a multiple of 3 and E or $\bar{E}$ otherwise. Figure 8 is a qualitative example of the correlation of librational energy levels for an oblate symmetric rotor from the free rotor to the high barrier limit.

An A state in $\bar{\bar{C}}_3$ corresponds to $A\bar{A} + E_o$ in G, and an E state in $\bar{\bar{C}}_3$ corresponds to $A\bar{E} + E\bar{A} + E_2$ in G. The symmetry of both μ and α in external axes is $A\bar{A} + E\bar{A}$ so the selection rules are the same for infrared and Raman transitions. Near the librator limit there are two transitions allowed to the $v_z = 1$ level ($A\bar{A} \longrightarrow A\bar{A}$, $E_o \longrightarrow E_o$), and three transitions allowed to the $v_{x,y} = 1$ level ($A\bar{A} \longrightarrow E\bar{A}$, $E_o \longrightarrow A\bar{E}$, E_2). For $\bar{A}$ vibrations the selection rules for vibration-libration transitions are the same as for the pure librations. The orientation transitions with an $\bar{A}$ vibration are

TABLE VI. THE CHARACTER TABLE FOR $(C_3, \bar{C}_{3V})$ AND CORRELATION TO THE GROUP $\bar{\bar{C}}_3$.

$(C_3, \bar{C}_{3V})$	$\bar{E}\bar{E}$	$(123)\bar{E}$	$(132)\bar{E}$	$E(\overline{123})$	$(123)(\overline{123})$	$(132)(\overline{123})$	$E(\overline{132})$	$(123)(\overline{132})$	$(132)(\overline{132})$	$e=\exp(\frac{2\pi i}{3})$		$\bar{\bar{C}}_3$
$A\bar{A}$	1	1	1	1	1	1	1	1	1	μ_z	$\alpha_{xx}+\alpha_{yy}, \alpha_{zz}$	A
$E\bar{A}$	1	e	e*	1	e	e*	1	e	e*	(μ_x, μ_y)	$(\alpha_{xx}-\alpha_{yy}, \alpha_{xy}), (\alpha_{yz}, \alpha_{xz})$	E
	1	e*	e	1	e*	e	1	e*	e			
$A\bar{E}$	1	1	1	e	e	e	e*	e*	e*			E
	1	1	1	e*	e*	e*	e	e	e			
E_o	1	e	e*	e*	1	e	e	e*	1			2A
	1	e*	e	e	1	e*	e*	e	1			
E_2	1	e	e*	e	e*	1	e*	1	e			E
	1	e*	e	e*	e	1	e	1	e*			

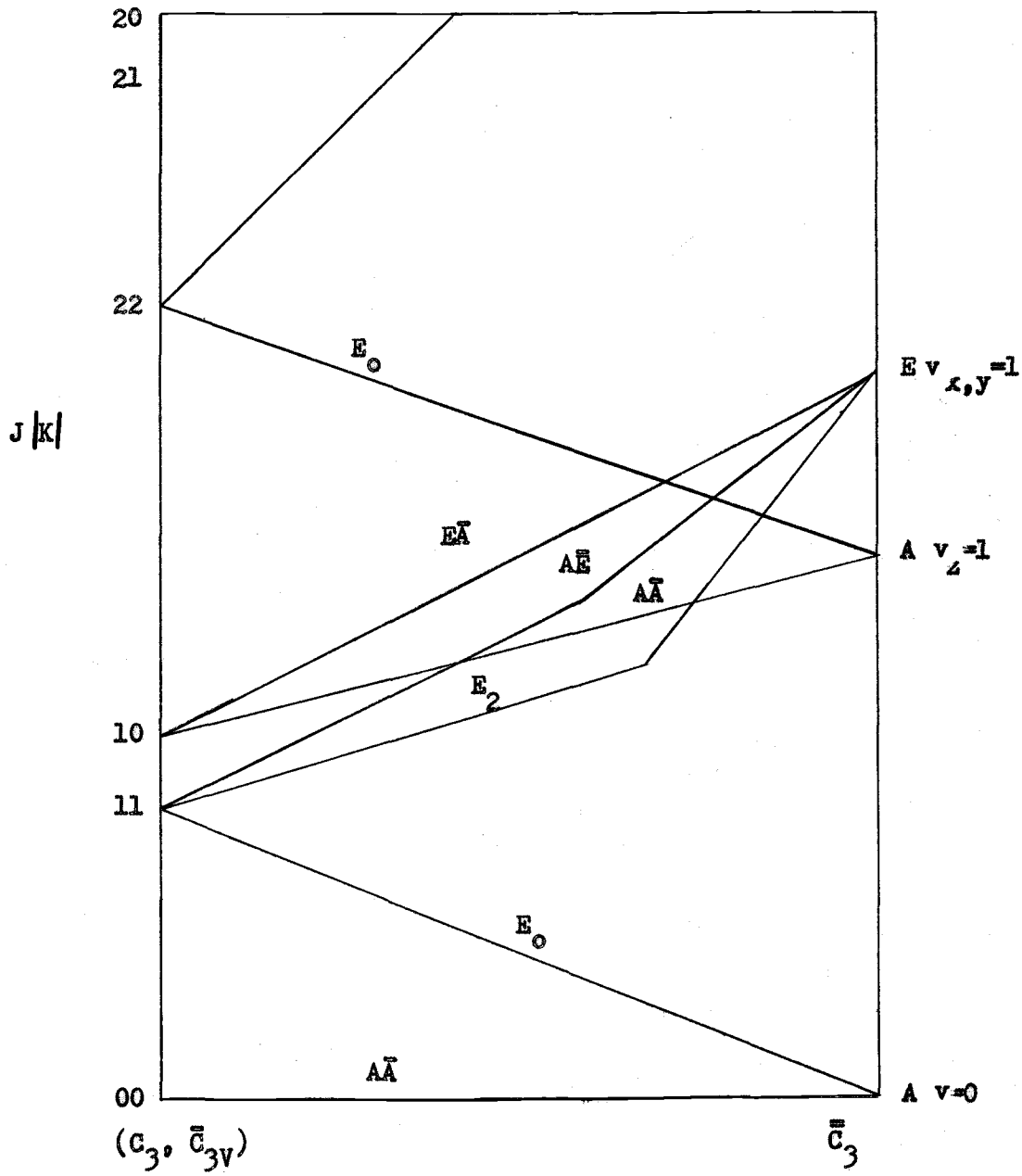

Figure 8. Correlation of rotational energy levels for an oblate symmetric rotor from the $(C_3, \bar{C}_{3v})$ free rotor limit to the $\bar{C}_3$ librator limit.

simply $A\bar{A} \longrightarrow A\bar{A}$ and $E_o \longrightarrow E_o$. For $\bar{E}$ vibrations the vibration-orientation transitions are $A\bar{A} \longrightarrow E_o$; $E_o \longrightarrow A\bar{A}$, E_o. Also, there are three vibration-libration transitions allowed to the $v_z = 1$ level ($A\bar{A} \longrightarrow E_o$; $E_o \longrightarrow A\bar{A}$, E_o) and five to the $v_{x,y} = 1$ level ($A\bar{A} \longrightarrow A\bar{E}$, E_2; $E_o \longrightarrow A\bar{E}$, $E\bar{A}$, E_2) for an $\bar{E}$ vibration.

Assuming an XY_3 molecule the nuclear spin states have the symmetry $A\bar{A}$ for $I_Y = 0$, $4A\bar{A} + 2A\bar{E}$ for $I_Y = 1/2$ and $11\ A\bar{A} + 8A\bar{E}$ for $I_Y = 1$ (160). Since the operations $\bar{E}$, $(\overline{123})$, and $(\overline{132})$ are all products of an even number of transpositions both bosons and fermions have the symmetry requirements that the overall wave function is $\Gamma\bar{A}$ where Γ can be A or E. Assuming a vibronic symmetry of $\bar{A}$, the symmetry of the rotational states is $\bar{A}$ for $\bar{A}$ nuclear spin and $\bar{E}$ for $\bar{E}$ nuclear spins. Thus the ground librator state has a state for $\bar{A}$ spin molecules ($A\bar{A}$) and a state for $\bar{E}$ spin molecules (E_o). Again, as in the linear case, the frequencies differ for molecules with different nuclear spin symmetry.

An example of this type of symmetry is found in NH_3 or ND_3 crystals where the space group is T^4 ($P2_13$) (111). A system appropriate for this discussion would be ND_3 isolated in an NH_3 crystal or vice versa. Rotation in the ammonia crystal is presumably hindred by the extensive hydrogen bonding. Although the external mode spectrum of ammonia has been studied quite extensively in the far-infrared (1) and in the Raman effect (117, 125) an unequivocal assignment of the librational modes is not at present possible. The symmetry species of such modes in the unit cell of T symmetry are:

molecular z axis: A + F,

molecular x,y axes: E + 2F.

Two librational modes, necessarily of F symmetry, have been found in the infrared, and two of undetermined symmetry, one presumably being of E symmetry, in the Raman. Recent unpublished work in this laboratory suggests that when the Raman observations are made under the same conditions of temperature and crystallinity as the infrared, at least one Raman mode is coincident with an infrared mode. This seems to indicate that the intensity due to libration about the z axis may be too small to be seen in either the Raman effect or the infrared.

Another possible example where this symmetry may be appropriate and where rotational motion may occur is PH_3 isolated in PD_3 and vice versa, although the structures of the various solid phases of phosphine are uncertain (73). If we assume a structure similar to ammonia then we can apply the symmetry considerations in this section. If the most intense transitions for an $A\bar{E}$ vibration are the orientation transitions one would expect a triplet ($A\bar{A} \longrightarrow E_o$, $E_o \longrightarrow A\bar{A}$, E_o). The orientation transitions for an $A\bar{A}$ vibration result in a single line ($A\bar{A} \longrightarrow A\bar{A}$, $E_o \longrightarrow E_o$). Assuming the librations about the molecular x and y axes to be more intense as in ammonia, the vibration-libration spectrum would consist of three lines ($A\bar{A} \longrightarrow E\bar{A}$; $E_o \longrightarrow E_2$, $A\bar{E}$). Since the orientation transition $A\bar{A} \longrightarrow A\bar{A}$ is not allowed at the free rotor limit the vibration-libration spectrum may be strong for an $A\bar{A}$ vibration. The infrared spectra of PH_3 in PD_3 and vice versa have been recorded by Huang (73).

For PH_3 isolated in PD_3 he observed a doublet split by 3 cm^{-1} for ν_2 (A_1), and a triplet over 5 cm^{-1} for ν_4 (E). For PD_3 isolated in PH_3 both ν_2 and ν_4 were a single broad feature. A possible explanation of these spectra is that ν_2 is a vibration-libration spectrum and ν_4 is a vibration-orientation spectrum. This would explain the loss in structure for the PD_3 spectra since the splittings would be smaller. This is given as a tentative explanation and a knowledge of the crystal structures would be needed before more definite statements could be made.

2. A $\bar{D}_{3h}$ Molecule in a D_3 Field

Since S is a rotational group, G is the direct product of two rotational groups, so G = 'D_3' x '$\bar{D}_3$'. The group at the high barrier limit is taken to be $\bar{\bar{D}}_3$. The correlation between states in $\bar{\bar{D}}_3$ and (D_3, $\bar{D}_{3h}$) is

$$A_1 \longrightarrow A_1\bar{A}_1 + A_2\bar{A}_2 + E\bar{E},$$

$$A_2 \longrightarrow A_1\bar{A}_2 + A_2\bar{A}_1 + E\bar{E},$$

and $$E \longrightarrow A_1\bar{E} + A_2\bar{E} + E\bar{A}_1 + E\bar{A}_2 + E\bar{E}.$$

The first excited librator states in $\bar{\bar{D}}_3$ are of symmetry $A_2 + E$. An energy level diagram is shown in Figure 9. The rules for K and M are the same for finding the symmetry of the free rotor states. For K = 0 the symmetry is $\bar{A}_1$ or $\bar{A}_2$ as J is even or odd, for K a multiple of 3 the symmetry is $\bar{A}_1 + \bar{A}_2$, and it is $\bar{E}$ otherwise (160).

In external axes, $\Gamma(\mu) = A_2\bar{A}_1 + E\bar{A}_1$ and $\Gamma(\alpha) = 2A_1\bar{A}_1 + 2E\bar{A}_1$;

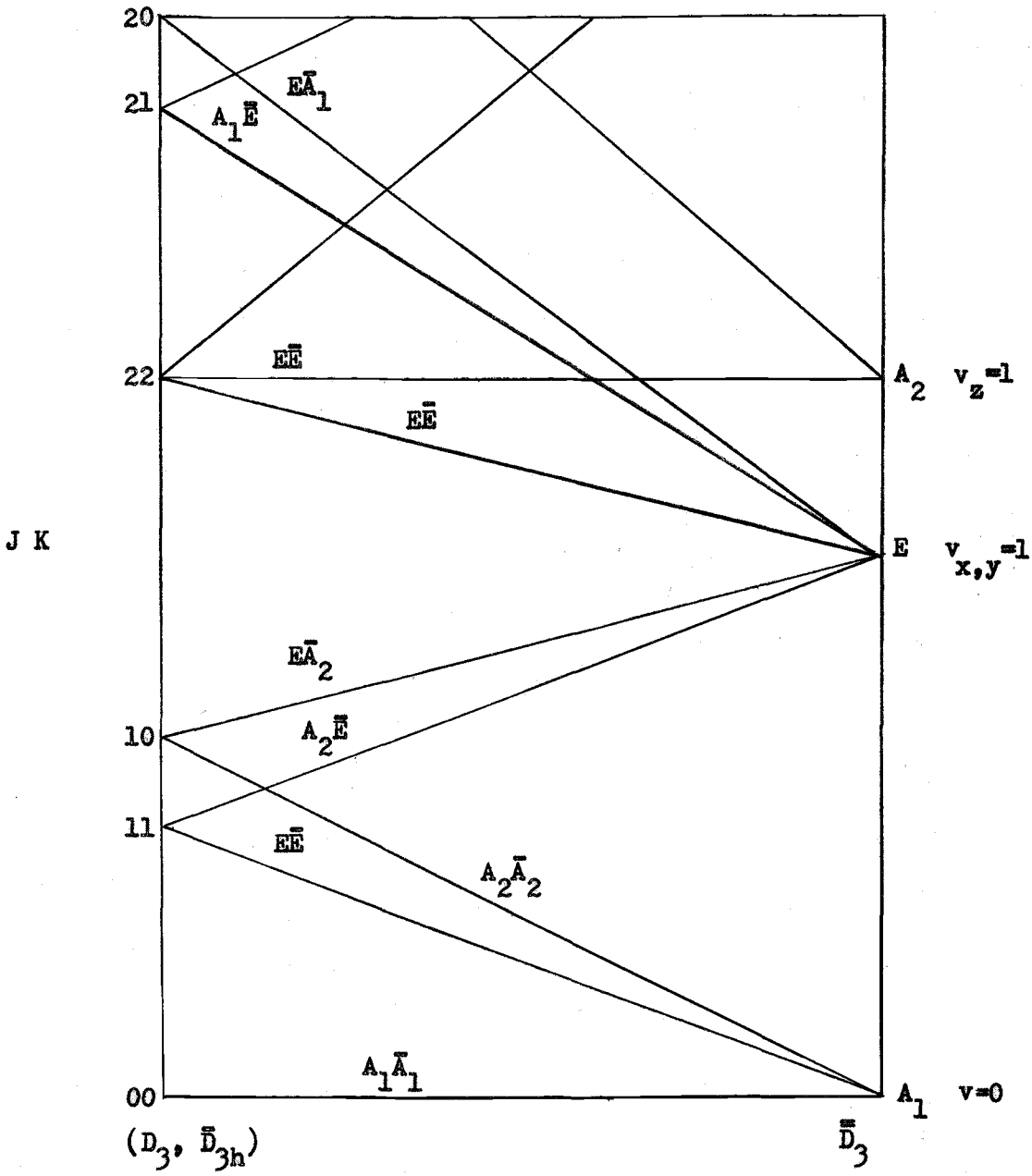

Figure 9. Correlation of rotational energy levels for an oblate symmetric rotor from the $(D_3, \bar{D}_{3h})$ free rotor limit to the $\bar{D}_3$ librator limit.

in internal axes $\Gamma(\mu) = A_1\bar{A}_2 + A_1\bar{E}$ and $\Gamma(\alpha) = 2A_1\bar{A}_1 + 2A_1\bar{E}$. Although a D_{3h} molecule has no equilibrium dipole moment at a D_3 site, librational transitions are permitted according to $\Gamma(\mu)$ in external coordinates, presumably due to interaction of the molecule with the surrounding crystal. The allowed infrared librational transitions near the librator limit for v = 0 to the $v_z = 1$, A_2 level, are $A_1\bar{A}_1 \longrightarrow A_2\bar{A}_1$, $A_2\bar{A}_2 \longrightarrow A_1\bar{A}_2$, and $E\bar{E} \longrightarrow E\bar{E}$, whereas only the $E\bar{E} \longrightarrow E\bar{E}$ is Raman allowed. The allowed transitions to the $v_{x,y} = 1$, E level, in both the infrared and Raman are $A_1\bar{A}_1 \longrightarrow E\bar{A}_1$, $A_2\bar{A}_2 \longrightarrow E\bar{A}_2$ and $E\bar{E} \longrightarrow A_1\bar{E}$, $A_2\bar{E}$, $E\bar{E}$.

Assuming an XY_3 molecule the nuclear spin wave functions are $A_1\bar{A}_1$ for $I_Y = 0$, $4A_1\bar{A}_1 + 2A_1\bar{E}$ for $I_Y = 1/2$, and $10\,A_1\bar{A}_1 + A_1\bar{A}_2 + 8A_1\bar{E}$ for $I_Y = 1$ (160). The overall wave function must be $\Gamma\bar{A}_1$ for Y a boson and $\Gamma\bar{A}_2$ for Y a fermion, where Γ can be A_1, A_2, or E. If the vibronic symmetry is $\bar{A}_1$, for $I_Y = 0$ only the $\Gamma\bar{A}_1$ librational states can exist. Similarly, for $I_Y = 1/2$ the librational states can be $\Gamma\bar{A}_2$ and $\Gamma\bar{E}$ with statistical weights of 4 and 2 respectively. If $I_Y = 1$ the librational states of symmetries $\Gamma\bar{A}_1$, $\Gamma\bar{A}_2$, and $\Gamma\bar{E}$ will be occupied with relative statistical weights 10:1:8.

The vibrational activity in the infrared and Raman effect follows the selection rules of the internal axes as a first approximation. The overall transition is governed by the selection rules in the external axes and some vibration-orientation or vibration-libration transitions may be formally allowed but would be expected to be weak. From the symmetry of μ in internal axes we see that

$A_1\bar{A}_2$ and $A_1\bar{E}$ vibrations are allowed in the infrared. Assuming the electronic symmetry to be $A_1\bar{A}_1$, the orientation transitions for an $A_1\bar{A}_2$ vibration must be $A_1\bar{A}_1 \longrightarrow A_2\bar{A}_2$ for $I_Y = 0$, $A_2\bar{A}_2 \longrightarrow A_1\bar{A}_1$ and $E\bar{E} \longrightarrow E\bar{E}$ for $I_Y = 1/2$, and all three of these for $I_Y = 1$ because of the nuclear spin requirements. So if the splittings in the ground state are large enough to be observed, the spectra would be a singlet, doublet, and triplet. Similarly the vibration-orientation spectra for an $A_1\bar{E}$ vibration would be a singlet for $I_Y = 0$ ($A_1\bar{A}_1 \longrightarrow E\bar{E}$), a quartet for $I_Y = 1/2$ ($E\bar{E} \longrightarrow A_1\bar{A}_1$, $E\bar{E}$, $A_2\bar{A}_2$ and $A_2\bar{A}_2 \longrightarrow E\bar{E}$) and a quintet for $I_Y = 1$ (all five transitions). Relative intensities can be assigned to vibration-orientation transitions from the nuclear spin statistical weights. In the Raman effect both $A_1\bar{A}_1$ and $A_1\bar{E}$ vibrations are allowed. The orientation transitions allowed with an $A_1\bar{A}_1$ vibration are only those to the same librational state so one would expect a single line for any nuclear spin. An $A_1\bar{E}$ vibration would follow the same selection rules in the Raman effect as in the infrared.

Example of this type of symmetry are found in the calcite family where the space group is D^6_{3d} (R3c) (164). However, the librator frequencies for motion about the threefold molecular axis have been assigned as 51 cm^{-1} in $NaNO_3$ and 92 cm^{-1} in $CaCO_3$ (65) which would imply a barrier (see Section III.F) so high that the splittings would be utterly negligible.

3. A $\bar{D}_{3h}$ Molecule in an O_h Field

Both S and $\bar{M}$ are direct product groups so there are two ways to

express G. In order to preserve the symmetry species of the molecule we choose G = '0' x '$\bar{D}_{3h}$'. This choice is also consistent with the rotational group for G which is '0' x '$\bar{D}_6$'. The largest group at a high barrier limit could be either $\bar{\bar{D}}_3$ or $\bar{\bar{C}}_{3V}$. The correlation between states in $\bar{\bar{D}}_3$ or $\bar{\bar{C}}_{3V}$ and states in (O_h, $\bar{D}_{3h}$) is given in Table VII. The first excited librator states in both $\bar{\bar{D}}_3$ and $\bar{\bar{C}}_{3V}$ are of symmetry $A_2 + E$. By knowing the symmetry of states at the free rotor limit, one can make an energy level diagram to either librator limit. The symmetry of states in O is given in Table III of King and Hornig (87). The Q group for $\bar{D}_{3h}$ is $\bar{D}_6$ and the symmetry of states in $\bar{D}_6$ was done by Wilson (160). The correspondence between symmetry species of $\bar{D}_6$ and $\bar{D}_{3h}$ is the following: $\bar{A}_1 \longrightarrow \bar{A}_1'$, $A_2 \longrightarrow \bar{A}_2'$, $\bar{E}' \longrightarrow \bar{E}^*$, $\bar{B}_1 + \bar{B}_2 \longrightarrow \bar{A}_1'' + \bar{A}_2''$, $\bar{E}'' \longrightarrow \bar{E}_*^*$. Now the symmetry of states in $\bar{D}_{3h}$ can be found from Table XV of Wilson (160).

Selection rules can be found by noting that in external axes $\Gamma(\mu) = F_1\bar{A}_1''$ and $\Gamma(\alpha) = A_1\bar{A}_1' + E\bar{A}_1' + F_2\bar{A}_1'$, while in internal axes $\Gamma(\mu) = A_1\bar{A}_2'' + A_1\bar{E}'$ and $\Gamma(\alpha) = 2A_1\bar{A}_1' + A_1\bar{E}' + A_1\bar{E}''$.

Assuming an XY_3 molecule the nuclear spin wave functions are $A_1\bar{A}_1'$ for $I_Y = 0$, $4A_1\bar{A}_1' + 2A_1\bar{E}'$ for $I_Y = 1/2$, and $10\ A_1\bar{A}_1' + A_1\bar{A}_2' + 8\ A_1\bar{E}'$ for $I_Y = 1$. The overall wave function must be $\Gamma\bar{A}_1'$ or $\Gamma\bar{A}_1''$ for Y a boson and $\Gamma\bar{A}_2'$ or $\Gamma\bar{A}_2''$ for Y a fermion where Γ is any symmetry species from O. The discussion of symmetry requirements is the same as for (D_3, $\bar{D}_{3h}$) where either ' or '' may modify the molecular symmetry species.

An example of this type of symmetry is found for the methyl

TABLE VII. CORRELATION OF $\bar{\bar{D}}_3$ AND $\bar{\bar{C}}_{3V}$ WITH (O_h, $\bar{D}_{3h}$).

$\bar{\bar{D}}_3$	(O_h, $\bar{D}_{3h}$)
A_1	$A_1\bar{A}_1' + F_2\bar{A}_1' + A_2\bar{A}_2' + F_1\bar{A}_2' + E\bar{E}'$ $+ F_1\bar{E}' + F_2\bar{E}' + A_1\bar{A}_1'' + F_2\bar{A}_1'' + A_2\bar{A}_2''$ $+ F_1\bar{A}_2'' + E\bar{E}'' + F_1\bar{E}'' + F_2\bar{E}''$
A_2	$A_2\bar{A}_1' + F_1\bar{A}_1' + A_1\bar{A}_2' + F_2\bar{A}_2' + E\bar{E}'$ $+ F_1\bar{E}' + F_2\bar{E}' + A_2\bar{A}_1'' + F_1\bar{A}'' + A_1\bar{A}_2''$ $+ F_2\bar{A}_2'' + E\bar{E}'' + F_1\bar{E}'' + F_2\bar{E}''$
E	$E\bar{A}_1' + F_1\bar{A}_1' + F_2\bar{A}_1' + E\bar{A}_2' + F_1\bar{A}_2' + F_2\bar{A}_2' + A_1\bar{E}'$ $+ A_2\bar{E}' + E\bar{E}' + 2F_1\bar{E}' + 2F_2\bar{E}' + E\bar{A}_1'' + F_1\bar{A}_1'' + F_2\bar{A}_1''$ $+ E\bar{A}_2'' + F_1\bar{A}'' + F_2\bar{A}_2'' + A_1\bar{E}'' + A_2\bar{E}'' + E\bar{E}'' + 2F_1\bar{E}'' + 2F_2\bar{E}''$

$\bar{\bar{C}}_{3V}$	(O_h, $\bar{D}_{3h}$)
A_1	$A_1\bar{A}_1' + F_2\bar{A}_1' + A_2\bar{A}_2' + F_1\bar{A}_2' + E\bar{E}' + F_1\bar{E}' + F_2\bar{E}'$ $+ A_2\bar{A}_1'' + F_1\bar{A}_1'' + A_1\bar{A}_2'' + F_2\bar{A}_2'' + E\bar{E}'' + F_1\bar{E}'' + F_2\bar{E}''$
A_2	$A_2\bar{A}_1' + F_1\bar{A}_1' + A_1\bar{A}_2' + F_2\bar{A}_2' + E\bar{E}' + F_1\bar{E}' + F_2\bar{E}'$ $+ A_1\bar{A}_1'' + F_2\bar{A}_1'' + A_2\bar{A}_2'' + F_1\bar{A}_2'' + E\bar{E}'' + F_1\bar{E}'' + F_2\bar{E}''$
E	$E\bar{A}_1' + F_1\bar{A}_1' + F_2\bar{A}_1' + E\bar{A}_2' + F_1\bar{A}_2' + F_2\bar{A}_2' + A_1\bar{E}' + A_2\bar{E}'$ $+ E\bar{E}' + 2F_1\bar{E}' + 2F_2\bar{E}' + E\bar{A}_1'' + F_1\bar{A}_1'' + F_2\bar{A}_1'' + E\bar{A}_2''$ $+ F_1\bar{A}_2'' + F_2\bar{A}_2'' + A_1\bar{E}'' + A_2\bar{E}'' + E\bar{E}'' + 2F_1\bar{E}'' + 2F_2\bar{E}''$

radical, CH_3 or CD_3, in an argon lattice. If one assumes a repulsion between argon atoms and protons or deuterons, then the high barrier limit has the symmetry $\bar{\bar{C}}_{3V}$. In an area near the high barrier limit the approximate energy levels for the ground librational state may be determined by using the appropriate linear combination of wave functions at the 48 minima for the librational state wave function. The assumption is made that only the smallest rotations in the group will contribute and these are rotations of 60° about the molecular threefold axis and 90° about a fourfold crystal axis. There are three different nonzero matrix elements for the wave functions at the 48 minima. The diagonal contribution is denoted by E_o, the matrix element between minima separated by a 60° rotation is denoted by α, and the matrix element is β for minima separated by a 90° rotation. Now the energy for a librational state of definite symmetry may be found in terms of E_o, α, and β by using the advanced methods of group theory found in Molecular Vibrations, Section 6-6 (161). These methods illustrate how to find the force constants for symmetry coordinates by knowing only the first row of the general F matrix and using only a single representative of a degenerate symmetry coordinate set. These two problems are exactly analogous. The number of operations in each class which represent a relative rotation of 60° or 90° and the character table is all that is needed. A further description will be found in the Appendix.

The A_1 librational ground state in $\bar{\bar{C}}_{3V}$ is made up of fourteen states in (O_h, $\bar{D}_{3h}$). The quantity E_o is common to the energy of all states so the relative energies in terms of α and β are given for

these states in Table VIII. The quantities α and β are assumed to be negative due to the contribution of the kinetic energy term so the lowest state has the symmetry $A_1\bar{A}_1'$ as one would expect. An energy diagram is shown in Figure 10 where for convenience we have chosen $\alpha=\beta$. The allowed transitions can be determined from the symmetries of μ and α in a manner previously described. Calculations similar to those in Section III.B.4 near the high barrier limit for α and β could be done but would require an estimate of the potential function and would need to be very elaborate. The frequency pattern may be determined in most cases without explicitly finding values for α and β.

The infrared work by Milligan and Jacox (101) shows the out-of plane bending mode (ν_2) for CH_3 and deuterated analogs in Ar. The evidence for rotation is from the structure in the ν_2 band of CH_3 which has reversible intensity changes with temperature. The band from CH_2D has three components but it is not clear whether this is due to rotational motion or not. The bands from CHD_2 and CD_3 consist of one rather broad feature.

The ν_2 vibration has the symmetry $A_1\bar{A}_2''$ so allowed orientation transitions are those which change by the symmetry $\Gamma(\mu) \times \Gamma(\nu_2) = F_1\bar{A}_1'' \times A_1\bar{A}_2'' = F_1\bar{A}_2'$. The ground vibronic state has the symmetry $A_1\bar{A}_2''$ (68) and since the total wave function must be $\Gamma\bar{A}_2'$ or $\Gamma\bar{A}_2''$ for CH_3, the rotational symmetry must be $\Gamma\bar{A}_1'$ or $\Gamma\bar{A}_1''$ for $A_1\bar{A}_1'$ nuclear spin symmetry and $\Gamma\bar{E}'$ or $\Gamma\bar{E}''$ for $A_1\bar{E}'$ nuclear spin. Assuming only the lowest levels are populated for each nuclear spin species from Figure 10 gives allowed orientation transitions for CH_3 of

TABLE VIII. THE RELATIVE HIGH BARRIER ENERGIES OF LIBRATIONAL STATES FROM (O_h, $\bar{D}_{3h}$) FORMING THE GROUND LIBRATIONAL STATE IN $\bar{\bar{C}}_{3v}$.

Symmetry	Energy
$A_1\bar{A}_1'$	$2\alpha + 6\beta$
$F_2\bar{A}_1'$	$2\alpha - 2\beta$
$A_2\bar{A}_2'$	$2\alpha - 6\beta$
$F_1\bar{A}_2'$	$2\alpha + 2\beta$
$E\bar{E}'$	$-\alpha$
$F_1\bar{E}'$	$-\alpha + \beta$
$F_2\bar{E}'$	$-\alpha - 2\beta$
$A_2\bar{A}_1''$	$-2\alpha - \beta$
$F_1\bar{A}_1''$	$-2\alpha + 2\beta$
$A_1\bar{A}_2''$	$-2\alpha + 6\beta$
$F_2\bar{A}_2''$	$-2\alpha - 2\beta$
$E\bar{E}''$	α
$F_1\bar{E}''$	$\alpha + 2\beta$
$F_2\bar{E}''$	$\alpha - 2\beta$

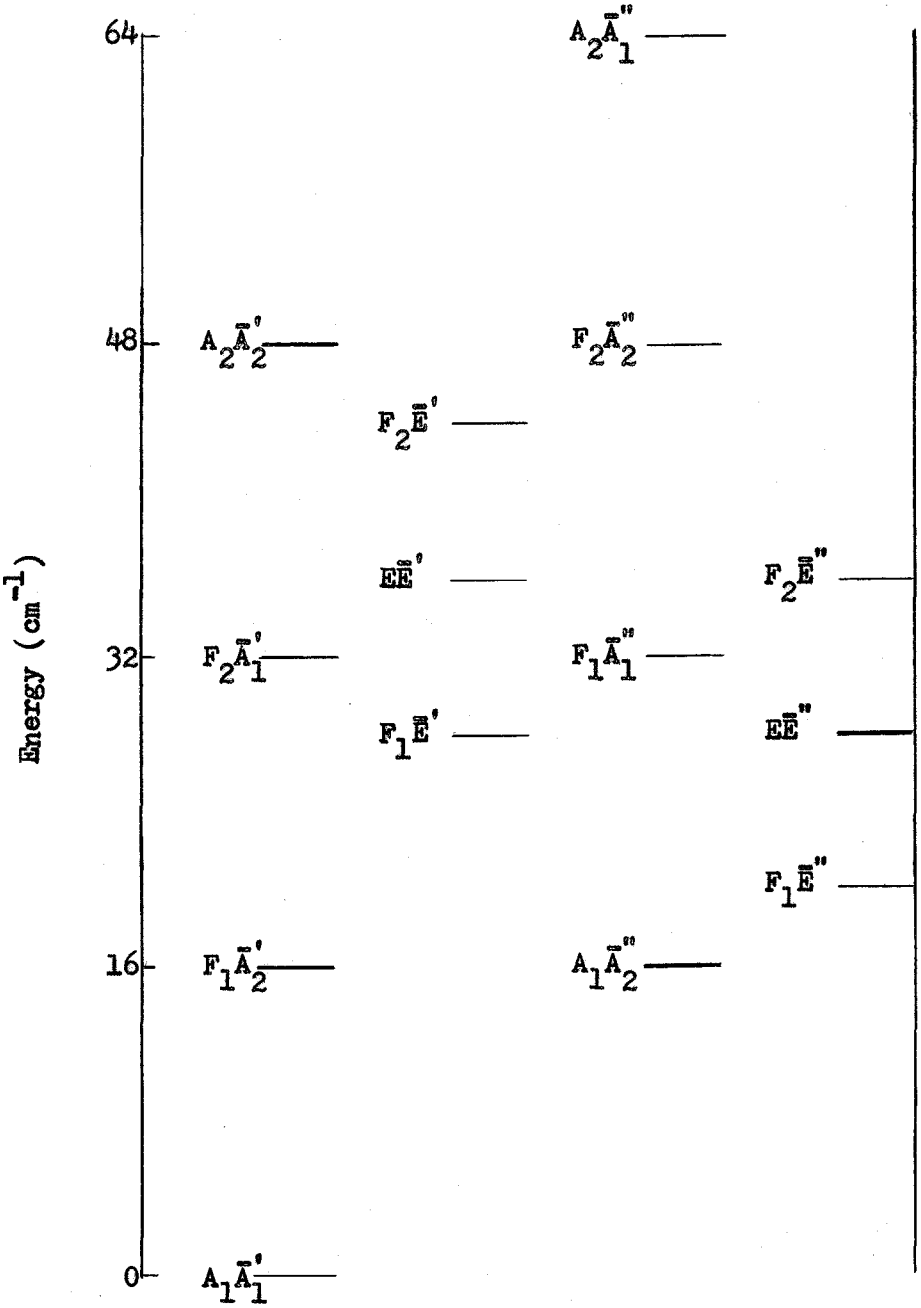

Figure 10. Ground state librational levels for (O_h, $\bar{\bar{D}}_{3h}$) near the $\bar{\bar{C}}_{3V}$ limit. For convenience we have chosen $\alpha = \beta = 4$ cm^{-1}, and the energy scale is approximately correct for CH_3.

$A_1\bar{A}_1' \longrightarrow F_1\bar{A}_2'$ and $F_1\bar{E}'' \longrightarrow F_1\bar{E}''$, $E\bar{E}''$, $F_2\bar{E}''$. The ν_2 spectrum would be expected to have three components with the $A_1\bar{A}_1' \longrightarrow F_1\bar{A}_2'$ and $F_1\bar{E}'' \longrightarrow F_2\bar{E}''$ transitions being coincident and at the highest frequency. The spectrum at 4°K (101) does have three components with the most intense at highest frequency. The separation of the lowest and highest frequency components is about 17 cm^{-1} or $1.8\tilde{B}$ (4β from Table VIII). This is only slightly smaller than the $2\tilde{B}$ separation of J = 0 and J = 1, but the difference between the J = 1 and J = 2 levels has changed from $4\tilde{B}$ to $.9\tilde{B}$ and $1.8\tilde{B}$. The observed ν_2 spectrum of CH_3 agrees with the hindered rotor model quite well.

The allowed transitions in CD_3 are those in CH_3 plus the additional transitions $F_1\bar{A}_2' \longrightarrow A_1\bar{A}_1'$, $F_2\bar{A}_1'$ and $A_1\bar{A}_2'' \longrightarrow F_1\bar{A}_1''$. The ν_2 spectrum for CD_3 would be expected to have four components if only the lowest levels are populated. The spacing between levels is reduced from the CH_3 case by a factor of two from $\tilde{B}$ and also an exponential factor depending on the barrier height. More than the lowest levels for each spin would be expected to be populated and this would allow more transitions. The ν_2 infrared band for CD_3 extends over about 12 cm^{-1} (101) and there is just one component. All the differences between CH_3 and CD_3 discussed above would help to explain this lack of structure.

4. A $\bar{C}_{3V}$ Molecule in an O_h Field

The group (O_h, $\bar{C}_{3V}$) is a subgroup of (O_h, $\bar{D}_{3h}$) and the appropriate symmetries for any problem can be found from the correlation between $\bar{D}_{3h}$ and $\bar{C}_{3V}$. In external axes $\Gamma(\mu) = F_1\bar{A}_2$ and

$\Gamma(\alpha) = A_1\bar{A}_1 + E\bar{A}_1 + F_2\bar{A}_1$.

An example fitting this symmetry is NH_3 isolated in a noble gas matrix. Again the high barrier limit is assumed to be $\bar{\bar{C}}_{3V}$. The A_1 ground librational state correlates to $A_1\bar{A}_1 + F_2\bar{A}_1 + A_2\bar{A}_2 + F_1\bar{A}_2 + E\bar{E} + F_1\bar{E} + F_2\bar{E}$ in G. The energies for these levels near the $\bar{\bar{C}}_{3V}$ limit can be found in the same manner as before, but now there are no minima separated by a 60° rotation so only the β elements for minima separated by 90° are considered. The relative energies in terms of β are given in Table IX and an energy diagram appropriate for NH_3 and ND_3 in Figure 11. The diagram is from the free rotor limit to the hindered rotor limit near $\bar{\bar{C}}_{3V}$ where it is assumed tunneling by 90° makes the largest contribution to the splitting of levels.

TABLE IX. THE RELATIVE HIGH BARRIER ENERGIES OF LIBRATIONAL STATES FROM (O_h, $\bar{\bar{C}}_{3V}$) FORMING THE GROUND LIBRATIONAL STATE IN $\bar{\bar{C}}_{3V}$.

Symmetry	Energy
$A_1\bar{A}_1$	6β
$F_2\bar{A}_1$	-2β
$F_1\bar{A}_2$	2β
$A_2\bar{A}_2$	-6β
$E\bar{E}$	0
$F_1\bar{E}$	2β
$F_2\bar{E}$	-2β

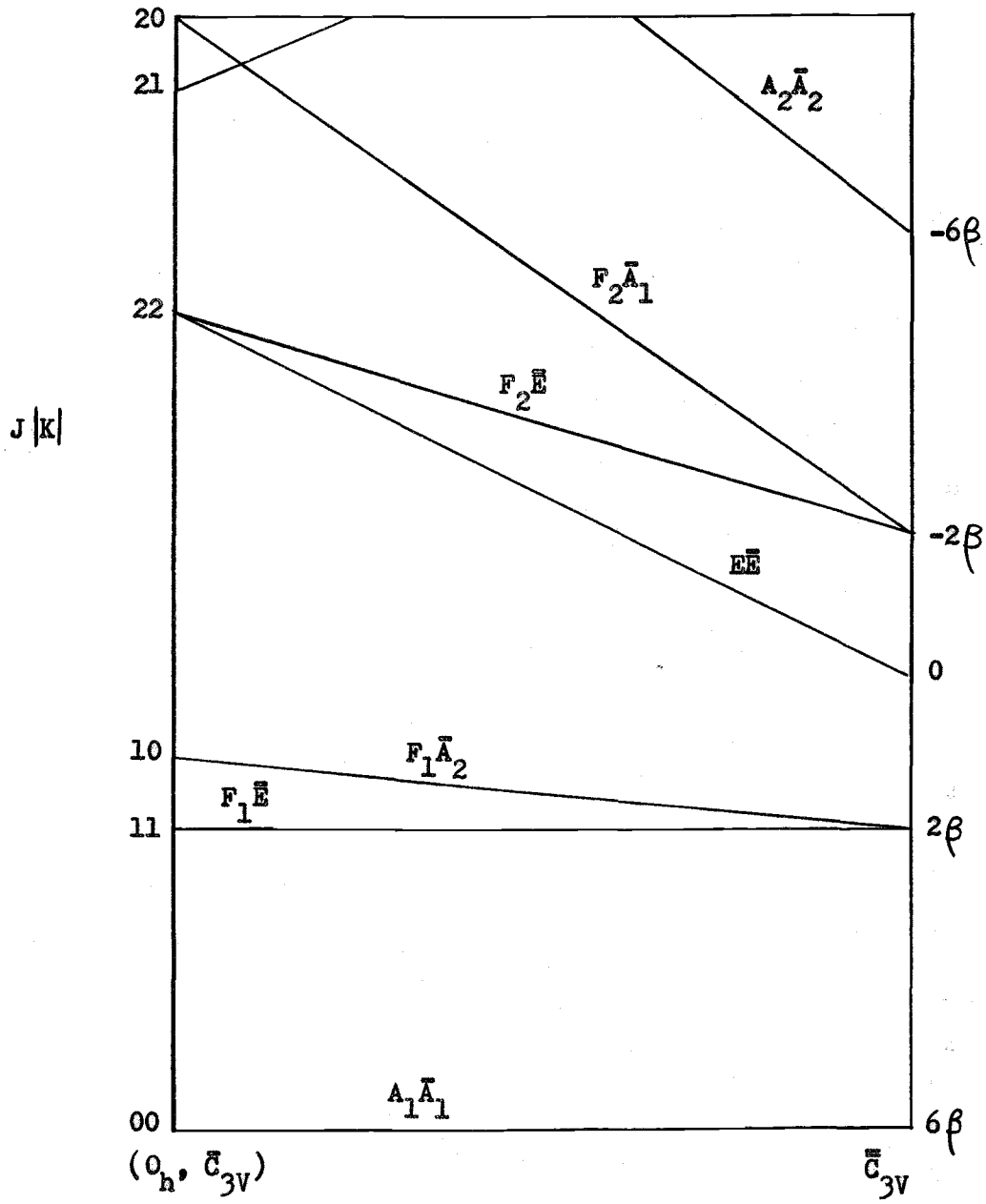

Figure 11. Correlation of ground state librational levels for an oblate symmetric rotor from the $(O_h, \bar{C}_{3V})$ free rotor limit to the $\bar{\bar{C}}_{3V}$ hindered rotor limit.

The experimental work on matrix isolated NH_3 has been done principally in Ar (69, 99) and N_2 (99, 115) although preliminary work was reported in Xe (10). The evidence from concentration studies (115) is that only one feature in the ν_2 region for the N_2 matrix is due to monomer, two are for dimers, and others at higher frequencies are from higher aggregates. The situation for ν_2 in Ar is more complicated with more than one feature assigned to the monomer, time dependent and temperature dependent intensities are observed, and features due to polymers are also present.

For the ν_2 vibration of symmetry $A_1\bar{A}_1$, the allowed infrared orientational transitions assuming the lowest $\bar{A}$ and $\bar{E}$ spin levels are occupied are $A_1\bar{A}_1 \longrightarrow F_1\bar{A}_2$, and $F_1\bar{E} \longrightarrow F_1\bar{E}$, $E\bar{E}$, $F_2\bar{E}$. The transitions $F_1\bar{E} \longrightarrow E\bar{E}$, $F_2\bar{E}$ are not allowed at the free rotor limit since this involves $\Delta K=1$, so these are expected to be somewhat weaker. At lowest temperatures, the $A_1\bar{A}_1 \longrightarrow F_1\bar{A}_2$ and $F_1\bar{E} \longrightarrow F_1\bar{E}$ lines would be the strongest and this agrees quite well with the work of Milligan, Hexter, and Dressler (99) at 4.2°K and Hopkins, Curl, and Pitzer (69) at 7°K, where they observed lines near 955 cm^{-1} and 974 cm^{-1}. Milligan, Hexter, and Dressler (99) also observe weaker features at 961, 972, and 980 cm^{-1} which are assigned as $E\bar{E} \longrightarrow F_2\bar{E}$, $F_1\bar{E} \longrightarrow E\bar{E}$, and $F_1\bar{E} \longrightarrow F_2\bar{E}$. The intensity of $E\bar{E} \longrightarrow F_2\bar{E}$ is much larger than one would expect at 4.2°K. Hopkins, Curl, and Pitzer (69) observe a band at 962 cm^{-1} at 33°K, but this band disappears at 7°K as one would expect since the energy difference between $F_1\bar{E}$ and $E\bar{E}$ is equivalent to about 24°K. Also the line at 956 cm^{-1} decreases in intensity at 33°K since $E\bar{E} \longrightarrow E\bar{E}$ is not allowed.

Features above 980 cm^{-1} are thought to be due to dimers and higher aggregates as they are in the N_2 matrix. The ν_2 spectrum of ND_3 in Ar at 4.2°K (99) can also be explained by this model if the lines at 749 cm^{-1} and 758 cm^{-1} are assigned as $F_1\bar{E} \longrightarrow F_1\bar{E}$ and $A_1\bar{A}_1 \longrightarrow F_1\bar{A}_2$, and the ones at 769 cm^{-1} and 778 cm^{-1} assigned as due to dimers. The preliminary work by Becker and Pimentel (10) of NH_3 in Xe at 20°K can be explained by assigning the strong feature at 973 cm^{-1} to $A_1\bar{A}_1 \longrightarrow F_1\bar{A}_2$, the weaker feature at 961 cm^{-1} to $E\bar{E} \longrightarrow F_2\bar{E}$, and the other bands to dimers.

The spectra of ν_2 suggest that NH_3 is a hindered rotor and is near the hindered rotor limit in the diagram. The assignment of the line near 962 cm^{-1} as $E\bar{E} \longrightarrow F_2\bar{E}$ means that the $F_2\bar{E}$ and $E\bar{E}$ levels are split by 6 cm^{-1} and they were degenerate at the free rotor limit. The assignment of $F_1\bar{E} \longrightarrow E\bar{E}$ below $A_1\bar{A}_1 \longrightarrow F_1\bar{A}_2$ and $F_1\bar{E} \longrightarrow F_2\bar{E}$ above, shows that NH_3 is a hindered rotor since the free rotor transitions would form one line $2\tilde{B}$ above $A_1\bar{A}_1 \longrightarrow F_1\bar{A}_2$, and it also shows that NH_3 is not at the hindered rotor limit where the transition $F_1\bar{E} \longrightarrow F_2\bar{E}$ would be coincident with $A_1\bar{A}_1 \longrightarrow F_1\bar{A}_2$. This model is only approximate, but it does provide a good explanation to the observed spectra.

D. The Spherical Rotor

1. A $\bar{T}_d$ Molecule in an O_h Field

We have $S = O_h$ and $\bar{M} = \bar{T}_d$ so $G = 'S'(P) \times 'M' = 'O' \times '\bar{T}_d'$. Since the $\{Q\}$ group for both O and T_d is O, the group for the rotational problem is $O \times \bar{O}$ as King and Hornig have shown (87). A $\bar{T}_d$ molecule of the type XY_4 in an O_h field may have a potential minimum if the Y atoms point toward the corners of the cube, in which case $\bar{\bar{H}} = \bar{\bar{T}}_d$, or if they point towards the midpoints of the edges, in which case $\bar{\bar{H}} = \bar{\bar{D}}_{2d}$. Another minimum which is appropriate is $\bar{\bar{C}}_{3V}$ which was used in the work of Nishiyama and Yamamoto (107, 108). The equilibrium position is found by starting with the Y atoms in the corners and rotating by 60° about one X-Y bond. The correlation of species in G, $\bar{\bar{T}}_d$, $\bar{\bar{D}}_{2d}$, and $\bar{\bar{C}}_{3V}$ is given in Table X. To go from $\bar{\bar{C}}_{3V}$ to $(O_h, \bar{T}_d)$ one must first go from $\bar{\bar{C}}_{3V}$ to $\bar{\bar{T}}_d$. The degeneracy factor is 24 for states in $\bar{\bar{T}}_d$, 72 for $\bar{\bar{D}}_{2d}$, and 96 for $\bar{\bar{C}}_{3V}$.

In the body-fixed axes $\Gamma(\mu) = A_1\bar{\bar{F}}_2$ and $\Gamma(\alpha) = A_1\bar{A}_1 + A_1\bar{\bar{E}} + A_1\bar{\bar{F}}_2$. In the space-fixed axes $\Gamma(\mu) = F_1\bar{A}_2$ and $\Gamma(\alpha) = A_1\bar{A}_1 + E\bar{A}_1 + F_2\bar{A}_1$. The nuclear spin wave functions have the symmetry $5A_1\bar{A}_1 + A_1\bar{\bar{E}} + 3A_1\bar{\bar{F}}_2$ for $I_Y = 1/2$ and $15A_1\bar{A}_1 + 6A_1\bar{\bar{E}} + 3A_1\bar{\bar{F}}_1 + 15A_1\bar{\bar{F}}_2$ for $I_Y = 1$. The overall wave function must be $\Gamma\bar{A}_1$ or $\Gamma\bar{A}_2$ ($\Gamma = A_1$, A_2, E, F_1, or F_2) and this is the same for bosons and fermions. Therefore, in a ground vibronic state of symmetry $A_1\bar{A}_1$, $\bar{A}_1$ spin molecules could occupy $\bar{A}_1$ and $\bar{A}_2$ rotational states, $\bar{\bar{E}}$ spin molecules could be in $\bar{\bar{E}}$ states, and $\bar{\bar{F}}_1$ or $\bar{\bar{F}}_2$ spin molecules in $\bar{\bar{F}}_1$ and $\bar{\bar{F}}_2$ states.

TABLE X. CORRELATION OF $\bar{\bar{T}}_d$ AND $\bar{\bar{D}}_{2d}$ WITH $(O_h, \bar{T}_d)$, AND $\bar{\bar{C}}_{3V}$ WITH $\bar{\bar{T}}_d$.

$\bar{\bar{T}}_d$	$(O_h, \bar{T}_d)$
A_1	$A_1\bar{A}_1 + A_2\bar{A}_2 + E\bar{E} + F_1\bar{F}_1 + F_2\bar{F}_2$
A_2	$A_2\bar{A}_1 + A_1\bar{A}_2 + E\bar{E} + F_2\bar{F}_1 + F_1\bar{F}_2$
E	$E\bar{A}_1 + E\bar{A}_2 + A_1\bar{E} + A_2\bar{E} + E\bar{E} + F_1\bar{F}_1 + F_2\bar{F}_1 + F_1\bar{F}_2 + F_2\bar{F}_2$
F_1	$F_1\bar{A}_1 + F_2\bar{A}_2 + F_1\bar{E} + F_2\bar{E} + A_1\bar{F}_1 + E\bar{F}_1 + F_1\bar{F}_1 + F_2\bar{F}_1 + A_2\bar{F}_2 + E\bar{F}_2 + F_1\bar{F}_2 + F_2\bar{F}_2$
F_2	$F_2\bar{A}_1 + F_1\bar{A}_2 + F_1\bar{E} + F_2\bar{E} + A_2\bar{F}_1 + E\bar{F}_1 + F_1\bar{F}_1 + F_2\bar{F}_1 + A_1\bar{F}_2 + E\bar{F}_2 + F_1\bar{F}_2 + F_2\bar{F}_2$
$\bar{\bar{D}}_{2d}$	$(O_h, \bar{T}_d)$
A_1	$A_1\bar{A}_1 + E\bar{A}_1 + F_2\bar{A}_2 + A_1\bar{E} + E\bar{E} + F_2\bar{E} + 2F_1\bar{F}_1 + F_2\bar{F}_1 + A_2\bar{F}_2 + E\bar{F}_2 + F_1\bar{F}_2 + F_2\bar{F}_2$
A_2	$F_1\bar{A}_1 + A_2\bar{A}_2 + E\bar{A}_2 + A_2\bar{E} + E\bar{E} + F_1\bar{E} + A_1\bar{F}_1 + E\bar{F}_1 + F_1\bar{F}_1 + F_2\bar{F}_1 + F_1\bar{F}_2 + 2F_2\bar{F}_2$
B_1	$F_2\bar{A}_1 + A_1\bar{A}_2 + E\bar{A}_2 + A_1\bar{E} + E\bar{E} + F_2\bar{E} + A_2\bar{F}_1 + E\bar{F}_1 + F_1\bar{F}_1 + F_2\bar{F}_1 + 2F_1\bar{F}_2 + F_2\bar{F}_2$
B_2	$A_2\bar{A}_1 + E\bar{A}_1 + F_1\bar{A}_2 + A_2\bar{E} + E\bar{E} + F_1\bar{E} + F_1\bar{F}_1 + 2F_2\bar{F}_1 + A_1\bar{F}_2 + E\bar{F}_2 + F_1\bar{F}_2 + F_2\bar{F}_2$
E	$F_1\bar{A}_1 + F_2\bar{A}_1 + F_1\bar{A}_2 + F_2\bar{A}_2 + 2F_1\bar{E} + 2F_2\bar{E} + A_1\bar{F}_1 + A_2\bar{F}_1 + 2E\bar{F}_1 + 2F_1\bar{F}_1 + 2F_2\bar{F}_1 + A_1\bar{F}_2 + A_2\bar{F}_2 + 2E\bar{F}_2 + 2F_1\bar{F}_2 + 2F_2\bar{F}_2$

$\bar{\bar{C}}_{3V}$	$\bar{\bar{T}}_d$
A_1	$A_1 + F_2$
A_2	$A_2 + F_1$
E	$E + F_1 + F_2$

The orientation transitions allowed near the $\bar{\bar{C}}_{3v}$ limit for ν_3 and ν_4 in the infrared, and all fundamentals in the Raman effect are given in Table XI assuming each spin species is in its lowest state. Some of these transitions are forbidden for a free rotor and may be quite weak, for example, the changes in librational states for ν_1.

The rotational energies at the $\bar{\bar{C}}_{3v}$ hindered rotor limit may be found for most states by the method previously described (Section III.C.3) assuming only tunneling by 90° is important. However, there are two levels each of symmetry $F_1\bar{F}_1$ and $F_2\bar{F}_2$ which correlate to the ground librator state (see Table X). The method does not work in general for a case like this, so a more complicated procedure was used.

The group G is divided into 96 left cosets with the members of each having the same relative rotation of the molecule with respect to the crystal. The coset with no relative rotation is the subgroup $\bar{\bar{C}}_{3v}$. A 96 x 96 matrix is formed where the only nonzero entries are for cosets which are related by 90° rotations. There are a number of ways of obtaining these remaining eigenvalues; from the trace properties, diagonalizing the matrix, and from the eigenvectors having the correct symmetry. In order to determine which eigenvalue belongs to which symmetry species, it is necessary to determine the eigenvectors and then the eigenvalues are found quite easily. There are two $F_1\bar{F}_1$ species making 18 eigenvectors which must be determined. The eigenvalues for the $F_2\bar{F}_2$ species are just the negative of those for the $F_1\bar{F}_1$ problem, and this is easily seen from the traces (see

TABLE XI. ALLOWED VIBRATION-ORIENTATION TRANSITIONS BETWEEN LIBRATIONAL STATES FOR A $\bar{T}_d$ MOLECULE IN AN O_h CRYSTAL FIELD NEAR THE $\bar{C}_{3V}$ HIGH BARRIER LIMIT, ASSUMING ONLY THE LOWEST SPIN STATES ARE POPULATED.

A. $\nu_1(A_1\bar{A}_1)$ Raman transitions

$A_1\bar{A}_1 \longrightarrow A_1\bar{A}_1,\ F_2\bar{A}_1$

$F_1\bar{F}_1 \longrightarrow A_2\bar{F}_1,\ E\bar{F}_1,\ F_1\bar{F}_1,\ F_2\bar{F}_1$

$E\bar{E} \longrightarrow E\bar{E},\ F_1\bar{E},\ F_2\bar{E}$

B. $\nu_2(A_1\bar{E})$ Raman transitions

$A_1\bar{A}_1 \longrightarrow E\bar{E},\ F_2\bar{E}$

$F_1\bar{F}_1 \longrightarrow A_2\bar{F}_1,\ E\bar{F}_1,\ F_1\bar{F}_1,\ F_2\bar{F}_1,\ E\bar{F}_2,\ F_1\bar{F}_2,\ F_2\bar{F}_2$

$E\bar{E} \longrightarrow A_1\bar{A}_1,\ F_2\bar{A}_1,\ A_2\bar{A}_2,\ F_1\bar{A}_2,\ E\bar{E},\ F_1\bar{E},\ F_2\bar{E}$

C. $\nu_3, \nu_4(A_1\bar{F}_2)$ Raman transitions

$A_1\bar{A}_1 \longrightarrow A_1\bar{F}_2,\ E\bar{F}_2,\ F_2\bar{F}_2$

$F_1\bar{F}_1 \longrightarrow A_2\bar{A}_2,\ F_1\bar{A}_2,\ E\bar{E},\ F_1\bar{E},\ F_2\bar{E},\ A_2\bar{F}_1,\ E\bar{F}_1,\ F_1\bar{F}_1,\ F_2\bar{F}_1,$
$E\bar{F}_2,\ F_1\bar{F}_2,\ F_2\bar{F}_2$

$E\bar{E} \longrightarrow A_2\bar{F}_1,\ E\bar{F}_1,\ F_1\bar{F}_1,\ F_2\bar{F}_1,\ A_1\bar{F}_2,\ E\bar{F}_2,\ F_1\bar{F}_2,\ F_2\bar{F}_2$

D. $\nu_3, \nu_4(A_1\bar{F}_2)$ Infrared transitions

$A_1\bar{A}_1 \longrightarrow F_1\bar{F}_1$

$F_1\bar{F}_1 \longrightarrow A_1\bar{A}_1,\ F_2\bar{A}_1,\ E\bar{E},\ F_1\bar{E},\ F_2\bar{E},\ E\bar{F}_1,\ F_1\bar{F}_1,\ F_2\bar{F}_1,\ A_1\bar{F}_2,$
$E\bar{F}_2,\ F_1\bar{F}_2,\ F_2\bar{F}_2$

$E\bar{E} \longrightarrow F_1\bar{F}_1,\ F_2\bar{F}_1,\ F_1\bar{F}_2,\ F_2\bar{F}_2$

Appendix C). The method of Wigner (159, 161) is used to construct 18 different linear combinations of 96 wave functions (one wave function for each potential minimum) and then the Schmidt orthogonalization procedure (161) could be used to construct 18 orthogonal eigenvectors. Actually the problem is much simpler than that since it can be shown (see Appendix C) that $H|\bar{i}\rangle = 4\beta|\bar{i}\rangle$, where H is the 96 x 96 matrix, $|\bar{i}\rangle$ is one of the 18 linear combinations (not orthogonalized), and β is the matrix element between minima separated by a 90° rotation. If we denote the orthogonalized eigenvectors by $|\bar{\bar{i}}\rangle$, then $|\bar{\bar{i}}\rangle = \sum_{\bar{i}=1}^{18} C_{\bar{i}\bar{\bar{i}}}|\bar{i}\rangle$

Now, $$H|\bar{\bar{i}}\rangle = H\sum_{\bar{i}=1}^{18} C_{\bar{i}\bar{\bar{i}}}|\bar{i}\rangle$$

$$= 4\beta \sum_{\bar{i}=1}^{18} C_{\bar{i}\bar{\bar{i}}}|\bar{i}\rangle = 4\beta|\bar{\bar{i}}\rangle$$

Therefore, $\langle\bar{\bar{j}}|H|\bar{\bar{i}}\rangle = 4\beta\langle\bar{\bar{j}}|\bar{\bar{i}}\rangle = 4\beta\delta_{ij}$.

Therefore, for the $F_1\bar{F}_1$ symmetry species, all 18 eigenvalues are 4β, and for the $F_2\bar{F}_2$ symmetry species, all 18 eigenvalues are -4β. The relative energies in terms of β for all states forming the ground librational state are given in Table XII and an energy diagram is shown in Figure 12.

Examples where the $\bar{\bar{C}}_{3V}$ limit is appropriate for the (O_h, T_d) group are the methane molecule in a noble gas matrix (108), the disordered molecules in neat methane where only nearest neighbor molecules are considered (80, 120, 165), and the NH_4^+ impurity in an NaCl-type lattice (153). The methane examples will be discussed in Chapter V after the Raman spectra are presented.

TABLE XII. THE RELATIVE HIGH BARRIER ENERGIES OF LIBRATIONAL STATES FROM (O_h, $\bar{T}_d$) FORMING THE GROUND LIBRATIONAL STATE IN $\bar{C}_{3v}$.

Symmetry	Energy
$A_1\bar{A}_1$	12β
$F_2\bar{A}_1$	4β
$A_2\bar{A}_2$	-4β
$E\bar{E}$	0
$F_1\bar{E}$	2β
$F_2\bar{E}$	-2β
$A_2\bar{F}_1$	-4β
$E\bar{F}_1$	2β
$F_1\bar{F}_1$	4β
$F_1\bar{F}_1$	4β
$F_2\bar{F}_1$	0
$A_1\bar{F}_2$	4β
$E\bar{F}_2$	-2β
$F_1\bar{F}_2$	0
$F_2\bar{F}_2$	-4β
$F_2\bar{F}_2$	-4β

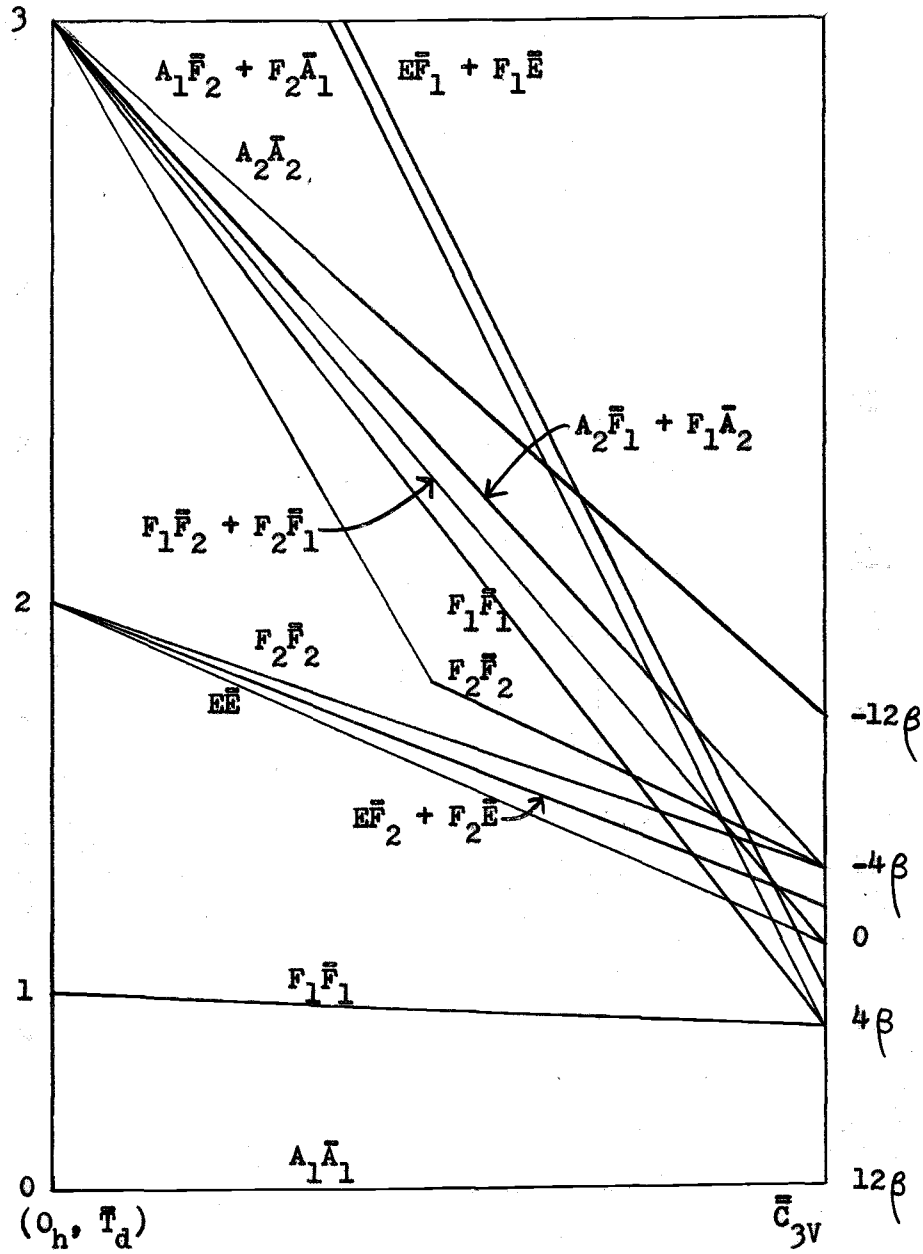

Figure 12. Correlation of ground state librational levels for a spherical rotor from the $(O_h, \bar{T}_d)$ free rotor limit to the $\bar{C}_{3V}$ hindered rotor limit.

Vedder and Hornig (153) reported the infrared spectra of NH_4^+ in KCl, KBr, and KI. They considered the free rotor model and also a model where rotation occurs about a N-H $\cdots$ X^- axis, where X^- is a halide ion. They concluded that there is no agreement with a free rotor and that some features, but not all, seem to be in agreement with rotation about a N-H $\cdots$ X^- axis. Assuming that only the $A_1\bar{A}_1$ and $F_1\bar{F}_1$ levels would be occupied at the lowest temperature of these experiments (5^oK), from the symmetry considerations of this section one would predict six principal transitions ($A_1\bar{A}_1 \longrightarrow F_1\bar{F}_1$; $F_1\bar{F}_1 \longrightarrow A_1\bar{A}_1$, $F_1\bar{F}_1$, $E\bar{E}$, $E\bar{F}_2 + F_2\bar{E}$, $F_2\bar{F}_2$) and others may be weakly allowed (see Table XI). The transitions from $F_1\bar{F}_1$ to states originating from J=2 are split into a triplet which is at a higher frequency than the $A_1\bar{A}_1 \longrightarrow F_1\bar{F}_1$ transition at low barriers, and at the hindered rotor limit (Figure 12) has two components lower in frequency and the $A_1\bar{A}_1 \longrightarrow F_1\bar{F}_1$ and $F_1\bar{F}_1 \longrightarrow F_2\bar{F}_2$ transitions are coincident (difference of 8β). This model may partially explain the ν_4 spectra, but there are too many lines, particularly at lower frequencies than the most intense features, which are not explained. The ν_3 spectra in general have much less structure than one would expect from this hindered rotor model, although the resolution was better for the ν_4 spectra. Additional experiments, such as Raman spectra of NH_4^+ or infrared and Raman spectra of ND_4^+, would be very helpful in making assignments.

2. A $\bar{T}_d$ Molecule in a T_d Field

In this example the group G is not a direct product since T_d

is one of the six exceptions. The method of finding the character table (see Table XIII) is to determine the class structure, then the number of species of each multiplicity, and then the characters follow rather easily knowing that this is a subgroup of $(O_h, \bar{T}_d)$ which is a direct product. The group at the librator limit is taken to be $\bar{\bar{T}}_d$ since T_d is the greatest common subgroup. The group $(T_d, \bar{T}_d)$ would be appropriate for the $\bar{T}_d$ molecule in a cubic crystal if the barrier to rotation by 90° about a crystal axis was large so that the molecule could only rotate about the threefold axes of the molecule or crystal. Also, in the ordered phase of NH_4Cl (139), the ammonium ion occupies a site of T_d symmetry, but the barrier is apparently much too high to permit splittings in any of the lower librator levels.

An A_1 state in $\bar{\bar{T}}_d$ corresponds to $A_1 + L_1 + E_2$ in G and an F_1 state in $\bar{\bar{T}}_d$ corresponds to $F_1 + F_3 + I_1 + I_2 + L_1 + L_2$ in G. The degeneracy factor is twelve so that A_1 states are twelve-fold degenerate and F_1 states are 36-fold degenerate at the librator limit. The free rotor states are found by correlation with the states for a $\bar{T}_d$ molecule in an O_h field. The energy diagram for the first few rotational states is shown in Figure 13.

For an XY_4 molecule and $I_Y = 1/2$ the nuclear spin functions have the symmetry $5A_1 + E_1 + 3F_2$ and for $I_Y = 1$ their symmetry is $15A_1 + 6E_1 + 3F_1 + 15F_2$. Since the group is not a direct product it is not immediately apparent which species the overall wave function must be for bosons and fermions. Correlation to the subgroup $\{E\bar{E}, 8E(\overline{123}), 3E(\overline{12})(\overline{34})\} = \text{'}\bar{T}\text{'}$ shows that the only species from G

TABLE XIII. THE CHARACTER TABLE FOR $(T_d, \bar{T}_d)$ AND CORRELATION TO THE GROUP $\bar{\bar{T}}_d$.

$(T_d, \bar{T}_d)$	$\bar{\bar{E}}\bar{\bar{E}}$	$8\bar{E}(\overline{123})$	$3\bar{E}(\overline{12})(\overline{34})$	$8(123)\bar{\bar{E}}$	$32(123)(\overline{123})$	$32(123)(\overline{132})$	$24(123)(\overline{12})(\overline{34})$	$24(12)(34)(\overline{123})$	$3(12)(34)\bar{\bar{E}}$	$9(12)(34)(\overline{12})(\overline{34})$	$36(1324)^*(\overline{1324})^*$	$36(12)^*(\overline{1324})^*$	$36(1324)^*(\overline{12})^*$	$36(12)^*(\overline{12})^*$		$\bar{\bar{T}}_d$
A_1	1	1	1	1	1	1	1	1	1	1	1	1	1	1	α int. α ext.	A_1
A_2	1	1	1	1	1	1	1	1	1	1	-1	-1	-1	-1		A_2
E_1	2	-1	2	2	-1	-1	2	-1	2	2	0	0	0	0	α int.	E
E_2	2	-1	2	-1	2	-1	-1	-1	2	2	0	0	0	0		A_1+A_2
E_3	2	-1	2	-1	-1	2	-1	-1	2	2	0	0	0	0		E
E_4	2	2	2	-1	-1	-1	-1	2	2	2	0	0	0	0	α ext.	E
F_1	3	0	-1	3	0	0	-1	0	3	-1	1	1	-1	-1		F_1
F_2	3	0	-1	3	0	0	-1	0	3	-1	-1	-1	1	1	μ int. α int.	F_2
F_3	3	3	3	0	0	0	0	-1	-1	-1	1	-1	1	-1		F_1
F_4	3	3	3	0	0	0	0	-1	-1	-1	-1	1	-1	1	μ ext. α ext.	F_2
I_1	6	0	-2	-3	0	0	1	0	6	-2	0	0	0	0		F_1+F_2
I_2	6	-3	6	0	0	0	0	1	-2	-2	0	0	0	0		F_1+F_2
L_1	9	0	-3	0	0	0	0	0	-3	1	1	-1	-1	1		$A_1+E+F_1+F_2$
L_2	9	0	-3	0	0	0	0	0	-3	1	-1	1	1	-1		$A_2+E+F_1+F_2$

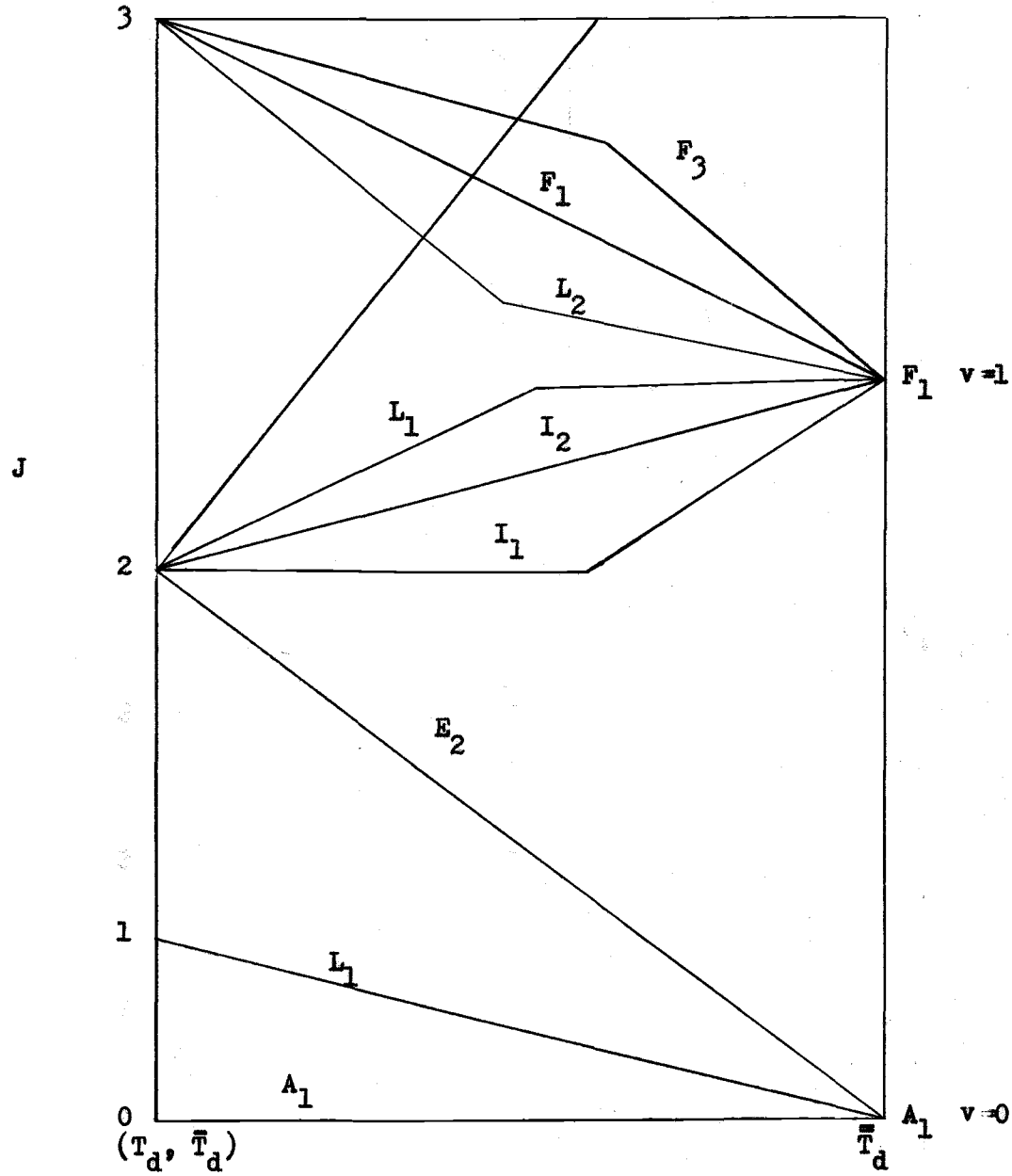

Figure 13. Correlation of rotational energy levels for a spherical rotor from the $(T_d, \bar{T}_d)$ free rotor limit to the $\bar{\bar{T}}_d$ librator limit.

which do correlate to the $\bar{A}$ species of '$\bar{T}$' are A_1, A_2, E_4, F_3, and F_4. The overall wave function must be $\bar{A}$ in '$\bar{T}$' for either bosons or fermions so in G the overall wave function must be A_1, A_2, E_4, F_3, or F_4. The only possibilities for the ground librator state are molecules with A_1 spin in the A_1 librator state, E_1 spin in the E_2 state, and F_1 or F_2 spin in the L_1 state; this is because $A_1 \times A_1 = \underline{A_1}$, $E_2 \times E_1 = E_3 + \underline{E_4}$ and $L_1 \times F_1(F_2) = \underline{F_3}(\underline{F_4}) + I_2 + L_1 + L_2$. So the ground librator state can have every type of nuclear spin as one would expect.

There are four librational v=0 $\longrightarrow$ v=1 transitions ($E_2 \longrightarrow I_2$, $L_1 \longrightarrow I_1$, L_1, L_2) allowed in both the infrared and Raman effect near the $\bar{\bar{T}}_d$ limit. The vibration-orientation transitions for an F_2 vibration are the same in the infrared and Raman effect and the spectra would show five lines ($A_1 \longrightarrow L_1$; $L_1 \longrightarrow A_1$, L_1, E_2; $E_2 \longrightarrow L_1$). An E_1 vibration is allowed in the Raman effect and the orientation transitions are $A_1 \longrightarrow E_2$, $L_1 \longrightarrow L_1$, and $E_2 \longrightarrow A_1$, so one would expect a triplet. An A_1 vibration is allowed in the Raman effect with no changes in librational states so again one expects a single line.

This example shows how to work with a group which is not a direct product. The molecular species have been given the same label (E becomes E_1) as in the group T_d. There are no simple rules for finding the direct product of two symmetry species as in the case of the regular point groups (161), but they can easily be found. Then the problem is solved in the same way as before.

3. A $\bar{T}_d$ Molecule in a D_{2d} Field

This is another example where G is not a direct product. The character table (see Table XIV) is found by restricting the characters in the direct product group $D_{2d} \times \bar{T}_d$ to the subgroup $(D_{2d}, \bar{T}_d)$. The group at the librator limit is taken to be $\bar{\bar{D}}_{2d}$. This symmetry is found for the CH_4 molecule in phase III (25, 80) and the CD_4 molecule in phase II (120). These molecules are ordered and so must be very near the $\bar{\bar{D}}_{2d}$ librator limit.

The first excited librator states in $\bar{\bar{D}}_{2d}$ have the symmetry $A_2 + E$. The A_1 ground librator state in $\bar{\bar{D}}_{2d}$ corresponds to $A_1 + E_1 + F_3 + I$ in G, the A_2 state to $A_3 + E_2 + F_1 + I$, and the E state to $E_3 + E_4 + E_5 + F_1 + F_2 + F_3 + F_4 + I$. The degeneracy factor is 12 for the librator states. The free rotor states are found by correlation with the group $(T_d, \bar{T}_d)$. The energy diagram for the first few rotational states is shown in Figure 14.

The nuclear spin wave functions have the same symmetry as in $(T_d, \bar{T}_d)$. Now correlation to the subgroup '$\bar{T}$' shows that the overall wave function must be A_1, A_2, A_3, A_4, or E_5 and this requirement is for both bosons and fermions. In the ground librator state molecules with A_1 spin must be in the A_1 state, E_1 spin in the E_1 state, F_1 or F_2 spin in either the F_3 or I states.

The vibration-orientation transitions are summarized in Table XV for a molecule having the symmetry $\bar{T}_d$. This treatment is an approximation for the methane example and depends on the intermolecular coupling being small.

TABLE XIV. THE CHARACTER TABLE FOR $(D_{2d}, \bar{T}_d)$ AND CORRELATION TO THE GROUP $\bar{\bar{D}}_{2d}$.

$(D_{2d}, \bar{T}_d)$	$\bar{E}\bar{E}$	$8E(\bar{1}\bar{2}\bar{3})$	$3E(\bar{1}\bar{2})(\bar{3}\bar{4})$	$(12)(34)\bar{E}$	$8(12)(34)(\bar{1}\bar{2}\bar{3})$	$3(12)(34)(\bar{1}\bar{2})(\bar{3}\bar{4})$	$2(13)(24)\bar{E}$	$8(13)(24)(\bar{1}\bar{2}\bar{3})$	$8(13)(24)(\bar{1}\bar{3}\bar{2})$	$6(13)(24)(\bar{1}\bar{2})(\bar{3}\bar{4})$	$12(1423)*(\bar{1}\bar{2}\bar{3}\bar{4})*$	$12(12)*(\bar{1}\bar{2}\bar{3}\bar{4})*$	$12(1423)*(\bar{1}\bar{2})*$	$12(12)*(\bar{1}\bar{2})*$	$\bar{\bar{D}}_{2d}$
A_1	1	1	1	1	1	1	1	1	1	1	1	1	1	1	A_1
A_2	1	1	1	1	1	1	1	1	1	1	-1	-1	-1	-1	B_1
A_3	1	1	1	1	1	1	-1	-1	-1	-1	1	-1	1	-1	A_2
A_4	1	1	1	1	1	1	-1	-1	-1	-1	-1	1	-1	1	B_2
E_1	2	-1	2	2	-1	2	2	-1	-1	2	0	0	0	0	A_1+B_1
E_2	2	-1	2	2	-1	2	-2	1	1	-2	0	0	0	0	A_2+B_2
E_3	2	-1	2	-2	1	-2	0	$\sqrt{3}$	$-\sqrt{3}$	0	0	0	0	0	E
E_4	2	-1	2	-2	1	-2	0	$-\sqrt{3}$	$\sqrt{3}$	0	0	0	0	0	E
E_5	2	2	2	-2	-2	-2	0	0	0	0	0	0	0	0	E
F_1	3	0	-1	3	0	-1	3	0	0	-1	1	1	-1	-1	A_2+E
F_2	3	0	-1	3	0	-1	3	0	0	-1	-1	-1	1	1	B_2+E
F_3	3	0	-1	3	0	-1	-3	0	0	1	1	-1	-1	1	A_1+E
F_4	3	0	-1	3	0	-1	-3	0	0	1	-1	1	1	-1	B_1+E
I	6	0	-2	-6	0	2	0	0	0	0	0	0	0	0	$A_1+A_2+B_1+B_2+E$

$\Gamma(\mu \text{ ext}) = A_4 + E_5 \qquad \Gamma(\alpha \text{ ext}) = 2A_1 + A_2 + A_4 + E_5$

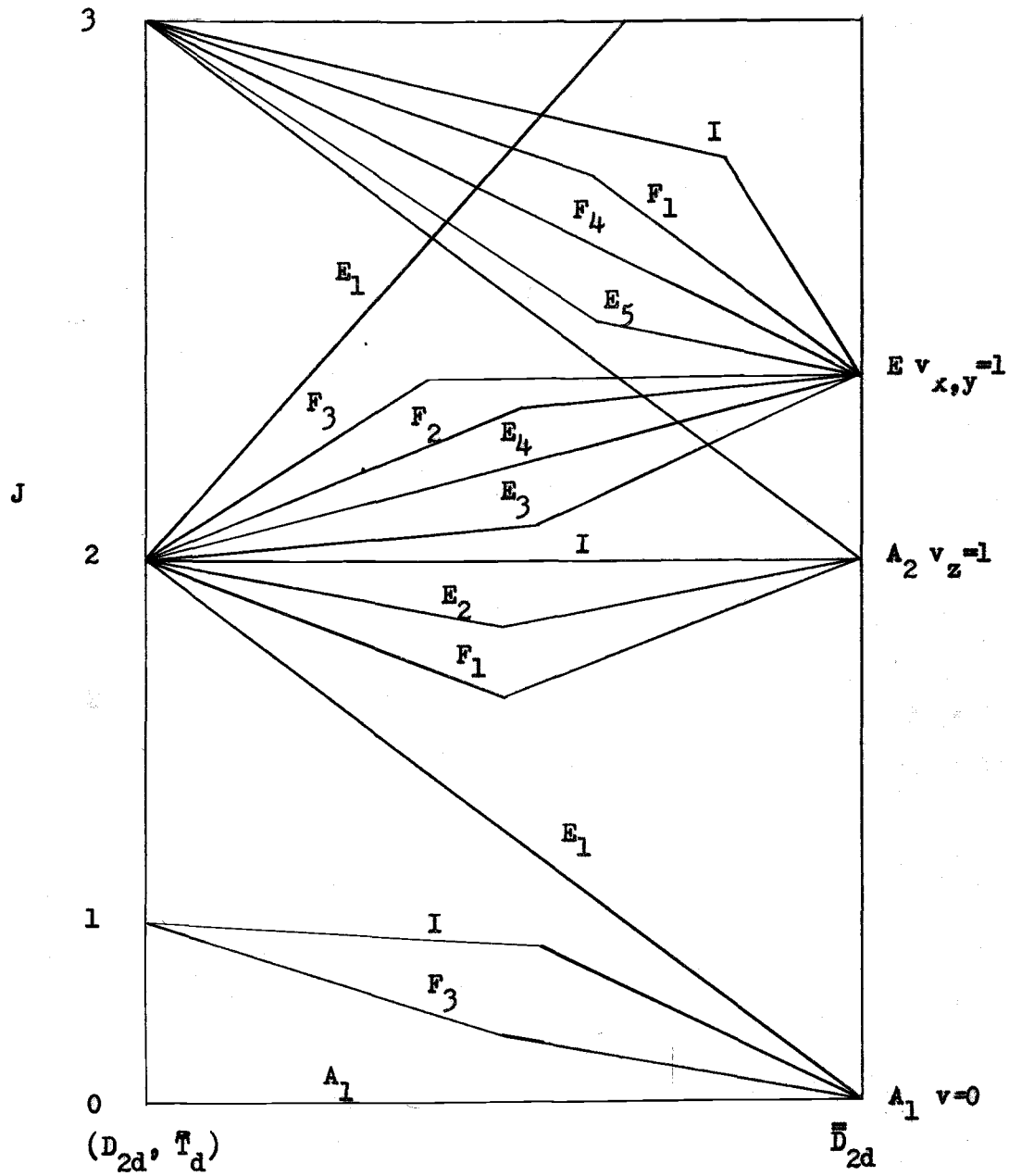

Figure 14. Correlation of rotational energy levels for a spherical rotor from the $(D_{2d}, \bar{T}_d)$ free rotor limit to the $\bar{D}_{2d}$ librator limit.

TABLE XV. ALLOWED VIBRATION-ORIENTATION TRANSITIONS BETWEEN LIBRATIONAL STATES FOR A $\bar{T}_d$ MOLECULE IN A D_{2d} CRYSTAL FIELD, NEAR THE $\bar{\bar{D}}_{2d}$ HIGH BARRIER LIMIT.

A. $\nu_1(A_1)$ Raman transitions

$A_1 \longrightarrow A_1$

$F_3 \longrightarrow F_3, I$

$I \longrightarrow F_3, I$

$E_1 \longrightarrow E_1$

B. $\nu_2(E_1)$ Raman transitions

$A_1 \longrightarrow E_1$

$F_3 \longrightarrow F_3, I$

$I \longrightarrow F_3, I$

$E_1 \longrightarrow A_1$

C. $\nu_3, \nu_4(F_2)$ Raman transitions

$A_1 \longrightarrow F_3, I$

$F_3 \longrightarrow A_1, F_3, I, E_1$

$I \longrightarrow A_1, F_3, I, E_1$

$E_1 \longrightarrow F_3, I$

D. $\nu_3, \nu_4(F_2)$ Infrared transitions

$A_1 \longrightarrow F_3, I$

$F_3 \longrightarrow A_1, I, E_1$

$I \longrightarrow A_1, F_3, I, E_1$

$E_1 \longrightarrow F_3, I$

E. The Asymmetric Rotor

1. A $\bar{C}_{2V}$ Molecule in an O_h Field

The group for this example is a direct product group and we set G = 'O' x '$\bar{C}_{2V}$' which preserves the molecular symmetry. In external axes $\Gamma(\mu) = F_1\bar{A}_2$ and $\Gamma(\alpha) = A_1\bar{A}_1 + E\bar{A}_1 + F_2\bar{A}_1$. The high barrier group is assumed to be $\bar{C}_{2V}$ where the twofold axis of the molecule lies along a <110> direction of the crystal. This has been determined for NO_2^- in NaCl-type lattices (106) and this is assumed for H_2O and NH_2 since the noble gas crystals are face-centered cubic (163). These examples will be discussed further at the end of this section. The correlation from the A_1 ground librator state in $\bar{C}_{2V}$ to G is $A_1 \longrightarrow A_1\bar{A}_1 + E\bar{A}_1 + F_2\bar{A}_1 + F_1\bar{A}_2 + F_2\bar{A}_2 + F_1\bar{B}_1 + F_2\bar{B}_1 + A_2\bar{B}_2 + E\bar{B}_2 + F_1\bar{B}_2$. The degeneracy factor is 24. The positions of the levels at the hindered rotor limit is found by assuming only minima separated by 90° contribute to the splittings. Matrix elements for minima separated by a 90° rotation perpendicular to the plane of the molecule are denoted by β. The other fourfold axes of the crystal bisect the principal axes in the plane of the molecule and the moments of inertia of the molecule about both fourfold crystal axes are $(I_a + I_b)/2$. The matrix elements for minima separated by a 90° rotation about these axes are denoted by α. The relative energies are given in Table XVI and an energy diagram in Figure 15. As an approximation for this diagram we let $\beta = \alpha/2$. These values would be found for a particular case by assuming a potential function and doing an elaborate

TABLE XVI. THE RELATIVE HIGH BARRIER ENERGIES OF LIBRATIONAL STATES FROM (O_h, $\bar{C}_{2V}$) FORMING THE GROUND LIBRATIONAL STATE IN $\bar{\bar{C}}_{2V}$.

Symmetry	Energy
$A_1\bar{A}_1$	$4\alpha + 2\beta$
$E\bar{A}_1$	$-2\alpha + 2\beta$
$F_2\bar{A}_1$	-2β
$F_1\bar{A}_2$	2α
$F_2\bar{A}_2$	-2α
$F_1\bar{B}_1$	2α
$F_2\bar{B}_1$	-2α
$A_2\bar{B}_2$	$-4\alpha - 2\beta$
$E\bar{B}_2$	$2\alpha - 2\beta$
$F_1\bar{B}_2$	2β

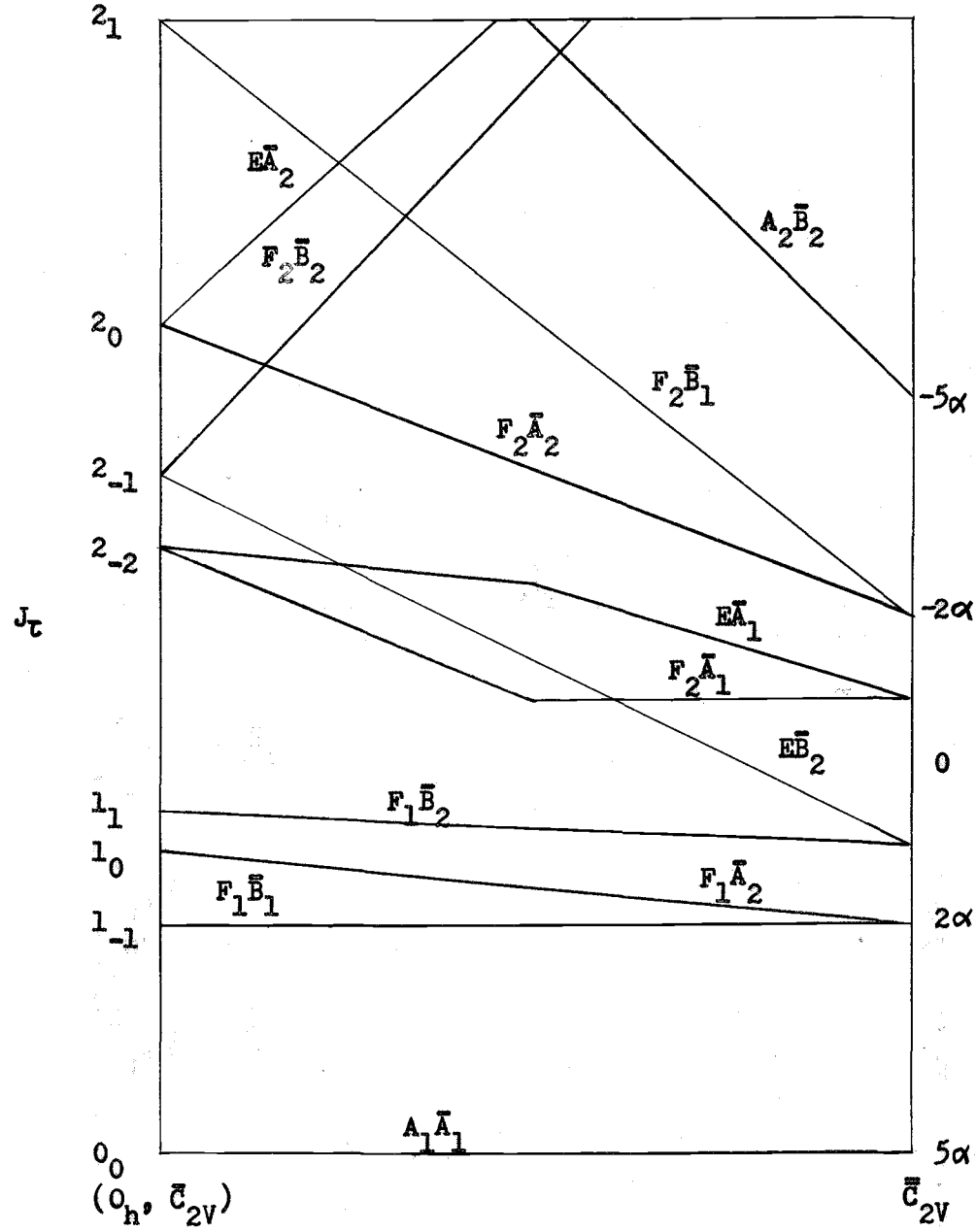

Figure 15. Correlation of ground state librational levels for an asymmetric rotor from the $(O_h, \bar{C}_{2V})$ free rotor limit to the $\bar{C}_{2V}$ hindered rotor limit. For convenience we have chosen $\beta = \alpha/2$.

calculation. The hindered rotor limit will be changed in general by the values of α and β.

The nuclear spin wave functions have the symmetry $A_1\bar{A}_1$ for ortho molecules and $A_1\bar{B}_2$ for para molecules. For a nonlinear XY_2 molecule the overall wave function must be $\Gamma\bar{A}_1$ or $\Gamma\bar{A}_2$ for Y a boson and $\Gamma\bar{B}_1$ or $\Gamma\bar{B}_2$ for Y a fermion. Assuming a vibronic state of symmetry $A_1\bar{A}_1$, ortho (para) molecules must be in $\Gamma\bar{A}_1$ or $\Gamma\bar{A}_2$ ($\Gamma\bar{B}_1$ or $\Gamma\bar{B}_2$) rotational states for Y a boson and vice versa for Y a fermion.

Assuming only the lowest spin states are populated greatly reduces the complexity in the selection rules. For $A_1\bar{A}_1$ vibrations (ν_1 and ν_2) the orientation transitions are $A_1\bar{A}_1 \longrightarrow F_1\bar{A}_2$; $F_1\bar{B}_1 \longrightarrow F_1\bar{B}_2$, $E\bar{B}_2$ in the infrared and $A_1\bar{A}_1 \longrightarrow A_1\bar{A}_1$, $E\bar{A}_1$, $F_2\bar{A}_1$; $F_1\bar{B}_1 \longrightarrow F_1\bar{B}_1$, $F_2\bar{B}_1$ in the Raman effect. The orientation transitions for ν_3 ($A_1\bar{B}_2$) are $A_1\bar{A}_1 \longrightarrow F_1\bar{B}_1$; $F_1\bar{B}_1 \longrightarrow A_1\bar{A}_1$, $E\bar{A}_1$, $F_2\bar{A}_1$ in the infrared and $A_1\bar{A}_1 \longrightarrow E\bar{B}_2$; $F_1\bar{B}_1 \longrightarrow F_1\bar{A}_2$, $F_2\bar{A}_2$ in the Raman effect.

The ground vibronic state for H_2O has the symmetry $A_1\bar{A}_1$. The overall wave function must be $\Gamma\bar{B}_1$ or $\Gamma\bar{B}_2$ since the proton is a fermion. The nuclear spin wave functions have the symmetry $3A_1\bar{A}_1$ (ortho) + $A_1\bar{B}_2$ (para). Therefore, para molecules must occupy $\Gamma\bar{A}_1$ or $\Gamma\bar{A}_2$ rotational states and ortho molecules must occupy $\Gamma\bar{B}_1$ or $\Gamma\bar{B}_2$ rotational states for the ground vibronic states. For the ν_1 and ν_2 vibrations which have the symmetry $A_1\bar{A}_1$, the allowed orientation transitions are those which change by the symmetry $\Gamma(\mu)$ = $F_1\bar{A}_2$. Assuming only the lowest levels for each spin are populated gives the allowed orientation transitions as $A_1\bar{A}_1 \longrightarrow F_1\bar{A}_2$ and $F_1\bar{B}_1 \longrightarrow F_1\bar{B}_2$, $E_2\bar{B}_2$. For the ν_3 vibration of symmetry $A_1\bar{B}_2$, the

allowed orientation transitions are $A_1\bar{A}_1 \longrightarrow F_1\bar{B}_1$ and $F_1\bar{B}_1 \longrightarrow A_1\bar{A}_1$, $E\bar{A}_1$, $F_2\bar{A}_1$. At liquid helium temperatures one would expect three line spectra for ν_1 and ν_2 and four lines for ν_3. Complications to this are from bands due to nonrotating molecules (126, 127) and polymers (152). Near the high barrier limit the ν_3 spectrum would become three lines. The observed spectra are quite complex (22, 53, 69, 126, 127, 128). The hindered rotor model is offered as one limit for H_2O to compare to the free rotor limit. The spectra seem to be explained better by a nearly free rotor although the differences between experiments make assignments quite difficult.

The ground vibronic state for NH_2 has the symmetry $A_1\bar{B}_1$ (68). The symmetry requirements are now that ortho molecules must occupy $\Gamma\bar{A}_1$ or $\Gamma\bar{A}_2$ rotational states and para molecules must occupy $\Gamma\bar{B}_1$ or $\Gamma\bar{B}_2$ rotational states in the ground vibronic state. The allowed vibration-orientation transitions are the same as for H_2O. The conclusions of McConnell (97), and Robinson and McCarty (130, 131) point to conversion of nearly all the para molecules to ortho at $4.2^{\circ}K$. This would eliminate rotational structure in the vibrational bands because the only allowed orientation transition would be $A_1\bar{A}_1 \longrightarrow F_1\bar{A}_2$ for ν_1 and ν_2, and $A_1\bar{A}_1 \longrightarrow F_1\bar{B}_1$ for ν_3. Milligan and Jacox (100) observed one component in the ν_3 region and three components in the ν_2 region of NH_2 in Ar at $14^{\circ}K$. A possible explanation of the ν_2 spectrum may be that the doublet at 1495 and 1498 cm^{-1} is due to nonrotating molecules and the peak at 1523 cm^{-1} is due to the $A_1\bar{A}_1 \longrightarrow F_1\bar{A}_2$ transition. This suggests that the ν_3 spectrum should show an additional line due to the $A_1\bar{A}_1 \longrightarrow F_1\bar{B}_1$ transition besides

the 3220 cm^{-1} line which appears. Robinson (131) also reported lines insensitive to temperature and this is consistent with non-rotating molecules. The $A_1\bar{A}_1 \longrightarrow F_1\bar{A}_2$ transition appears to be about .9 the free rotor value, but a lack of information on para molecules and states originating from $J = 2$ make any conclusions about NH_2 being a hindered rotor rather uncertain.

The ground vibronic state for NO_2^- has the symmetry $A_1\bar{A}_1$. Since ^{16}O is a boson, the overall wave function must be $\Gamma\bar{A}_1$ or $\Gamma\bar{A}_2$. The nuclear spin wave function has the symmetry $A_1\bar{A}_1$ so in the ground vibronic state only the $\bar{A}_1$ or $\bar{A}_2$ rotational levels may be occupied. Assuming there are only ortho molecules and that the hindered rotor limit is appropriate, orientation transitions from the two lowest levels are $A_1\bar{A}_1 \longrightarrow F_1\bar{A}_2$, and $F_1\bar{A}_2 \longrightarrow A_1\bar{A}_1$, $F_2\bar{A}_1$, $E\bar{A}_1$ for ν_1 and ν_2. The corresponding transitions for ν_3 are $A_1\bar{A}_1 \longrightarrow F_1\bar{B}_1$ and $F_1\bar{A}_2 \longrightarrow F_1B_2$, $E\bar{B}_2$. The observed spectra are much more complicated than this and the hindered rotor model of Narayanamurti, Seward, and Pohl (106) involves librational changes as well. Their one dimensional model does not seem to be realistic but explains the spectra quite well. Without some simplifying assumptions, interpreting the spectra would be quite difficult.

F. Summary

The symmetry species of either internal or external quantities may be found quite easily when G is a direct product. If G is not a direct product then no simple statements can be made. There are four cases of direct products to consider, two involving rotational groups and two involving direct product groups.

i) If S is a rotational group then G = 'S' x '$\bar{M}$' (P). The electric tensors in external axes have their usual symmetry species from S times the totally symmetric species from $\bar{M}$(P). The electric tensors in internal coordinates have the symmetry species that they have in the group $\bar{M}$(P) times the totally symmetric species from S. The molecular symmetries from $\bar{M}$ are found by correlating to $\bar{M}$(P) and multiplying by the totally symmetric species from S. Examples of this type are found in the groups (C_3, $\bar{C}_{3V}$) and (D_3, $\bar{D}_{3h}$).

ii) If $\bar{M}$ is a rotational group then G = 'S'(P) x '$\bar{M}$'. The discussion is the same as in case i) except for interchanging S and $\bar{M}$. The symmetry species from S are found in G by correlating to S(P).

iii) If neither S nor $\bar{M}$ is a rotational group and if S is a direct product group then G = 'S'(P) x '$\bar{M}$'. All the molecular symmetries have their usual symmetry species from $\bar{M}$, including the electric tensors in internal coordinates, times the totally symmetric species from S(P). The symmetry species for a quantity in external axes have the symmetry species in S(P), which is found from correlation with S, times either the totally symmetric species or an antisymmetric species from $\bar{M}$, depending on whether the symmetry species

in S was symmetric or antisymmetric to the operation involved in the direct product (i or σ_h). The antisymmetric species from $\bar{M}$ is the representation which has the character +1 for all P's and -1 for all P*'s; for $\bar{M} = \bar{T}_d$ this is $\bar{A}_2$, for $\bar{M} = \bar{D}_{3h}$ this is $\bar{A}_1''$, etc. If S contains i, then μ(external) has the antisymmetric species in $\bar{M}$ and α(external) has the totally symmetric species in $\bar{M}$; this is because μ is u and α is g with respect to i. If the direct product is with $\{E, \sigma_h\}$ then a primed species in S has the antisymmetric species in $\bar{M}$. An example of this case is found in the group $(O_h, \bar{T}_d)$ where the molecular species were preserved, but in the external axes $\Gamma(\mu) = F_1\bar{A}_2$ and $\Gamma(\alpha) = A_1\bar{A}_1 + E\bar{A}_1 + F_2\bar{A}_1$. If both S and $\bar{M}$ are direct product groups, then this case is the simplest to use since the molecular symmetries do not change in going from $\bar{M}$ to G.

iv) If neither S nor $\bar{M}$ is a rotational group and if $\bar{M}$ is a direct product group then G = 'S' x '$\bar{M}$'(P). Again the discussion parallels that of case iii), interchanging S and $\bar{M}$. This case is chosen for diatomic molecules where the number of molecular symmetry species is a minimum.

To gain some feeling for the splittings to be expected in consequence of tunneling effects, we summarize some asymptotic formulas appropriate for the group $(O_h, \bar{C}_{\infty v})$ near the $\bar{C}_{4v}$ limit. The librational frequency is $\tilde{\nu}_L = 4(\tilde{B}\tilde{V}_o)^{\frac{1}{2}}$ where $\tilde{B}$, the rotational constant, and $\tilde{V}_o$, the barrier height, are expressed in cm^{-1}. The splitting of the A_{1g} and F_{1u} levels in the ground state is of the order of

$$(E_{F_{1u}} - E_{A_{1g}})/\tilde{\nu}_L \approx \alpha \exp(-\frac{\pi^2}{16}\alpha) \quad \text{(see the Appendix)}$$

where

$$\alpha = 2\left(\frac{\tilde{V}_o}{\tilde{B}}\right)^{\frac{1}{2}} = \frac{1}{2}\,\frac{\tilde{\nu}_L}{\tilde{B}}$$

Thus we may write

$$\Delta E = E_{F_{1u}} - E_{A_{1g}} \approx 2\alpha^2\tilde{B}\exp(-\frac{\pi^2}{16}\alpha).$$

For $\alpha = 16$, $\Delta E \approx .03\ \tilde{B}$ and if $\tilde{B} = 10\ cm^{-1}$, then $\tilde{\nu}_L = 320\ cm^{-1}$ and $\Delta E \approx .3\ cm^{-1}$; however, if $\tilde{B} = .5\ cm^{-1}$ and $\tilde{\nu}_L = 50\ cm^{-1}$, then $\alpha = 50$ and $\Delta E \approx 10^{-10}\ cm^{-1}$. We conclude that splittings may be observed only for relatively large $\tilde{B}$ and relatively small α.

Using just the symmetry of the problem to obtain information has many advantages. A correlation diagram of the energy levels between the free rotor and high barrier limits can be easily made for any system and can be extended to include any desired energy levels. The most readily available information from a qualitative scheme is the number of components to expect in the spectra of a system. The magnitude of the splitting or the order of close-lying states must be found from calculations, and then certain assumptions must be made about the potential function. In certain cases the hindered rotor limit makes a good approximation.

We have used the full symmetry group in classifying all the states. The studies by Hougen (71, 72) were most helpful in understanding the rotational problem for the full group and the treatise by Longuet-Higgins (93) was particularly useful for classifying the nuclear spin states from the permutation groups.

IV. RAMAN SPECTRA OF METHANE IN NOBLE GAS MATRICES AND THE LOWEST TEMPERATURE CRYSTAL PHASES

In order to determine more about the rotational motion of methane, a series of experiments were performed using the Raman effect. Since the most intense transitions in the Raman effect are usually different from those in the infrared (66, 67), much additional information can be determined. Previous Raman work has not resolved any structure in the vibrational bands of matrix isolated methane (21) nor comparable structure to the ν_3 infrared spectrum of neat methane (2, 25), therefore comparisons with infrared data could not be made.

A. Experimental Methods

The Raman experiment was performed using a Cary 82 spectrophotometer and an argon ion laser as a light source. The lasers used were Coherent Radiation Laboratory model 52B and Spectra-Physics model 164. The first experiments used a Model CS-202 Displex TM Helium Refrigerator made by Air Products and Chemicals, Inc. to achieve low temperatures and later a liquid helium dewar made by Hofman Laboratories, Inc., was used.

The Cary 82 spectrophotometer is designed for use with a laser source. The optical system has three monochromators and there is a multiplier phototube used for detection. The frequency calibration was done with a 1/3 watt neon light and an argon ion laser.

An argon ion laser has two strong lines at 4880Å and 5145Å. The power output is comparable for both lines, but spectra with a

smaller noise level were obtained with the 5145Å line and this line was used more frequently. The maximum power for the 5145Å line was about .70 watts using the Coherent Radiation Laboratory laser and 1.8 watts with the Spectra-Physics laser.

The Displex TM Helium Refrigerator uses commercial-grade helium as a refrigerant and operates from 12°K to 300°K. The Hofman dewar has liquid helium as a coolant which boils at 4.2°K. The volume of the liquid helium well is one liter and this amount of helium will last about four hours. The helium dewar was precooled with liquid nitrogen in both wells. The pressure before a liquid helium transfer was 10^{-6} torr. Just prior to a transfer the inner well is emptied of liquid nitrogen. The transfer tube used is a standard flexible model made by Janis Research Company, Inc.

The samples were prepared by introducing a gas or gas mixture into a bulb evacuated to a pressure of less than 10^{-4} torr. The noble gases and CH_4 were from the Matheson Co. The CH_4 is C.P. grade (99.0%), the Ar is ultra-high purity (99.999%), and the Kr and Xe are both research grade (99.995%). The CH_3D and CD_4 are supplied by Volk and are believed to have 99% isotopic purity. However, the CH_3D sample was found to contain O_2 and N_2 from analyzing the Raman spectrum. The mixtures were prepared by first introducing the particular methane isotope into the bulb until the desired pressure was reached. Then the noble gas was introduced until the desired pressure was reached by keeping the pressure outside the bulb always greater than that inside, so that the flow was always into the bulb. The concentrations of methane are expressed

as a percentage of the partial pressure of methane to the total pressure of the mixture. The mixtures were left at room temperature for at least 24 hours to insure a uniform sample.

The sample tip used for the Displex experiments was an aluminum bar of square 1" x 1" cross-section extending about 2" from the Displex cold finger, the long axis being horizontal (see Figure 16). The sample tip used for the helium dewar experiments was a copper cone whose axis was in a vertical position (see Figure 16). Both of these tips were in thermal contact with the cold finger by using a crushed indium washer. It was found from the Displex experiments that spectra with the lowest noise level and greatest intensity were obtained when the angle between the incoming laser beam and the face of the aluminum block was about 20° (see Figure 16). The copper cone was designed to have this same angle and then small adjustments from vertical could be made to improve the spectra.

The temperature of both of these systems was measured with a chromel versus gold-.07% iron thermocouple. The reference junction was in an ice-water bath at $0^{\circ}C$. The temperature is believed to be accurate to $\pm 1^{\circ}$ from checks with ice-water baths versus liquid nitrogen at the boiling point. The cold junction in both cases was on the cold finger just away from the sample tip. In addition the Displex unit has a hydrogen vapor pressure gauge which is useful in the range 12-25°K. The temperature of the sample is not known precisely, but it is assumed to be nearly that of the cold tip. So the temperatures reported for the cold tips represent a lower limit for the samples.

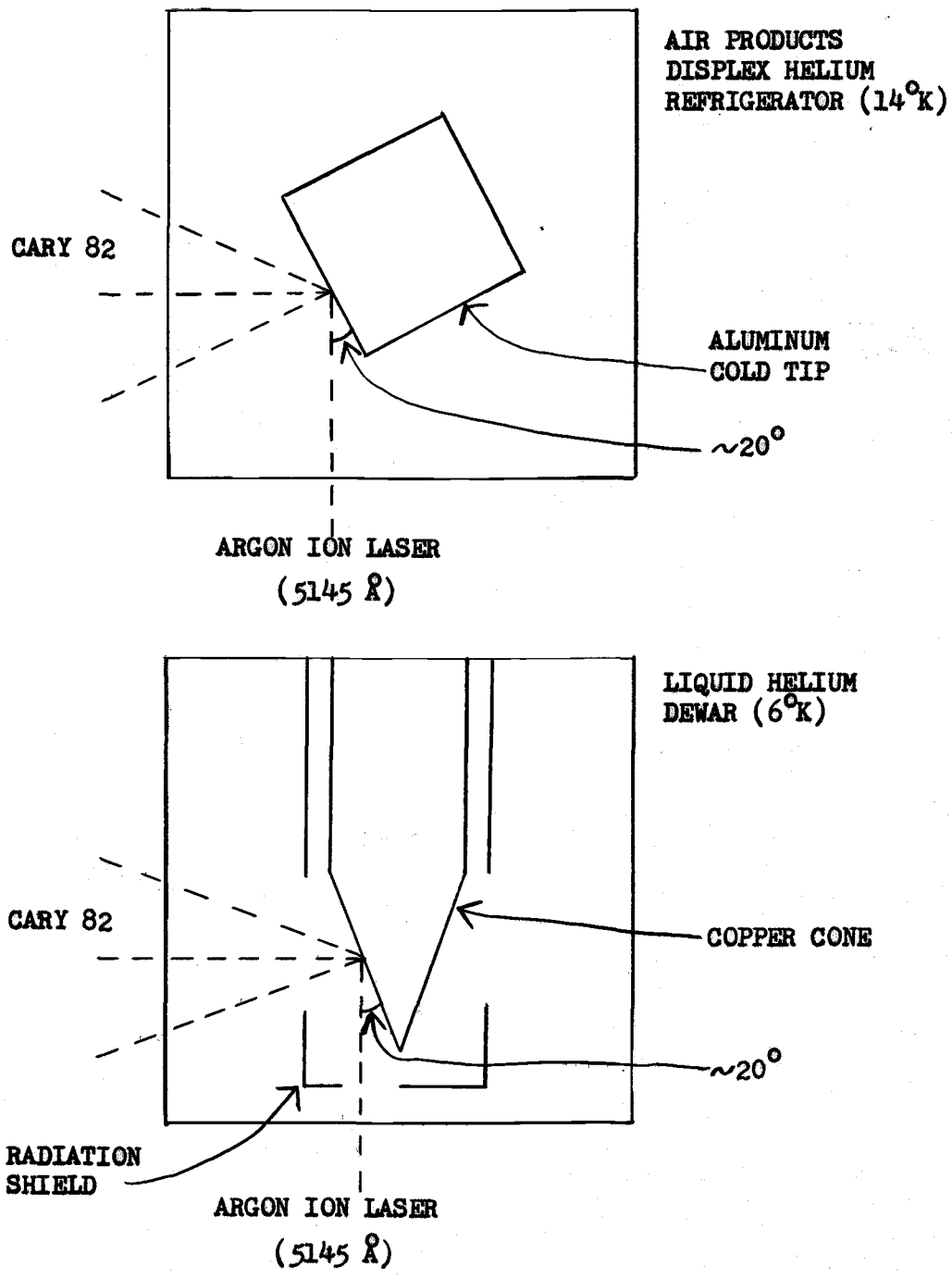

Figure 16. Schematic diagrams of the experimental apparatus for low temperature Raman spectroscopy.

The gas samples are sprayed onto the cold tip at a temperature of $14^{\circ}K$ using the Displex unit or $6^{\circ}K$ using the helium dewar. The temperature of the Displex experiment was varied by opening a valve allowing some helium to bypass the refrigeration cycle. The temperature of the copper cone with the helium dewar was found to vary considerably depending on the laser power. At the maximum power of 1.8 watts, the temperature was greater than $20^{\circ}K$. When the power was .5 watts, the heating was small ($\sim .5^{\circ}$) and this is the laser power used in most of the helium dewar experiments.

B. Vibrational Symmetries

An XY_4 molecule has four fundamental modes of vibration. These are pictured on page 100 of reference 67. The symmetric stretch is $\nu_1(A_1)$, the doubly degenerate bend is $\nu_2(E)$, the antisymmetric stretch is $\nu_3(F_2)$, and the triply degenerate bend is $\nu_4(F_2)$. The notation for a tetrahedral XYZ_3 molecule with a central X atom follows that for the XY_4 molecule. When the symmetry is lowered from T_d to C_{3V} a mode of F_2 symmetry becomes A_1+E and, for example, the ν_3 fundamental becomes $\nu_3(A_1) + \nu_3(E)$.

The selection rules for XY_4 molecules allow all four fundamentals in the Raman effect and all six fundamentals for XYZ_3 molecules. In the matrix diluted sample the $\nu_4(F_2)$ bend for CH_4 and CD_4 ($\nu_4(A_1)$ and $\nu_4(E)$ for CH_3D) is too weak to be seen although it appeared in neat CH_4. The $\nu_3(F_2)$ stretch and $\nu_4(F_2)$ bend are infrared active for XY_4 molecules and again all six fundamentals are active for XYZ_3 molecules. Therefore comparisons between infrared and Raman spectra are limited to the ν_3 band for CH_4 and CD_4 and can be made for all but $\nu_4(A_1)$ and $\nu_4(E)$ for CH_3D. Very important conclusions can also be made between ν_2 and ν_3 of CH_4 and CD_4 since the selection rules differ for E and F_2 bands.

In discussing the experimental results it will be necessary to occasionally refer to the group theory in Chapter III although a detailed analysis will be carried out in Chapter V. The symmetry group for matrix isolated CH_4 and CD_4 is $(O_h, \bar{T}_d)$ since the crystal structure of Ar, Kr, and Xe is face-centered cubic (163), the site

symmetry being O_h. Similarly, the group for matrix isolated CH_3D is $(O_h, \bar{C}_{3V})$. The symmetry group for the rotating molecules in neat CH_4 is assumed to be $(O_h, \bar{T}_d)$ from the corresponding structure of Phase II CD_4, and assuming only nearest neighbors contribute to the crystal field (80).

C. Methane in Noble Gas Matrices

1. CH_4 in Argon

The spectra of CH_4 in Ar (Figure 17) show a strong ν_1 line with a low frequency shoulder, a rather weak ν_2 band with possibly three components, and a ν_3 band with at least four components.

The low frequency part of ν_1 depends on the deposition rate and concentration. For deposition at a moderate rate (2-3 ml/min) the low frequency band is fairly well-defined and has about 8 per cent the intensity of the principal line. At slow deposition rates (.1-.2 ml/min) the low frequency component is broadened and not resolved. This band is also stronger with increasing concentration of CH_4. After warming the sample to 25°K for about 30 minutes the ν_1 spectrum shows an intense low frequency peak. This is attributed to preferential sublimation of argon atoms and formation of methane microcrystals by Chamberland, Belzile and Cabana (23, 57). This interpretation is supported by the behavior of ν_1 in that the faster deposit or higher concentration gives a more resolved low frequency component and that this band is near the position of ν_1 in neat methane.

The ν_2 band has two peaks separated by 20 cm^{-1} with the possibility of a third, between them. Using the gas phase notation (67), these transitions would correspond to Q(1) and S(0). An octahedral field splits S(0) for ν_2 (see Table XI) into two components ($A_1\bar{A}_1 \longrightarrow E\bar{E}$, $F_2\bar{E}$). A third peak may either be R(1) or the other part of S(0). Since the gas phase separation of Q(1) and S(0)

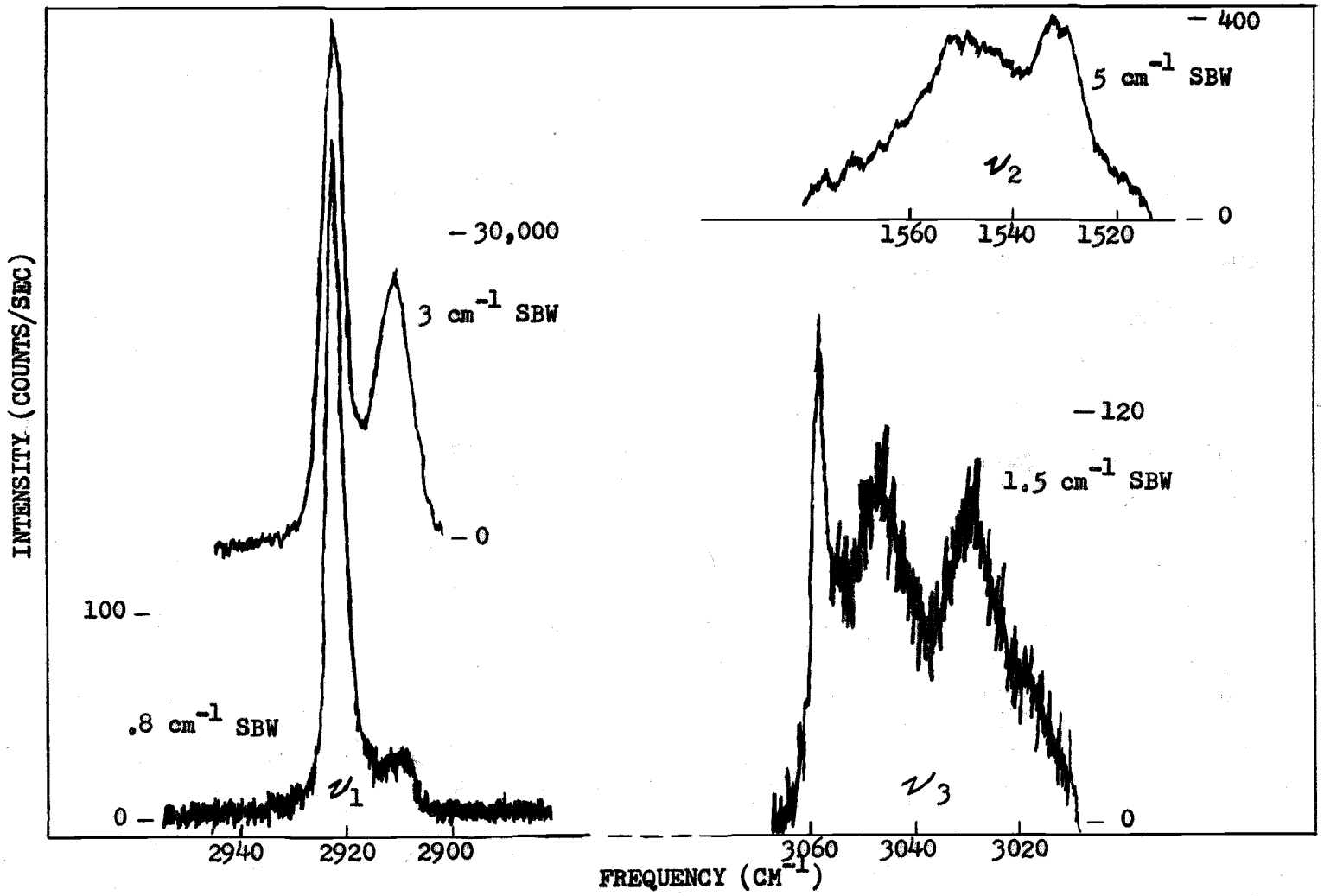

Figure 17. Raman spectra of 2% CH_4 in argon at 14°K. The upper trace of ν_1 was recorded after the sample was warmed to 25°K for 30 minutes then cooled again to 14°K.

is $6\tilde{B}$ or 31.4 cm^{-1} (66), CH_4 must be considered a hindered rotor if the structure is due to rotation.

The ν_3 region has four principal components. The feature at 3018 cm^{-1} is seen to grow markedly on warming the matrix and is assigned to CH_4 aggregates. The very sharp peak at 3057 cm^{-1} is assigned as the A_1 component of $2\nu_2$ in resonance with ν_1. Additional support for the $2\nu_2$ assignment is that A_1 molecular transitions are isotropic and therefore usually have relatively narrow lines. The other components at 3028 cm^{-1} and 3046 cm^{-1} are assigned as Q(1) and S(0) respectively. S(0) for ν_3 is also split by an octahedral field ($A_1\bar{A}_1 \longrightarrow E\bar{F}_2$, $F_2\bar{F}_2$), but neither another component of S(0) nor R(1) could be resolved. The separation of Q(1) and S(0) is 18 cm^{-1} compared to the 33.1 cm^{-1} gas phase value ($6\tilde{B}\ (1 + \zeta_3)$).

2. CH_4 in Krypton

The spectra of CH_4 in Kr (Figure 18) differ from those with Ar as the host in that the bands due to methane aggregates are absent. The ν_1 spectrum shows a slight broadening at lower frequencies, but nothing resembling the band in Ar. The ν_3 spectrum is also missing the lowest frequency component which appeared in Ar. This difference can be accounted for in part by the fact that Kr has a much lower vapor pressure than Ar and loss of Kr due to sublimation should be much less.

The ν_2 and ν_3 bands show structure which is comparable to that in Ar. The ν_2 region has a well-defined triplet. The two most intense bands are separated by 22 cm^{-1} and in the gas phase notation

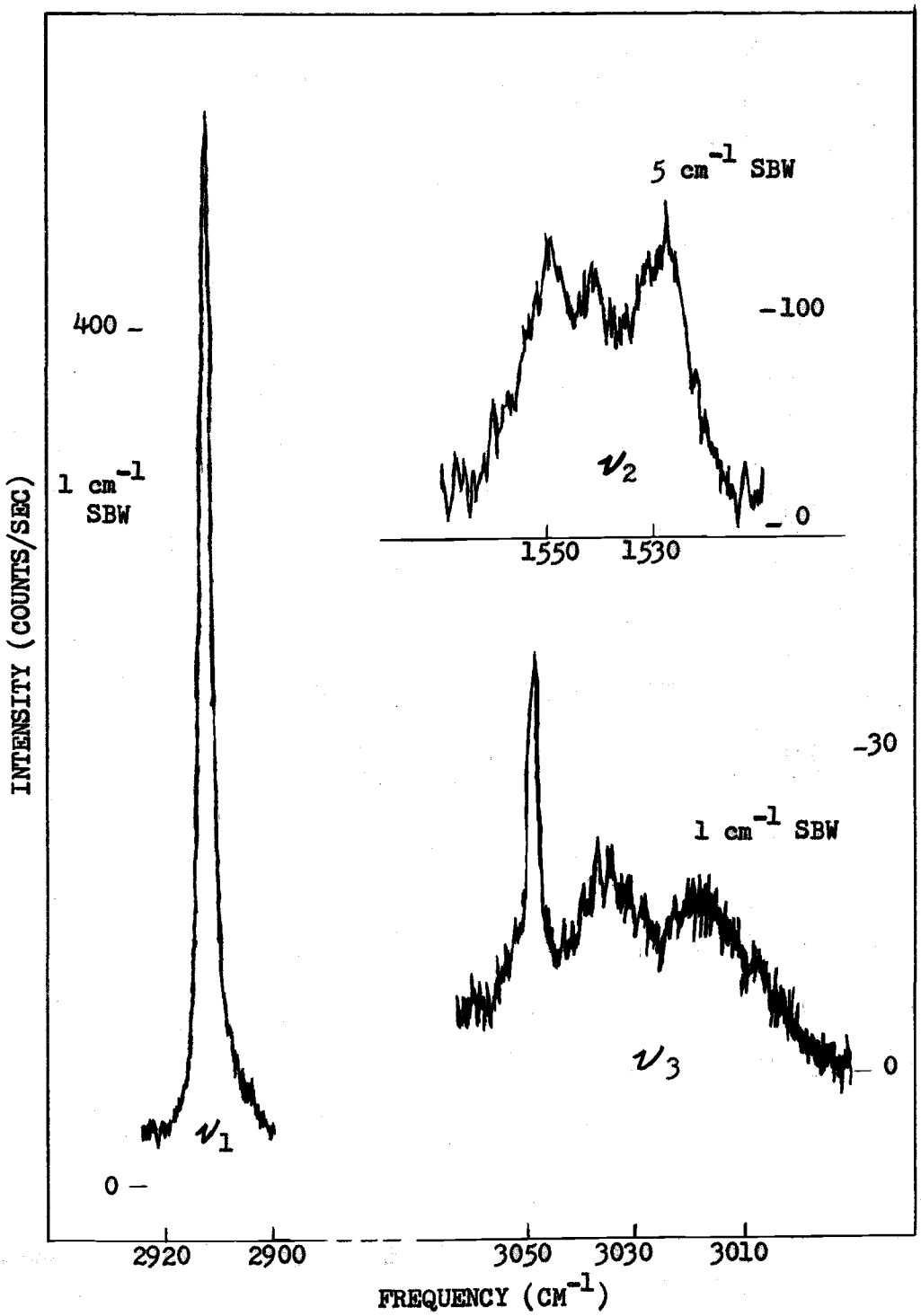

Figure 18. Raman spectra of 2% CH_4 in krypton at 14°K.

would be assigned as Q(1) and S(0). The third feature may either be part of S(0) or R(1). The ν_3 region has two rather broad bands assigned as Q(1) and S(0) which are separated by 18 cm^{-1}. There is a low frequency shoulder to S(0) which again may either be the other component of S(0) or R(1). The very sharp feature at 3049 cm^{-1} is assigned as the A_1 component of $2\nu_2$.

3. CH_4 in Xenon

The spectra of CH_4 in Xe (Figure 19) have no evidence of methane aggregates. The ν_1 spectrum is a very sharp and symmetric feature. The ν_2 band is quite weak with the Q(1) line observed, but a very broad feature in the region where S(0) is expected. The ν_3 region has three components, assigned as Q(1), S(0), and $2\nu_2$. The separation of Q(1) and S(0) is 22 cm^{-1} for ν_3.

The observed Raman frequencies for CH_4 in the noble gas matrices are listed in Table XVII. The effect of the size of the noble gas lattices is seen in the shifts in frequency of the vibrations. This is noted in both the stretching (ν_1 and ν_3) and bending (ν_2) regions. The diameters of the vacant lattice sites are 3.8Å for Ar, 4.0Å for Kr, and 4.4Å for Xe (36). The diameter of the CH_4 molecule is 4.1Å (23). The spectra show the trend of decreasing frequency with increasing lattice site. This pattern is consistent with the CH_4 molecule occupying a substitutional site (23).

4. CD_4 in Xenon

The spectra of CD_4 in Xe (Figure 20) provide a general comparison

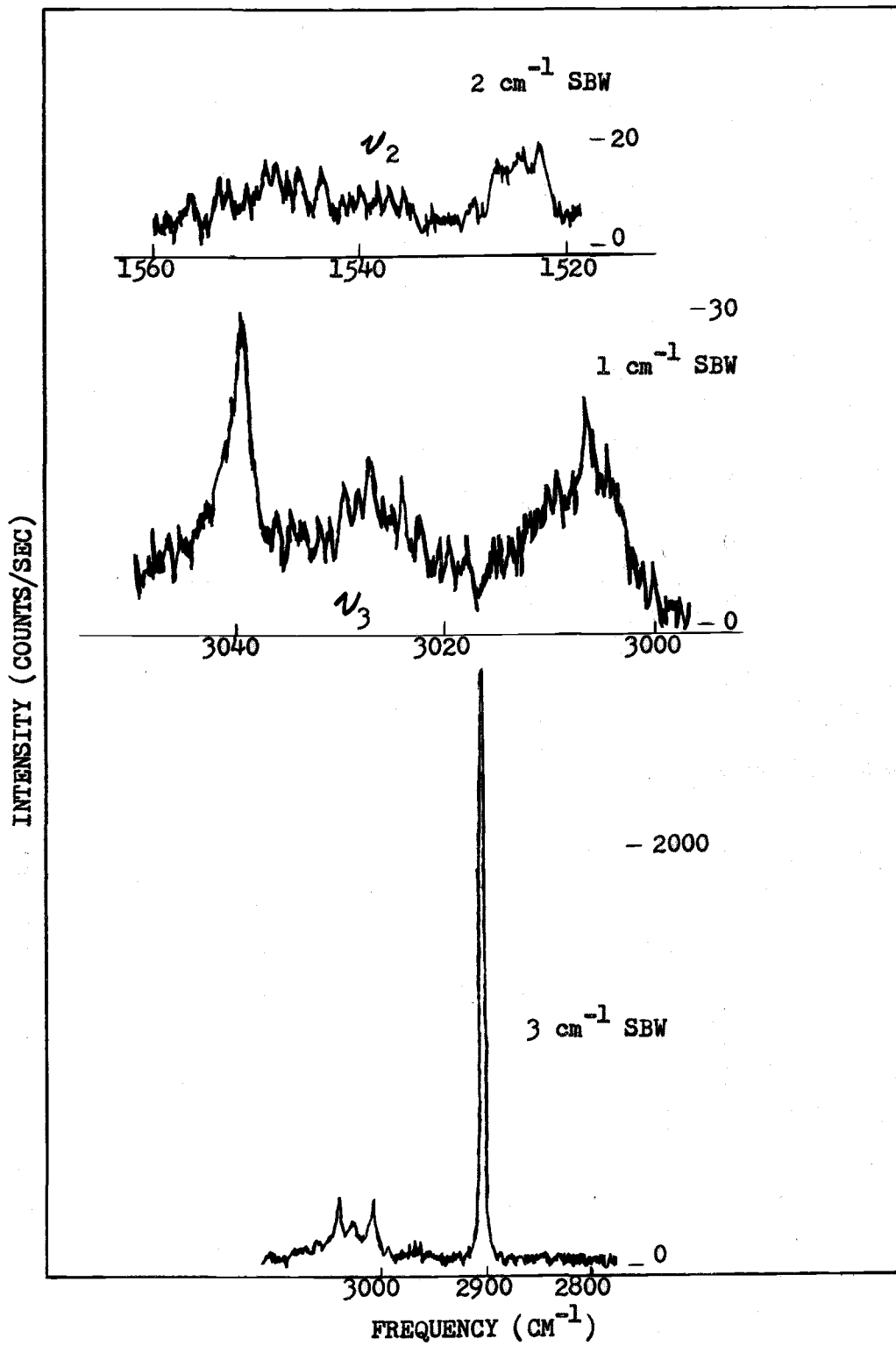

Figure 19. Raman spectra of 2% CH_4 in xenon at 6°K.

TABLE XVII. OBSERVED RAMAN FREQUENCIES OF 2% METHANE IN THE NOBLE GAS MATRICES, AT O SITES IN NEAT CH_4, AND COMPARISONS WITH INFRARED FREQUENCIES.

Raman Frequency, cm^{-1}

		CH_4/Ar (14°K)	CH_4/Kr (14°K)	$CH_4(O)$ (6°K)	$CH_4(O)$ (12°K)[1]	CH_4/Xe (6°K)	CD_4/Xe
ν_1		2922	2913	2908	2907	2901	2090
ν_2	Q(1)	1532	1527	1527	1530	1524	
			1541	1545			1087 (broad)
	S(0)	1552	1549	1552	1553		
	S(1)			1560			
ν_3	Q(1)	3028	3018	(3011)[2]		3006	2250
	R(1)			3019			
	S(0)	3046	3036	3036	3037	3028	2261
	S(1)			3044			
$2\nu_2(A_1)$		3057	3049			3039	2167

Infrared Frequency, cm^{-1}

		CH_4/Ar[3] (10°K)	CH_4Kr[3] (8°K)	$CH_4(O)$[2] (9°K)	CH_4/Xe[3] (8°K)
ν_3	P(1)	3021.6	3010.1	3004	2995.6
	Q(1)	3028.6	3018.3	3011	3005.3
	R(0)	3037.4	3026.5	3020.3	3013.3
	R(1)		3030.0	3026.4	3018.3

1. Reference 2
2. Reference 25
3. Reference 23

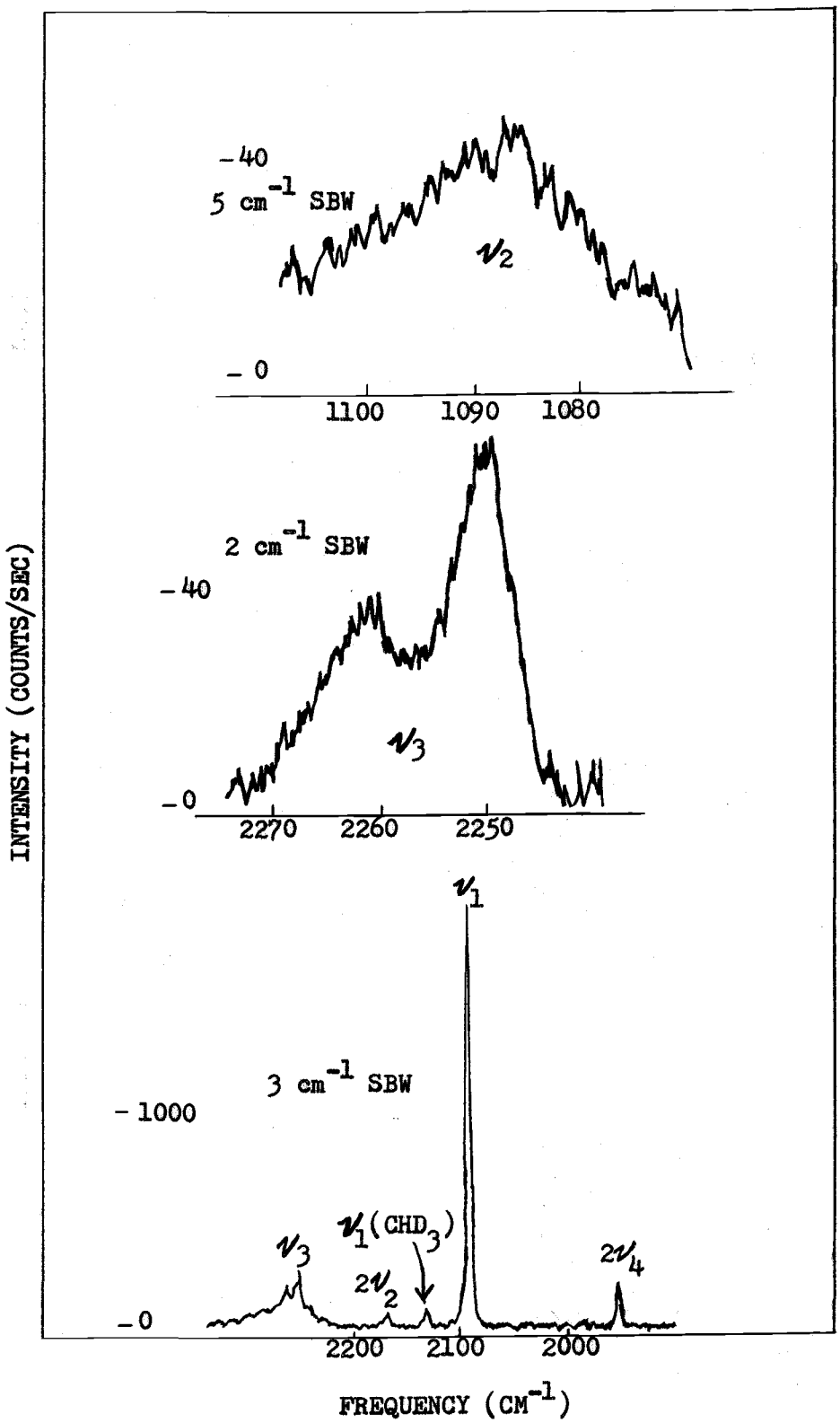

Figure 20. Raman spectra of 2% CD_4 in xenon at 6°K.

with CH_4 and more specifically the ν_3 band is free of the $2\nu_2$ feature. The ν_1 region shows a strong symmetrical ν_1 band in resonance with $2\nu_4$ and $2\nu_2$, and ν_1 for CHD_3 also appears. The ν_2 band is weak and broad and does not show any structure. There are two principal components which make up ν_3 and these are assigned as Q(1) and S(0). The difference is 11 cm^{-1} which is just half of that for CH_4. There is also a weak feature lying below ν_3 which is assigned as $\nu_3(E)$ of CHD_3. These observed frequencies are tabulated in Table XVII. The CD_4 sample is believed to have 99 per cent isotopic purity and this would give 4 per cent CHD_3 which agrees with the intensities observed. The CHD_3 assignments have been made using the infrared results of Chapados and Cabana (25). Comparisons between CH_4 and CD_4 in Xe give support to the assignment of $2\nu_2$ in resonance with ν_1 and the conclusion that the sharp feature does not belong to the ν_3 mode in CH_4.

5. <u>CH_3D in Argon</u>

The spectra of CH_3D in Ar (Figure 21) show four of the six fundamentals, $\nu_4(A_1)$ and $\nu_4(E)$ are not observed. The $\nu_2(E)$ mode appears at 1468 cm^{-1} and is very weak; ν_1 is at 2203 cm^{-1} and has a low frequency component at 2194 cm^{-1} which is presumably due to aggregates as in CH_4 (23); $\nu_3(A_1)$ is in resonance with the A_1 part of $2\nu_2$ and these frequencies are 2970 cm^{-1} and 2910 cm^{-1}; and $\nu_3(E)$ is broad with resolvable features at 3014 cm^{-1} and 3026 cm^{-1}. Also appearing is the A_1 part of the overtone, $2\nu_4(E)$, at 2310 cm^{-1} in resonance with ν_1. The evidence for rotation of CH_3D appears to be

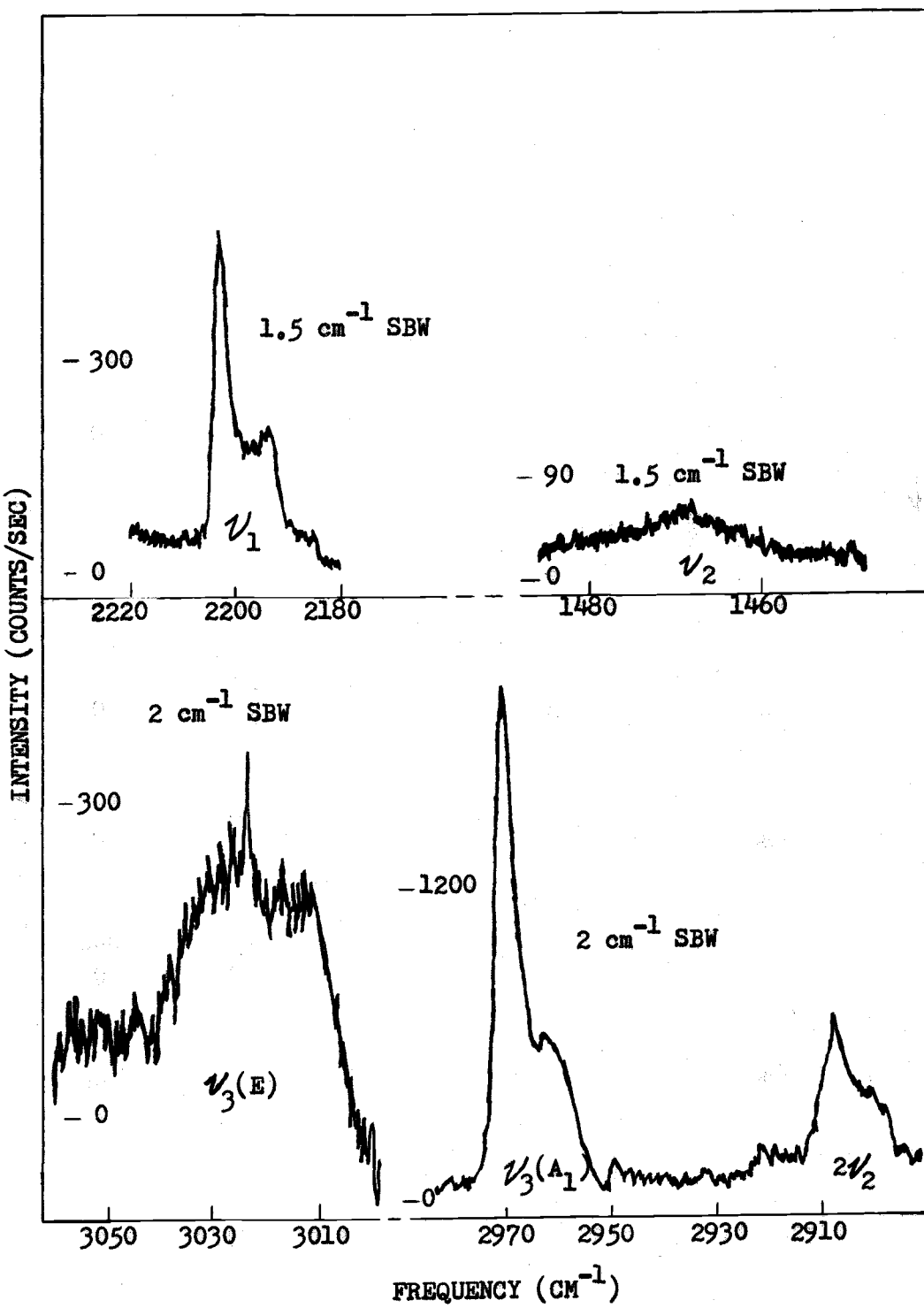

Figure 21. Raman spectra of 2% CH_3D in argon at 14°K.

limited to the $\nu_3(E)$ band where the 12 cm^{-1} splitting corresponds to a gas phase value of 23 cm^{-1} (from data in (67)). Thus if this splitting is due to rotational motion, the CH_3D molecule must also be a hindered rotor.

D. Lowest Temperature Crystal Phases of Methane

1. Neat CH_4

The Raman studies of neat CH_4 were done both with the Displex unit at about 14°K and the liquid helium dewar at about 6°K. There are features which are both temperature dependent and temperature independent. The lowest temperature crystal phase of CH_4 is designated phase III by Ballik, Gannon, and Morrison (5, 6) but has usually been labeled as phase II. The lowest temperature phase of CH_4 is believed to have the same structure as phase II of CD_4 (see Section II.B.3). The assignments will be made on the basis of the James-Keenan model (76), which is six ordered molecules on D_{2d} sites and two rotating molecules on O sites per primitive cell. The neat methane lattice to a good approximation (6, 80, 165) has rotating molecules at sites very similar to those in the noble gas crystals. Since the cubic cell dimension of CH_4 is intermediate to those of Kr and Xe (6, 36, 163) it is reasonable to compare the spectra of the O site molecules to the Kr and Xe matrix spectra (Table XVII).

The ν_1 region (Figure 22) consists of a doublet with the stronger line assigned to ordered molecules and the weaker line to rotating molecules. The frequency of the weaker line falls in the middle of the positions of ν_1 in Kr and Xe and its intensity is slightly greater.

The ν_2 spectrum at 6°K (Figure 23) appears to have five components, two principal ones and three weaker features. The 1524 cm^{-1} component is assigned to the ordered molecules and the rest of the

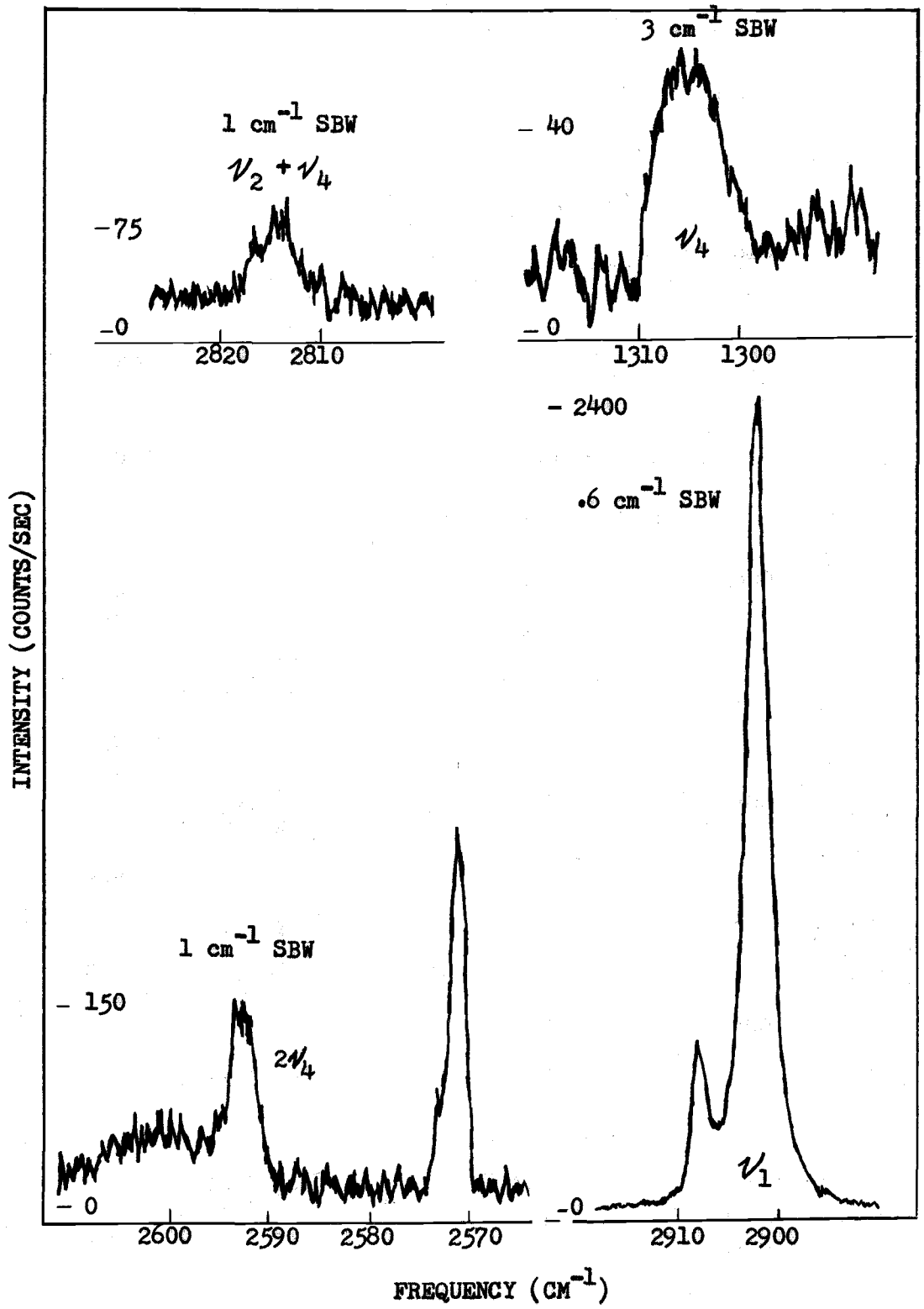

Figure 22. Raman spectra of neat CH_4 at 6°K

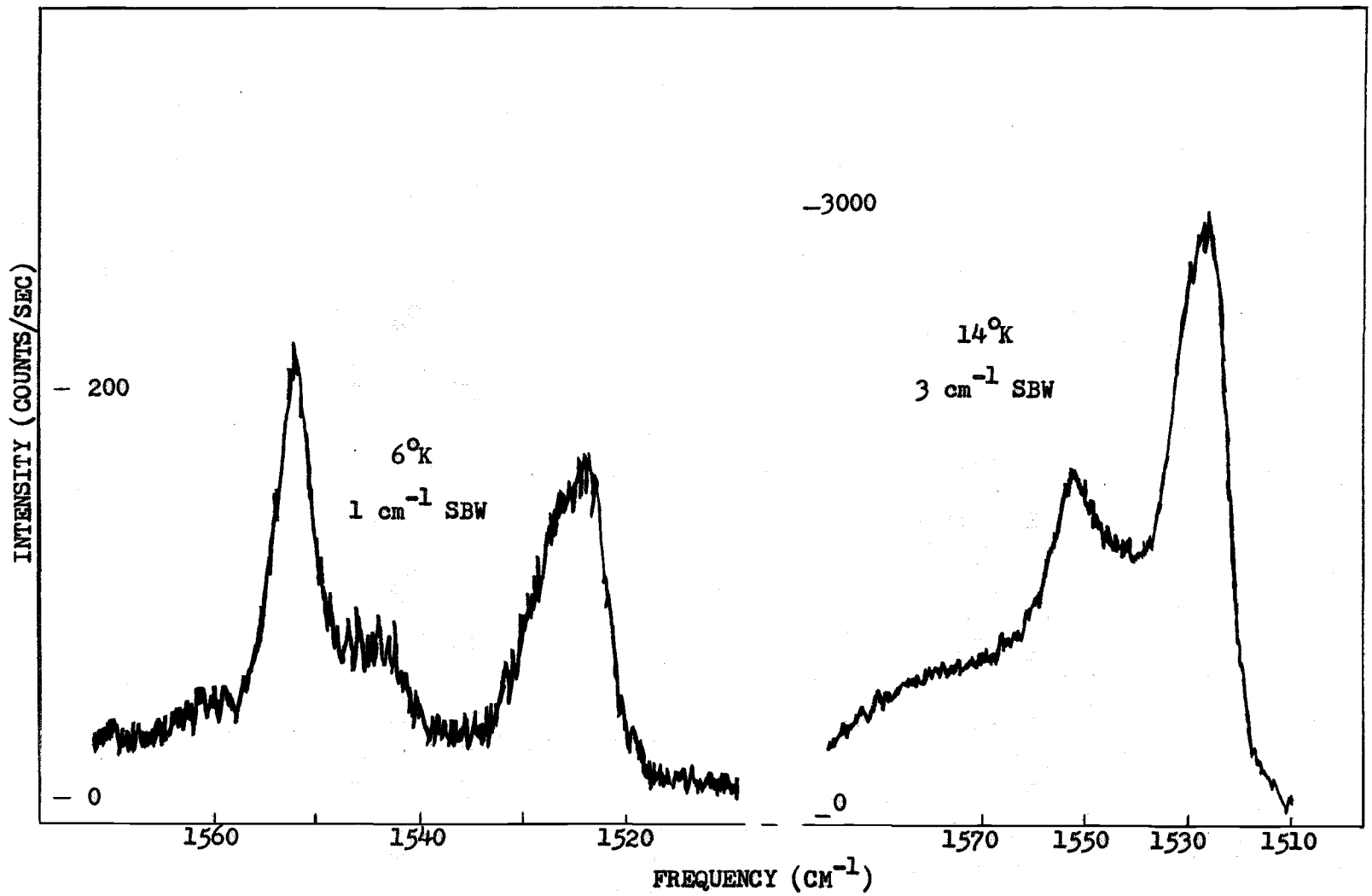

Figure 23. Raman ν_2 spectra of neat CH_4 at 6°K and 14°K.

spectrum is assigned to rotating molecules. The intense feature at 1552 cm^{-1} is assigned as one component of S(0) and its intensity increases markedly in going from 14°K to 6°K, consistent with the rotational assignment.

The ν_3 area at 6°K (Figure 24) consists of a very sharp and intense line at 3010 cm^{-1} and three much weaker bands at higher frequencies. The 3010 cm^{-1} feature is assigned to ordered molecules and the bands at 3019, 3036, and 3044 cm^{-1} are assigned as R(1), S(0), and S(1) respectively. There does not appear to be a coincidence between the Raman 3010 cm^{-1} line and the infrared 3008.5 cm^{-1} line (25). The intensity of S(0) increases and the intensity of S(1) decreases in going from 14°K to 6°K, again consistent with rotational assignments for both features. The Q(1) transition is assigned to 3011 cm^{-1} by Chapados and Cabana (25) and is certainly under the 3010 cm^{-1} line. The sharp feature due to $2\nu_2$ does not appear in neat CH_4 as it does in the matrices. A similar behavior is found in CD_4 where $2\nu_2$ is sharp in the Xe matrix (Figure 20) but in phase III of CD_4 it is found to be relatively weaker and very broad (Figure 25).

The spectrum of ν_4 (Figure 22) is a very weak feature at 1305 cm^{-1}, 2500 times weaker than ν_1. This intensity factor explains why ν_4 is not seen in a matrix.

There are three weak bands observed in the lattice region and the model predicts three Raman active lattice modes.

Other modes which appear (Figure 22) are the $2\nu_4$ overtone and the $\nu_2 + \nu_4$ combination. The $2\nu_4$ spectrum shows three components.

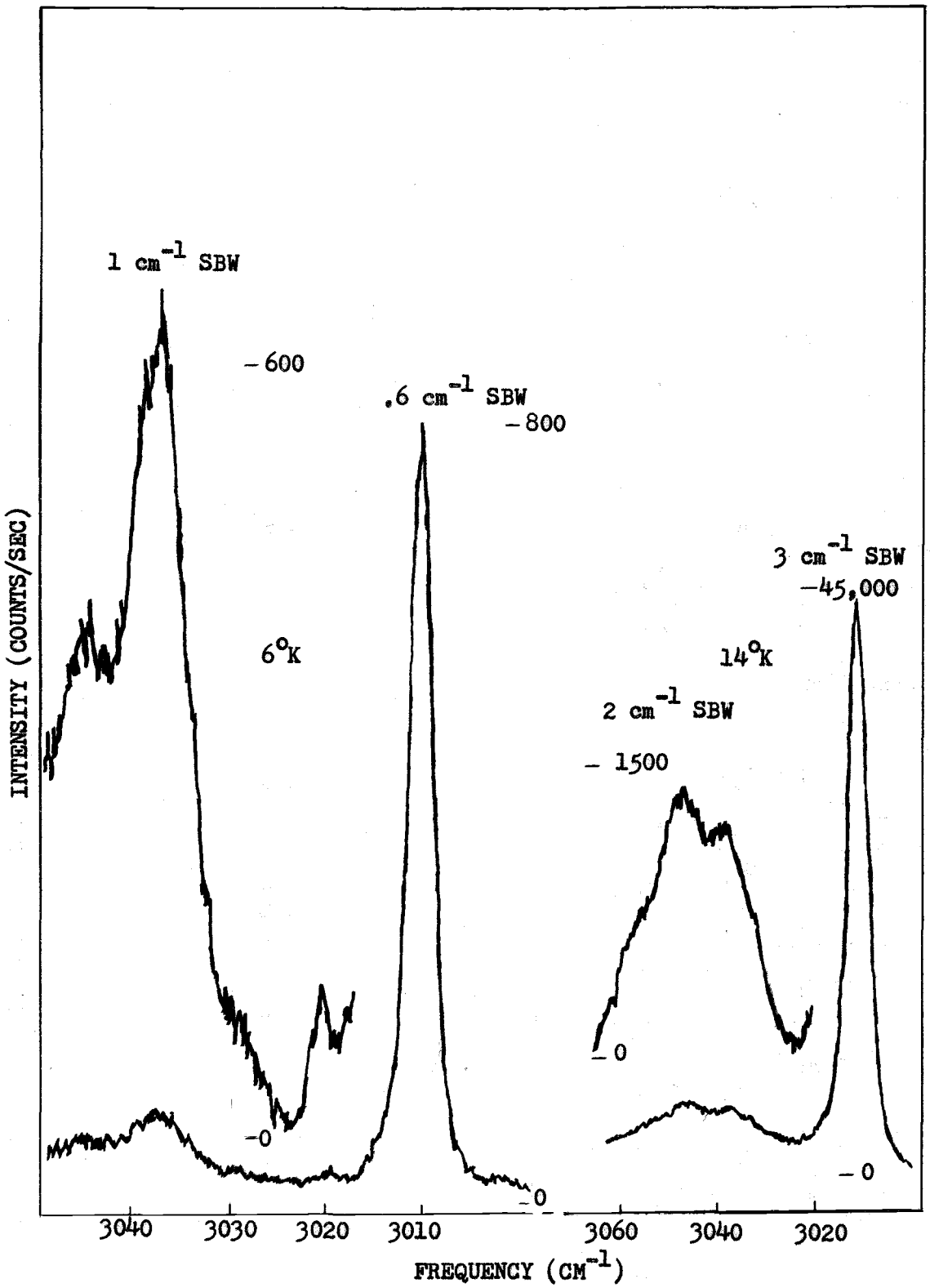

Figure 24. Raman ν_3 spectra of neat CH_4 at 6°K and 14°K.

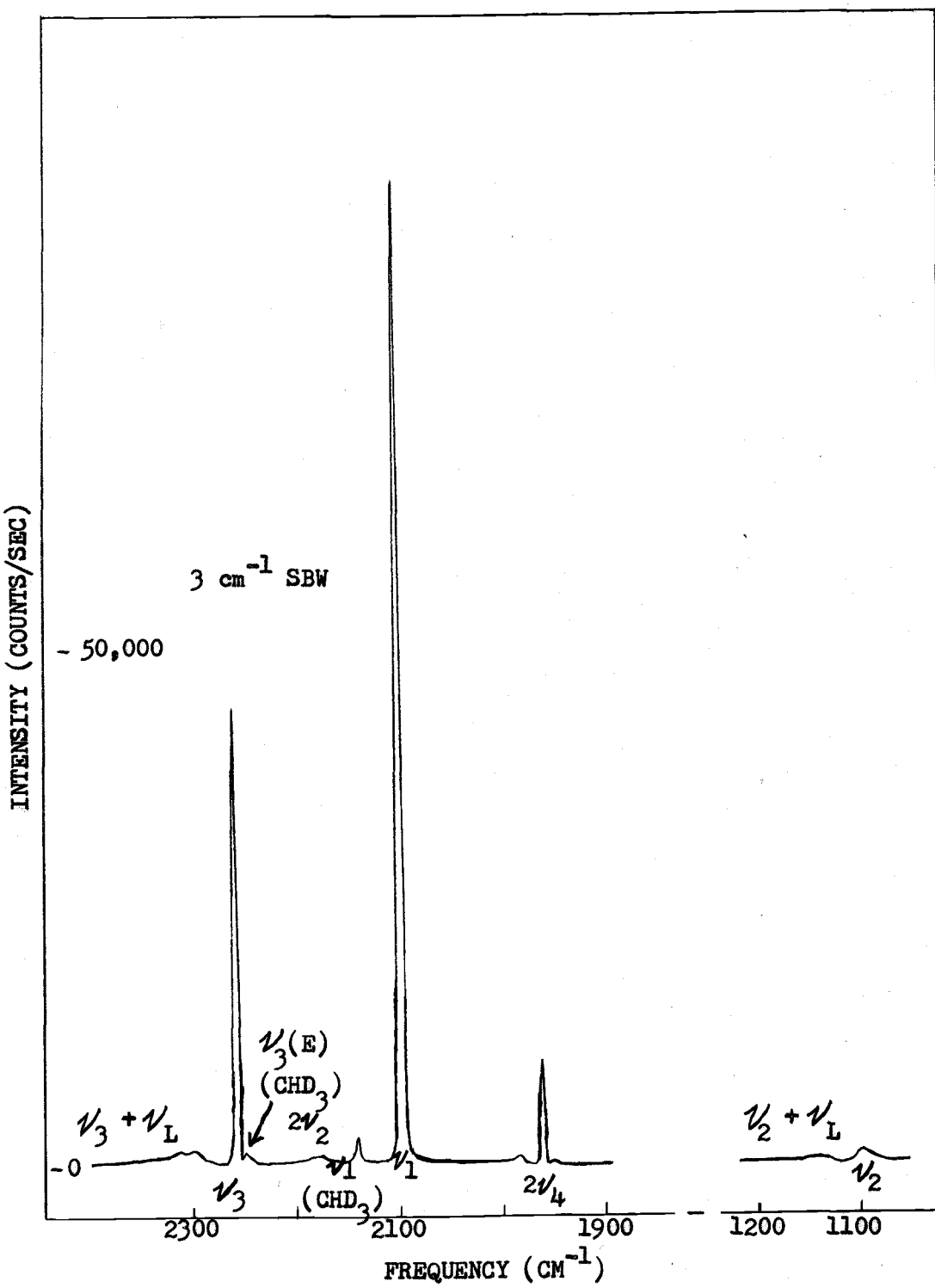

Figure 25. Raman spectrum of neat CD_4 at 6°K.

The first overtone of all F modes in O_h have the symmetries $A_{1g} + E_g + F_{2g}$, all Raman active, and it is possible that these would be correct assignments although two phonon spectra in crystals can be much more complicated than that. The $\nu_2 + \nu_4$ spectrum shows a single band which is consistent with all symmetry combinations of ν_2 and ν_4 being $F_{1g} + F_{2g} + F_{1u} + F_{2u}$ with only the F_{2g} part active in the Raman effect.

The neat CH_4 spectra consist of features which are assigned to ordered and disordered molecules. The features arising from ordered molecules at D_{2d} sites (Table XVIII) have the same relative intensities at 14°K and 6°K which is consistent with no rotation. The features belonging to rotating molecules at O sites do show temperature dependence and also compare favorably with the frequencies of CH_4 in Kr and Xe. The proposed O_h factor group and D_{2d} site for the ordered molecules predicts two and sometimes three components for the intramolecular modes (Table XIX) and in all cases only one is observed, thus the intermolecular forces are believed to be small.

2. Neat CD_4

The Raman studies of CD_4 (Figure 25) were performed at 6°K in phase III. Most of the features observed were reported by Anderson and Savoie (2), but there are some new features (see Table XX) and the behavior of $2\nu_2$ is most helpful in interpreting the Raman spectra of neat CH_4. In the Xe matrix (Figure 20), $2\nu_2$ is a sharp feature with nearly the intensity of ν_1 (CHD_3), but in neat CD_4 (Figure 25), $2\nu_2$ is very broad and much weaker than ν_1 (CHD_3). The contribution

TABLE XVIII. OBSERVED FREQUENCIES AND RELATIVE INTENSITIES OF MOLECULES AT D_{2d} SITES IN NEAT CH_4.

	Frequency, cm^{-1}			Relative Intensity
	Raman		Infrared	Raman
	(6°K)	(12°K)[4]		(6°K)
ν_1	2902	2901		2500
ν_2	1524	1526		40
ν_3	3010	3009	3008.5[5]	800
ν_4	1305		1301.3[5]	1
lattice modes	55		53[6]	1
	59		75[6]	.5
	72			1
$2\nu_4$	2571			90
	2593			40
	2601			10
$\nu_2 + \nu_4$	2814			20

4. Reference 2
5. Reference 25
6. Reference 135

TABLE XIX. FACTOR GROUP AND SITE SYMMETRIES FOR ORDERED MOLECULES IN NEAT CH_4.

Mode	Free Molecule (T_d)	Site (D_{2d})	Factor Group (O_h)
ν_1	A_1	A_1	$A_{1g}+E_g+A_{2u}+E_u$
ν_2	E	A_1+B_1	$A_{1g}+A_{2g}+2E_g+A_{1u}+A_{2u}+2E_u$
L	F_1	A_2+E	$2F_{1g}+F_{2g}+F_{1u}+2F_{2u}$
ν_3, ν_4, T	F_2	B_2+E	$F_{1g}+2F_{2g}+2F_{1u}+F_{2u}$

TABLE XX. OBSERVED RAMAN FREQUENCIES IN PHASE III OF NEAT CD_4.

Assignment	Frequency (cm^{-1}) (6^oK)	(12^oK)[7]
ν_2	1092	1093
ν_2+lattice modes	1135	
$2\nu_4$	1943	
	1955	1954
	1977	
ν_1	2092	2090
ν_1 (CHD_3)	2135	
$2\nu_2$	2175	
ν_3 ($^{13}CD_4$)[8]		2238
ν_3 (E) (CHD_3)	2244	2243
ν_3	2252	2252
ν_3+lattice modes	2295	2293
	2307	2305
ν_3 (A_1) (CHD_3)	2985	

7. Reference 2

8. Reference 25

of $2\nu_2$ to the ν_3 spectrum of neat CH_4 is assumed to be just a broad band as in neat CD_4.

V. INTERPRETATION OF METHANE SPECTRA

A. CH_4 and CD_4 in the Noble Gas Matrices

The appropriate group for CH_4 or CD_4 substituted in a noble gas matrix is $(O_h, \bar{T}_d)$. Using the results of Yasuda (165), Nishiyama and Yamamoto (108) have determined the lowest minima to occur at a position corresponding to the $\bar{\bar{C}}_{3V}$ high barrier limit. Their calculations have been compared to the infrared work for CH_4 and CD_4 in noble gas matrices (20, 23, 46, 47). In section III.D.1 the general group theory was presented, the energy levels found (Table XII) assuming tunneling through 90° is important, and an energy level diagram (Figure 12) drawn from the $(O_h, \bar{T}_d)$ free rotor limit to the $\bar{\bar{C}}_{3V}$ high barrier limit. The Raman spectra will be interpreted using both the hindered rotor model and the results obtained by Nishiyama and Yamamoto (107, 108), and compared to the infrared experiments. The allowed infrared and Raman transitions between rotational levels for the ν_2 and ν_3 vibrational bands are shown in Figure 26 along with the corresponding gas phase notation.

The difference in Raman selection rules for ν_2 and ν_3 (see Figure 26) is quite important in interpreting the spectra. The strong transitions from the $A_1\bar{A}_1$ librational ground state are $A_1\bar{A}_1 \rightarrow E\bar{E}$, $F_2\bar{E}$ for ν_2 and $A_1\bar{A}_1 \rightarrow E\bar{F}_2$, $F_2\bar{F}_2$ for ν_3 ($A_1\bar{A}_1 \rightarrow A_1\bar{F}_2$ is forbidden for a free rotor and is assumed to be weak). To a good approximation (87, 108, also see Table XII) the $E\bar{F}_2$ and $F_2\bar{E}$ levels are degenerate, so one would expect the same splitting from the Q

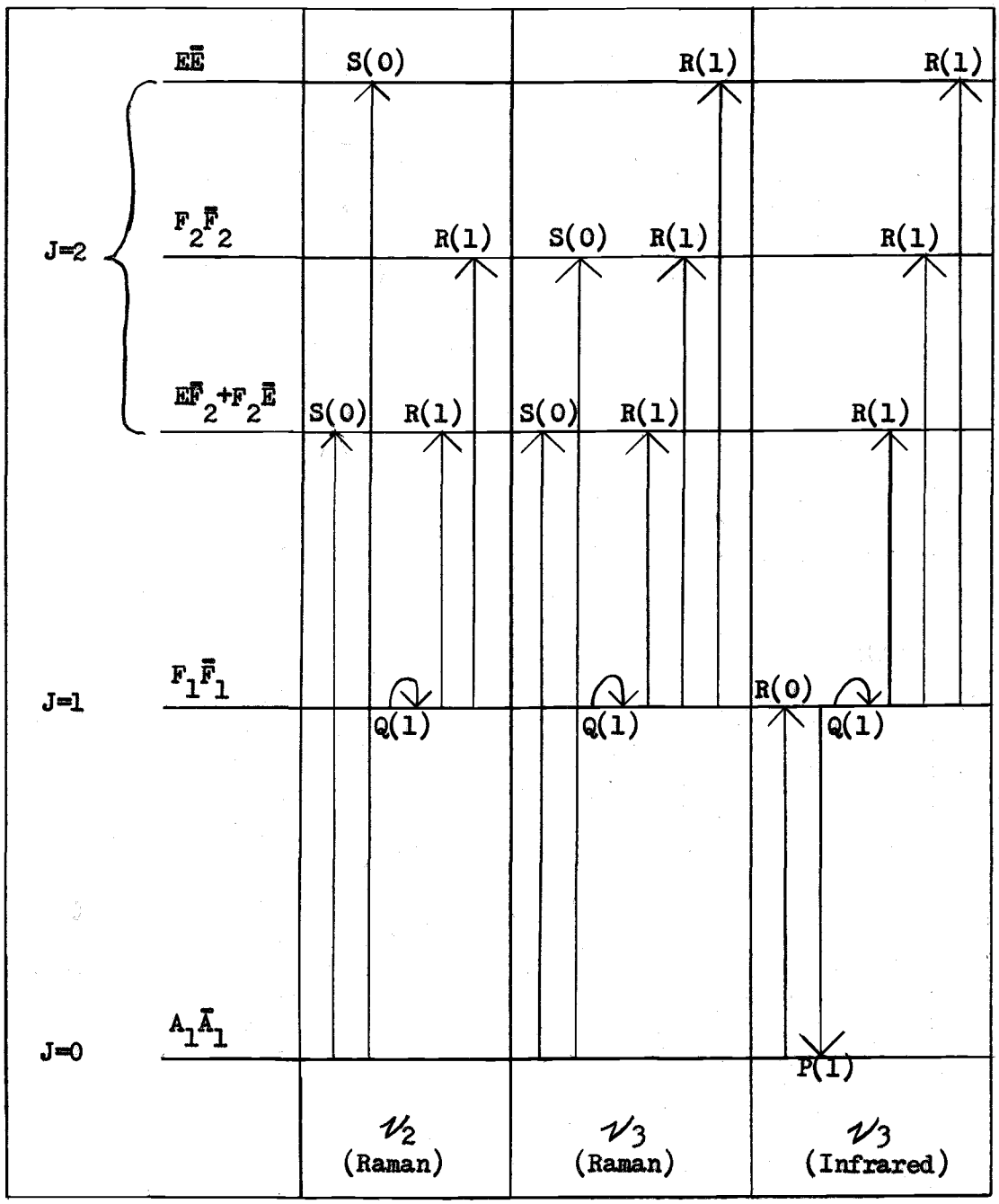

Figure 26. Allowed transitions between rotational levels accompanying vibrations in the Raman effect (ν_2 and ν_3) and the infrared (ν_3), and the corresponding gas phase notation. Only the J=0 and J=1 levels are assumed to be populated.

line for ν_2 and ν_3 from transitions to these levels, but different splittings for transitions to the $E\bar{E}$ (ν_2) and $F_2\bar{F}_2$ (ν_3) levels. The Coriolis effect is small ($\sim 1\,cm^{-1}$) for ν_3 (66, 107, 108) and will be ignored as a first approximation.

1. The ν_2 Region

The Raman spectra of ν_2 for CH_4 in Ar, Kr, and Xe have a similar structure. The clearest ν_2 spectrum is for CH_4 in Kr (Figure 18) which clearly shows three components at 1527, 1541, and 1549 cm^{-1}. Only the $A_1\bar{A}_1$ and $F_1\bar{F}_1$ levels would be expected to be populated at the 14°K temperature of the experiment, assuming the nuclear spin conversion of $A_1\bar{E}$ to $A_1\bar{F}_2$ spin molecules is rapid (47). The 1527 cm^{-1} feature is assigned as Q(1) ($F_1\bar{F}_1 \longrightarrow F_1\bar{F}_1$) since it is the lowest frequency transition which is allowed. The feature at 1549 cm^{-1} is assigned as the $A_1\bar{A}_1 \longrightarrow E\bar{E}$ transition since there is nothing comparable to that 22 cm^{-1} above the Q line in ν_3. The 1541 cm^{-1} feature could either be the $A_1\bar{A}_1 \longrightarrow F_2\bar{E}$ transition or a transition corresponding to R(1) in the gas phase ($F_1\bar{F}_1 \longrightarrow E\bar{F}_2$, $F_2\bar{F}_2$). Since the S lines are generally more intense than the R lines in the Raman effect (66, 67), it seems more likely that the 1541 cm^{-1} feature is due to the $A_1\bar{A}_1 \longrightarrow F_2\bar{E}$ transition. This will be discussed further after the ν_3 section. This assignment is compatible with the ν_2 spectra of CH_4 in Ar and Xe where the splittings have decreased for Ar and increased for Xe since the barriers to rotation decrease with an increasing size of the vacancy (108, 165).

2. The ν_3 Region

The Raman spectra of ν_3 for CH_4 in Ar, Kr, and Xe are similar except for the band at 3018 cm^{-1} in Ar which is assigned to aggregates. The spectra are complicated by the sharp A_1 component of $2\nu_2$ which is in resonance with ν_1. Comparisons with the ν_3 infrared spectra (23) give added proof that the structure is due to rotational splittings. Since the clearest ν_2 spectrum was for CH_4 in Kr, the ν_3 band in Kr will be examined in detail. The ν_3 Raman spectrum of CH_4 in Kr (Figure 18) has components at 3018, 3036, and 3049 cm^{-1}. The sharp peak at 3049 cm^{-1} is assigned as $2\nu_2$ and the 3036 cm^{-1} feature has a low frequency shoulder. The lowest frequency band at 3018 cm^{-1} is again assigned as the Q(1) line ($F_1\bar{F}_1 \longrightarrow F_1\bar{F}_1$). The ν_3 infrared spectrum (23) has four lines at 3010.1, 3018.3, 3026.5, and 3030.0 cm^{-1} which are assigned as P(1), Q(1), R(0), and R(1) (23, 108). The agreement with the Q(1) assignment is quite good. The lines designated P(1) and R(0) are forbidden in the Raman effect and there are no Raman features corresponding to these lines. The fact that the infrared and Raman spectra of ν_3 are so different discounts any thoughts that the structure might be due to polymers or multiple sites since coincidences would be expected. There are transitions allowed in the Raman which correspond to an R(1) line ($F_1\bar{F}_1 \longrightarrow E\bar{E}$, $F_2\bar{E} + E\bar{F}_2$, $F_2\bar{F}_2$), but there is not a line in the Raman spectrum which corresponds to the 3030.0 cm^{-1} line in the infrared. The 3036 cm^{-1} feature is 18 cm^{-1} above the Q(1) line and is assigned as the transition $A_1\bar{A}_1 \longrightarrow F_2\bar{F}_2$. The assignment of the $A_1\bar{A}_1 \longrightarrow F_2\bar{E}$

transition in ν_2 as 14 cm^{-1} above Q(1) means the $A_1\bar{A}_1 \longrightarrow E\bar{F}_2$ transition for ν_3 should also be 14 cm^{-1} above Q(1). This is about the position of the shoulder to the 3036 cm^{-1} feature so this is consistent with the ν_2 assignment.

The ν_3 Raman spectrum of CD_4 in Xe (Figure 20) has two principal components at 2250 and 2261 cm^{-1} which are assigned at the $F_1\bar{F}_1 \longrightarrow F_1\bar{F}_1$ and $A_1\bar{A}_1 \longrightarrow F_2\bar{F}_2$ transitions respectively. The Q(1) line at 2250 cm^{-1} is more intense than the 2261 cm^{-1} feature and this is in agreement with the relatively larger statistical weight for F spin CD_4 molecules (160). The splitting is just half of that for CH_4 in Xe, which is larger than expected for a hindered rotor. This does agree fairly well with the calculation of Nishiyama (107) which is 12.7 cm^{-1} for the $A_1\bar{A}_1 \longrightarrow F_2\bar{F}_2$ splitting for CD_4 in Xe.

3. Discussion

The assignments for CH_4 in Kr from the Raman and infrared experiments determine the positions of the rotational energy levels. These are compared in parentheses to the calculations of Nishiyama and Yamamoto (108) below along with the incomplete assignment for CD_4 in Xe with Nishiyama's calculations (107), in addition comparisons with the free rotor values (66, 67) are made.

Symmetry	Energy (cm^{-1})			
	CH_4/Kr	Free Rotor	CD_4/Xe	Free Rotor
$E\bar{E}$	22 (48.8)	31.4	(24.8)	15.8
$F_2\bar{F}_2$	18 (27.2)	31.4	11 (12.7)	15.8
$E\bar{F}_2 + F_2\bar{E}$	14 (19.6)	31.4	(9.0)	15.8
$F_1\bar{F}_1$	8.2 (8.3)	10.5	(3.8)	5.3
$A_1\bar{A}_1$	0 (0)	0	0 (0)	0

The order of the levels for CH_4 in Kr is the same, but the energies are much higher for the calculations, in fact the $E\bar{E}$ level is much higher than for the free rotor (31.4 cm^{-1}). The diagram in Figure 12 shows that the $E\bar{E}$ level is below the $E\bar{F}_2 + F_2\bar{E}$ and $F_2\bar{F}_2$ levels at the hindered rotor limit so the assignment of $E\bar{E}$ suggests that CH_4 is somewhere in between the free rotor and hindered rotor limits. The Raman assignments predict that the infrared ν_3 spectrum would show a triplet for R(1) at 6, 10, and 14 cm^{-1} above the Q line. The observed spectrum (23) has one component for R(1), 11.7 cm^{-1} above the Q line. The Coriolis effect may decrease the ν_3 spacings in the infrared since R^- transitions are allowed (67), and increase the ν_3 spacings in the Raman since S^+ transitions are the strongest (66, 67). Some of the R(1) components may be under the R(0) line or may be too weak to be seen. The assignment of the 1541 cm^{-1} line in ν_2 to the $A_1\bar{A}_1 \longrightarrow F_2\bar{E}$ transition agrees with the $E\bar{F}_2 + F_2\bar{E}$ level being below the $F_2\bar{F}_2$ level ((108) and Figure 12) and neither the $F_1\bar{F}_1 \longrightarrow E\bar{F}_2 + F_2\bar{E}$ or $F_2\bar{F}_2$ transitions could be 14 cm^{-1} above the Q line.

The Raman assignments of $E\bar{E}$, $F_2\bar{E} + E\bar{F}_2$ for CH_4 in Kr agree with the ν_2 and ν_3 Raman bands, but not too well for the ν_3 infrared band. The calculations of Nishiyama and Yamamoto (108) explain the infrared spectra well, but the spacings are too large to explain the Raman experiment. Additional information which supports the Raman assignments will be found from the spectra of neat CH_4.

B. CH_3D in Argon

While the infrared spectra have been studied for CH_3D in Ar, Kr, and Xe, the most apparent time dependence was found in the $\nu_4(A_1)$ band in Kr and this is the band reported in detail by Hopkins, Curl, and Pitzer (69). They also have the $\nu_4(A_1)$ and $\nu_4(E)$ bands for the hosts Ar, Kr, and Xe. The Raman results reported here for CH_3D in Ar are limited in rotational studies to $\nu_3(E)$. The Q branch is the strongest feature in the Raman for A_1 modes and no structure was observed for ν_1 and $\nu_3(A_1)$. The ν_4 modes are too weak to be seen in the Raman and so comparisons with infrared data are not possible.

The group for CH_3D in the noble gas matrices is $(O_h, \bar{C}_{3V})$. From the potential function found for CH_4 (165), it seems likely that both $\bar{\bar{C}}_{3V}$ and $\bar{\bar{C}}_S$ are appropriate high barrier groups depending on whether the D atom is along a three-fold axis of the crystal or just a dihedral plane. This uncertainty in the high barrier group makes a detailed analysis quite difficult in terms of a hindered rotor model. A rather qualitative discussion will follow on the results indicating rotational motion.

The $\nu_4(A_1)$ band for CH_3D in Kr has lines at 1300 and 1306 cm^{-1} which exhibit the greatest change in intensity with time. The line at 1306 cm^{-1} increases in intensity and is assigned as the $A_1\bar{A}_1 \longrightarrow F_1\bar{A}_2$ transition, the 1300 cm^{-1} line decreases in intensity and is assigned as the Q line ($F_1\bar{\bar{E}} \longrightarrow F_1\bar{E}$). This is consistent with the nuclear spin conversion from $\bar{\bar{E}}$ to $\bar{A}_1$ spin species. There are two other weaker lines at 1295 and 1303.5 cm^{-1} which change very little with time and assignments for these are uncertain. They could be

assigned as the transitions $F_1\bar{A}_2 \longrightarrow A_1\bar{A}_1$ and $F_1\bar{E} \longrightarrow E\bar{E}$ respectively, but there should be another transition ($F_1\bar{E} \longrightarrow F_2\bar{E}$) at higher frequency and this is not observed. The observed time dependent intensities does indicate rotational motion for CH_3D and this is consistent with the other bands as well. The $\nu_4(A_1)$ bands in Ar and Xe are quite similar, but with the spacing between lines somewhat smaller for Ar and larger for Xe, which is consistent with smaller barriers to rotation in the larger cavities. The $\nu_4(E)$ band is different in appearance since it is a perpendicular band and there is the additional complication of the Coriolis effect, but again rotational motion is suggested. The Raman spectrum of $\nu_3(E)$ in Ar has two principal features split by 12 cm^{-1}. Assuming these are the $F_1\bar{E} \longrightarrow F_1\bar{A}_2$ and $A_1\bar{A}_1 \longrightarrow F_1\bar{E}$ transitions, the corresponding gas phase difference is 23 cm^{-1}, so this points more to hindered rotation. The infrared and Raman evidence for CH_3D is consistent with hindered rotation, but a detailed analysis may need to include translational effects since the center of mass is not at the carbon atom.

C. Neat CH_4

The molecules in neat CH_4 are assumed to be in two different sites in the lowest temperature phase (5, 6) according to the James-Keenan model (76, 80). If only nearest neighbor molecules are considered, the crystal field for the rotating molecules has the symmetry O_h (80, 165). Kataoka, Okada, and Yamamoto (80) have calculated the rotational levels for neat CH_4 and the crystal field parameters are intermediate to those for Kr and Xe. Therefore, the rotating molecules at 0 sites can to a good approximation be treated as matrix isolated molecules and the same symmetry considerations used for CH_4 in noble gas matrices can be used for neat methane.

1. The ν_2 Region

The ν_2 Raman spectrum of neat CH_4 at 6^oK and 14^oK is shown in Figure 23. The 6^oK spectrum has components at 1527, 1545, 1552, and 1560 cm^{-1} assigned to rotating molecules. The spectrum at 14^oK does not show all of this structure. The 1527 cm^{-1} feature appears as a shoulder on the 1524 cm^{-1} peak assigned to the ordered molecules at D_{2d} sites. The 1527 cm^{-1} feature is assigned as Q(1) ($F_1\bar{F}_1 \longrightarrow F_1\bar{F}_1$) and compares to the Q(1) assignment in Kr of 1527 cm^{-1} and in Xe of 1524 cm^{-1}. The strongest band at 1552 cm^{-1} is assigned to the transition $A_1\bar{A}_1 \longrightarrow E\bar{E}$. This is 25 cm^{-1} above the Q line compared with 22 cm^{-1} for CH_4 in Kr. The band at 1545 cm^{-1} is assigned to the transition $A_1\bar{A}_1 \longrightarrow F_2\bar{E}$ and there is additional support for this from the ν_3 spectra. The 1560 cm^{-1} feature is assigned as S(1)

which could include the transitions $F_1\bar{F}_1 \longrightarrow A_2\bar{F}_1$, $F_1\bar{F}_1$, $F_2\bar{F}_1$ + $F_1\bar{F}_2$, $F_2\bar{F}_2$ (see Table XI). The intensity of the 1552 cm^{-1} band is seen to increase markedly when the temperature is lowered from 14°K to 6°K which agrees well with this rotational assignment. The weaker band at 1545 cm^{-1} also seems to increase in intensity which is consistent with its assignment ($A_1\bar{A}_1 \longrightarrow F_2\bar{E}$). The features above 1524 cm^{-1} are very similar to the ν_2 matrix spectra and this is the reason for assigning just the 1524 cm^{-1} line to the molecules at D_{2d} sites.

2. <u>The ν_3 Region</u>

The ν_3 Raman spectrum of neat CH_4 at 6°K and 14°K is shown in Figure 24. The ν_3 infrared spectrum of neat CH_4 at 9°K has been reported by Chapados and Cabana (25). The infrared assignments for rotating molecules at 3004, 3011, 3020.3, and 3026.4 cm^{-1} are denoted by P(1), Q(1), R(0), and R(1) respectively. All the features above the 3010 cm^{-1} line in the Raman spectrum of ν_3 are assigned to rotating molecules, assuming $2\nu_2$ is broad and relatively weaker as in neat CD_4 (Figure 25). The Raman spectrum at 6°K again shows more structure than that at 14°K. The Q(1) line which appeared as a shoulder to the 3008.5 cm^{-1} line in the infrared (25) is certainly under the very strong feature at 3010 cm^{-1}. The strongest line above 3010 cm^{-1} at 6°K is the 3036 cm^{-1} line and this is assigned to the $A_1\bar{A}_1 \longrightarrow F_2\bar{F}_2$ transition which is 25 cm^{-1} above the Q(1) line, assuming the 3011 cm^{-1} infrared assignment. The 3036 cm^{-1} line is much less intense at 14°K. The shoulder below the 3036 cm^{-1}

line is assigned to the transition $A_1\bar{A}_1 \longrightarrow E\bar{F}_2$. This assignment agrees with the ν_2 assignment and also with the shape of ν_3 in the noble gas matrices. The feature at 3019 cm^{-1} is assigned to the $F_1\bar{F}_1 \longrightarrow E\bar{F}_2 + F_2\bar{E}$ transition. The infrared spectra (25) place the $F_1\bar{F}_1$ state 9 cm^{-1} above the ground state and the Raman ν_2 spectrum (Figure 23) sets the $F_2\bar{E}$ level 18 cm^{-1} above the ground state, so the transition $F_1\bar{F}_1 \longrightarrow E\bar{F}_2 + F_2\bar{E}$ should appear 9 cm^{-1} above the Q(1) line and this agrees quite well with its position. The R(0) or $A_1\bar{A}_1 \longrightarrow F_1\bar{F}_1$ transition is also 9 cm^{-1} above the Q(1) line, but is forbidden in the Raman effect. The $F_1\bar{F}_1 \longrightarrow E\bar{F}_2 + F_2\bar{E}$ transition is also allowed in the infrared and must be either under the R(0) line or too weak to be observed. The position of the $E\bar{E}$ and $F_2\bar{F}_2$ levels at 25 cm^{-1} above the $A_1\bar{A}_1$ level determines the $F_1\bar{F}_1 \longrightarrow E\bar{E}$, $F_2\bar{F}_2$ transitions to appear 16 cm^{-1} above the Q(1) line which agrees well with the R(1) feature observed in the infrared (25). The band at 3044 cm^{-1} is assigned as S(1) ($F_1\bar{F}_1 \longrightarrow A_2\bar{A}_2$, $F_1\bar{A}_2 + A_2\bar{F}_1$, $F_1\bar{F}_1$, $F_2\bar{F}_1 + F_1\bar{F}_2$, $F_2\bar{F}_2$) and is 33 cm^{-1} above the Q(1) line, the same as the S(1) feature in ν_2.

3. Discussion

The assignments for neat CH_4 from the infrared and Raman experiments determine the positions of the rotational energy levels for the lowest states and an average position for the states originating from J=3 (see Figure 12). The energy levels are listed below with the calculated levels (80) in parentheses.

Symmetry	Energy (cm^{-1})
J = 3	42
$E\bar{E}$	25 (47)
$F_2\bar{F}_2$	25 (30)
$E\bar{F}_2 + F_2\bar{E}$	18 (21)
$F_1\bar{F}_1$	9 (9)
$A_1\bar{A}_1$	0 (0)

Again the assigned levels from experimental data are more closely spaced than the calculated ones. The assigned positions are also in agreement with the inelastic neutron scattering experiments of Kapulla and Glaser (79) at 4.4°K where they observed peaks at energy differences corresponding to 8.5, 15, and 23 cm^{-1} and assigned these as R(0), R(1), and S(0) respectively. There is good agreement between these assignments and all experimental evidence. The treatment of the ν_3 spectra again ignores the Coriolis effect, but any differences would be quite small. The assignment of the $E\bar{F}_2 + F_2\bar{E}$ level from both the ν_2 and ν_3 Raman spectra adds support to the assignment of this level for the noble gas matrix experiments, where the spectra are much weaker causing more uncertainties in the assignments. The earlier Raman spectra of neat CH_4 by Anderson and Savoie (2) are in agreement with the spectra reported here, although they did not observe the weak features. The Raman spectra of neat CH_4 adds additional evidence to that in Section II.B.3 supporting the James-Keenan model (76) for the lowest temperature phase (phase III) of CH_4.

VI. CONCLUSIONS

The description of rotational levels for molecules in crystalline solids has been accomplished using methods of group theory. The group theory has been solved for a molecule of any symmetry at a site in a crystal field of any symmetry and a diagram of rotational energy levels may be found from the free rotor limit to any of the high barrier or librator limits. The pattern of energy levels can usually be determined near a high barrier limit using methods of group theory with some simplifying assumptions. Selection rules are then applied to predict spectra in the infrared and Raman effect.

Examples of many different symmetries have been presented and compared to experimental results when appropriate. From these considerations it was possible to show that the ν_2 infrared spectrum of CH_3 in argon (101) fit the spectrum predicted by the energy level pattern at the hindered rotor limit (Figure 10), and that the ν_2 infrared spectrum of NH_3 in argon (69, 99) fit the spectrum predicted by the energy level pattern near the hindered rotor limit (Figure 11). Many of the other comparisons may require much more elaborate calculations than the ones given here before reaching an agreement between theory and experiment.

The Raman spectra were presented for neat methane and methane in noble gas matrices and provide new evidence in support of the James-Keenan model (76, 80) for phase III (5, 6) of CH_4, and in support of rotational motion for methane in the noble gas matrices. The rotational motion is determined to be hindered for methane, but

the assignments neither agree with the energy level pattern at or near the hindered rotor limit (Figure 12) nor with the levels calculated by Yamamoto and co-workers (80, 108). Their calculations do agree with the assignments as to the order of the rotational states, but the spacings are smaller than the calculated ones. The calculation for CD_4 (107) is in good agreement with the present Raman findings.

The usefulness of group theory as it is applied to the rotation of molecules in crystals has been presented along with examples of the kinds of information which can be obtained by these methods.

BIBLIOGRAPHY

1. A. Anderson and S. H. Walmsley, Mol. Phys. 9, 1 (1965).

2. A. Anderson and R. Savoie, J. Chem. Phys. 43, 3468 (1965).

3. R. L. Armstrong, J. Chem. Phys. 36, 2429 (1962).

4. R. L. Armstrong, J. Chem. Phys. 44, 530 (1966).

5. E. A. Ballik, D. J. Gannon, and J. A. Morrison, J. Chem. Phys. 57, 1793 (1972).

6. E. A. Ballik, D. J. Gannon, and J. A. Morrison, J. Chem. Phys. 58, 5639 (1973).

7. A. J. Barnes, J. B. Davies, H. E. Hallam, G. F. Scrimshaw, G. C. Hayward, and R. C. Milward, Chem. Comm., 1089 (1969).

8. A. J. Barnes, H. E. Hallam, and G. F. Scrimshaw, Trans. Faraday Soc. 65, 3159 (1969).

9. C. S. Barrett, L. Meyer, and J. Wasserman, J. Chem. Phys. 44, 998 (1966).

10. E. D. Becker and G. C. Pimentel, J. Chem. Phys. 25, 224 (1956).

11. S. S. Bhatnagar, E. J. Allin, and H. L. Welsh, Can. J. Phys. 40, 9 (1962).

12. H. Boerner, Representations of Groups (American Elsevier, New York, 1970).

13. D. N. Bol'shutkin, V. M. Gasau, A. I. Prokhvatilov, and A. I. Erenburg, J. Struct. Chem. 12, 313 (1971).

14. M. T. Bowers and W. H. Flygare, J. Chem. Phys. 44, 1389 (1966).

15. M. T. Bowers, G. I. Kerley, and W. H. Flygare, J. Chem. Phys. 45, 3399 (1966).

16. W. E. Bron and R. W. Dreyfus, Phys. Rev. 164, 304 (1967).

17. L. C. Brunel and M. Peyron, C. R. Acad. Sci. (Paris), Ser. C 262, 1297 (1966).

18. P. R. Bunker and D. Papousek, J. Mol. Spectrosc. 32, 419 (1969).

19. P. R. Bunker, Vibrational Spectra and Structure (Marcel Dekker, New York, to be published), Vol. III.

20. A. Cabana, G. B. Savitsky, and D. F. Hornig, J. Chem. Phys. 39, 2942 (1963).

21. A. Cabana, A. Anderson, and R. Savoie, J. Chem. Phys. 42, 1122 (1965).

22. E. Catalano and D. E. Milligan, J. Chem. Phys. 30, 45 (1959).

23. A. Chamberland, R. Belzile, and A. Cabana, Can. J. Chem. 48, 1129 (1970).

24. C. K. Chan, M. V. Klein, and B. Wedding, Phys. Rev. Letters 17, 521 (1966).

25. C. Chapados and A. Cabana, Can. J. Chem. 50, 3521 (1972).

26. K. Clusius, Z. Physik, Chem. B3, 41 (1929).

27. K. Clusius, L. Popp, and A. Frank, Physica 4, 1105 (1937).

28. K. Clusius and L. Popp, Z. Physik, Chem. B46, 63 (1940).

29. J. H. Colwell, E. K. Gill, and J. A. Morrison, J. Chem. Phys. 36, 2223 (1962).

30. J. H. Colwell, E. K. Gill, and J. A. Morrison, J. Chem. Phys. 39, 635 (1963).

31. J. H. Colwell, J. Chem. Phys. 51, 3820 (1969).

32. M. A. Cundill and W. F. Sherman, Phys. Rev. 168, 1007 (1968).

33. H. M. Cundy, Proc. Roy. Soc. (London) A164, 420 (1938).

34. J. B. Davies and H. E. Hallam, J. C. S. Faraday II 67, 3176 (1971).

35. A. F. Devonshire, Proc. Roy. Soc. (London) A153, 601 (1936).

36. E. R. Dobbs and G. O. Jones, Rep. Progr. Phys. 20, 560 (1957).

37. B. Dorner and H. Stiller, Inelastic Scattering of Neutrons, Vol. 2 (I.A.E.A., Vienna, 1965) p. 291.

38. P. A. Egelstaff, J. Chem. Phys. 53, 2590 (1970).

39. G. E. Ewing, J. Chem. Phys. 40, 179 (1964).

40. G. Feher, I. W. Shepherd, and H. B. Shore, Phys. Rev. Lett. 17, 1142 (1966).

41. W. R. Fenner and M. V. Klein, Light Scattering Spectra of Solids, edited by G. Wright (Springer, New York, 1969).

42. G. R. Field and W. F. Sherman, J. Chem. Phys. 47, 2378 (1967).

43. W. H. Flygare, J. Chem. Phys. 39, 2263 (1963).

44. S. N. Foner, E. L. Cochran, V. A. Bowers, and C. K. Jen, Phys. Rev. Lett. 1, 91 (1958).

45. A. Frank and K. Clusius, Z. Physik. Chem. B36, 291 (1937).

46. F. H. Frayer and G. E. Ewing, J. Chem. Phys. 46, 1994 (1967).

47. F. H. Frayer and G. E. Ewing, J. Chem. Phys. 48, 781 (1968).

48. H. Friedmann and S. Kimel, J. Chem. Phys. 41, 2552 (1964).

49. H. Friedmann and S. Kimel, J. Chem. Phys. 43, 3925 (1965).

50. H. Friedmann and S. Kimel, J. Chem. Phys. 44, 4359 (1966).

51. H. Friedmann and S. Kimel, J. Chem. Phys. 47, 3589 (1967).

52. H. Friedmann, A. Shalom, and S. Kimel, J. Chem. Phys. 50, 2496 (1969).

53. J. A. Glasel, J. Chem. Phys. 33, 252 (1960).

54. R. G. Gordon, J. Chem. Phys. 43, 1307 (1965).

55. R. G. Gordon, J. Chem. Phys. 44, 1830 (1966).

56. S. Greer and L. Meyer, Z. Angew, Phys. 27, 198 (1969).

57. S. Greer and L. Meyer, J. Chem. Phys. 50, 4299 (1969).

58. S. Greer and L. Meyer, J. Chem. Phys. 52, 468 (1970).

59. W. N. Hardy, I. F. Silvera, and J. P. McTague, Phys. Rev. Letters 26, 127 (1971).

60. Y. D. Harker and R. M. Brugger, J. Chem. Phys. 46, 220 (1967).

61. K. B. Harvey and H. F. Shurvell, Chem. Commun. 1967, 490.

62. K. B. Harvey and H. F. Shurvell, Can. J. Chem. 45, 2689 (1967).

63. K. B. Harvey and H. F. Shurvell, J. Mol. Spectry. 25, 120 (1968).

64. P. Van Hecke, P. Grobet, and L. van Gerven, J. Mag. Resonance 7, 117 (1972).

65. K. H. Hellwege, W. Lesch, M. Plihal, and G. Schaack, Z. Physik 232, 61 (1970).

66. J. Herranz and B. P. Stoicheff, J. Mol. Spectrosc. 10, 448 (1963).

67. G. Herzberg, Molecular Spectra and Molecular Structure. II. Infrared and Raman Spectra of Polyatomic Molecules (D. Van Nostrand Co., Inc., Princeton, N. J., 1945).

68. G. Herzberg, Molecular Spectra and Molecular Structure. III. Electronic Spectra and Electronic Structure of Polyatomic Molecules (D. VanNostrand Co., Inc., Princeton, N. J., 1966).

69. H. P. Hopkins, Jr., R. F. Curl, Jr., and K. S. Pitzer, J. Chem. Phys. 48, 2959 (1968).

70. G. K. Horton, Am. J. Phys. 36, 93 (1968).

71. J. T. Hougen, J. Chem. Phys. 37, 1433 (1962).

72. J. T. Hougen, J. Chem. Phys. 39, 358 (1963).

73. T.-H. Huang, Ph.D. Thesis, Oregon State University (1973).

74. N. Jacobi, J. Chem. Phys. 57, 2505 (1972).

75. N. Jacobi and O. Schnepp, J. Chem. Phys. 57, 2516 (1972).

76. H. M. James and T. A. Keenan, J. Chem. Phys. 31, 12 (1959).

77. S. Kapphan and F. Luty, J. Phys. Chem. Solids 34, 969 (1973).

78. H. Kapulla and W. Glaser, Phys. Letters 31A, 158 (1970).

79. H. Kapulla and W. Glaser, Neutron Inelastic Scattering 1972, (I.A.E.A., Vienna, 1972) p. 841.

80. Y. Kataoka, K. Okada, and T. Yamamoto, Chem. Phys. Lett. 19, 365 (1973).

81. B. Katz, A. Ron, and O. Schnepp, J. Chem. Phys. 46, 1926 (1967).

82. B. Katz, A. Ron, and O. Schnepp, J. Chem. Phys. 47, 5303 (1967).

83. B. Keller and F. Kneubuhl, Solid State Commun. 8, 867 (1970).

84. L. F. Keyser and G. W. Robinson, J. Chem. Phys. 44, 3225 (1966).

85. L. F. Keyser and G. W. Robinson, J. Chem. Phys. 45, 1694 (1966).

86. H. F. King, Ph.D. Thesis, Princeton (1960).

87. H. F. King and D. F. Hornig, J. Chem. Phys. 44, 4520 (1966).

88. M. V. Klein, B. Wedding and M. A. Levine, Phys. Rev. 180, 902 (1969).

89. A. Kruis, L. Popp, and K. Clusius, Z. Electrochem. 43, 664 (1937).

90. W. Kuhn and F. Luty, Solid State Commun. 2, 281 (1964).

91. J. C. Kwok, Ph.D. Thesis, California Institute of Technology, 1964.

92. W. N. Lawless, J. Phys. Chem. Solids 28, 1755 (1967).

93. H. C. Longuet-Higgins, Mol. Phys. 6, 445 (1963).

94. A. Maki and J. C. Decius, J. Chem. Phys. 31, 772 (1959).

95. D. E. Mann, N. Acquista, and D. White, J. Chem. Phys. 44, 3453 (1966).

96. M. G. Mason, W. G. Von Holle, and D. W. Robinson, J. Chem. Phys. 54, 3491 (1971).

97. H. McConnell, J. Chem. Phys. 29, 1422 (1958).

98. R. E. Miller and J. C. Decius, J. Chem. Phys. 59, 4871 (1973).

99. D. E. Milligan, R. M. Hexter, and K. Dressler, J. Chem. Phys. 34, 1009 (1961).

100. D. E. Milligan and M. E. Jacox, J. Chem. Phys. 43, 4487 (1965).

101. D. E. Milligan and M. E. Jacox, J. Chem. Phys. 47, 5146 (1967).

102. H. H. Mooy, Nature 127, 707 (1931).

103. H. H. Mooy, Proc. Acad. Sci. 34, 550 (1931).

104. T. Nagamiya, Prog. Theor. Phys. 6, 702 (1951).

105. V. Narayanamurti, Phys. Rev. Lett. 13, 693 (1964).

106. V. Narayanamurti, W. D. Seward, and R. O. Pohl, Phys. Rev. 148, 481 (1966).

107. K. Nishiyama, J. Chem. Phys. 56, 5096 (1972).

108. K. Nishiyama and T. Yamamoto, J. Chem. Phys. 58, 1001 (1973).

109. J. Noolandi, Can. J. Phys. 48, 2032 (1970).

110. T. Oka, J. Mol. Spectrosc. 48, 503 (1973).

111. I. Olovsson and D. H. Templeton, Acta Cryst. 12, 832 (1959).

112. L. Pauling, Phys. Rev. 36, 430 (1930).

113. J. G. Peascoe and M. V. Klein, J. Chem. Phys. 59, 2394 (1973).

114. J. G. Peascoe, W. R. Fenner, and M. V. Klein, J. Chem. Phys. 60, 4208 (1974).

115. G. C. Pimentel, M. D. Bulanin, and M. Van Thiel, J. Chem. Phys. 36, 500 (1962).

116. G. C. Pimentel and S. W. Charles, Pure Appl. Chem. 7, 111 (1963).

117. A. S. Pine, C. J. Glassbrenner, and G. Dresselhaus, Phonons: Proceedings International Conference on Phonons, Rennes, France, 1971. (Flammarion, Paris, 1972).

118. G. L. Pollack, Rev. Mod. Phys. 36, 748 (1964).

119. W. Press, B. Dorner, and H. Stiller, Solid State Commun. 9, 1113 (1971).

120. W. Press, J. Chem. Phys. 56, 2597 (1972).

121. W. Press, (Private Communication to J. A. Morrison) March, 1972.

122. W. C. Price, W. F. Sherman, G. R. Wilkinson, Proc. Roy. Sco. A255, 5 (1960).

123. W. C. Price, W. F. Sherman, and G. R. Wilkinson, Spectrochim. Acta 16, 663 (1960).

124. W. R. C. Prior and E. J. Allin, Can. J. Phys. 51, 405 (1973).

125. F. P. Reding and D. F. Hornig, J. Chem. Phys. 22, 1926 (1954).

126. R. L. Redington and D. E. Milligan, J. Chem. Phys. 37, 2162 (1962).

127. R. L. Redington and D. E. Milligan, J. Chem. Phys. 39, 1276 (1963).

128. D. W. Robinson, J. Chem. Phys. 39, 3430 (1963).

129. D. W. Robinson and W. G. Von Holle, J. Chem. Phys. 44, 410 (1966).

130. G. W. Robinson and M. McCarty, Jr., J. Chem. Phys. 30, 999 (1959).

131. G. W. Robinson, Advan. Chem. Ser. 36, 16 (1962).

132. O. Runolfeson and S. Mango, Phys. Letters 28A, 254 (1968).

133. P. Sauer, Z. Physik 194, 360 (1966).

134. P. Sauer, O. Schirmer, and J. Schneider, Phys. Status Solidi 16, 79 (1966).

135. R. Savoie and R. P. Fournier, Chem. Phys. Lett. 7, 1 (1970).

136. A. Schallamach, Nature 143, 375 (1939).

137. A. Schallamach, Proc. Roy. Soc. A171, 569 (1939).

138. L. J. Schoen, D. E. Mann, C. Knobler, and D. White, J. Chem. Phys. 37, 1146 (1962).

139. N. E. Schumaker and C. W. Garland, J. Chem. Phys. 53, 392 (1970).

140. W. P. Seward and V. Narayanamurti, Phys. Rev. 148, 463 (1966).

141. W. F. Sherman, G. R. Wilkinson, and J. L. Jacobson, Abstracts from 7th European Molecular Spectroscopy Conference, Budapest, 1963.

142. H. B. Shore, Phys. Rev. Lett. 17, 1142 (1966).

143. H. B. Shore, Phys. Rev. 151, 570 (1966).

144. H. F. Shurvell and K. B. Harvey, Can. Spectroscopy 14, 32 (1969).

145. K. Skold, J. Chem. Phys. 49, 2443 (1968).

146. D. Smith, J. Chem. Phys. 58, 3833 (1973).

147. T. E. Stern, Proc. Roy. Soc. (London) A130, 551 (1931).

148. H. Stiller and T. Springer, Z. Naturf. 26a, 575 (1971).

149. A. J. Tursi and E. R. Nixon, J. Chem. Phys. 52, 1521 (1970).

150. J. Van Kranendonk and H. P. Gush, Phys. Lett. 1, 22 (1962).

151. J. Van Kranendonk and G. Karl, Rev. Mod. Phys. 40, 531 (1968).

152. M. Van Thiel, E. D. Becker, G. C. Pimentel, J. Chem. Phys. 27, 486 (1957).

153. W. Vedder and D. F. Hornig, J. Chem. Phys. 35, 1560 (1961).

154. J. M. P. J. Verstegen, H. Goldring, S. Kimel, and B. Katz, J. Chem. Phys. 44, 3216 (1966).

155. W. G. Von Holle and D. W. Robinson, J. Chem. Phys. 53, 3768 (1970).

156. B. Wedding and M. V. Klein, Phys. Rev. 177, 1274 (1969).

157. G. H. Wegdam, J. B. te Beek, H. van der Linden, and J. van der Elsken, J. Chem. Phys. 55, 5207 (1971).

158. K. F. Weinmann and F. Luty, Bull. Am. Phys. Soc. 12, 82 (1967).

159. E. Wigner, Gott. Nachr. 1930, p. 133.

160. E. B. Wilson, J. Chem. Phys. 3, 276 (1935).

161. E. B. Wilson, J. C. Decius, and P. C. Cross, Molecular Vibrations (McGraw-Hill, New York, 1955).

162. K. P. Wong, J. D. Noble, M. Bloom, and S. Alexander, J. Mag. Resonance 1, 55 (1969).

163. R. W. G. Wyckoff, Crystal Structures (Interscience, New York, 1948), 2nd ed., Vol. 1.

164. R. W. G. Wyckoff, Crystal Structures (Interscience, New York, 1948), 2nd ed., Vol. 2.

165. H. Yasuda, Prog. Theor. Phys. 45, 1361 (1971).

APPENDIX

A. Summary of Energies and Integrals for (O_h, $\bar{\bar{C}}_{\infty v}$) Near the $\bar{\bar{C}}_{4v}$ High Barrier Limit

$$E_o^A 1g = \alpha_o + 4\beta_o - 4\epsilon_o\alpha_o$$

$$E_o^F 1u = \alpha_o$$

$$E_o^E g = \alpha_o - 2\beta_o + 2\epsilon_o\alpha_o$$

$$\alpha_o = \langle\psi_{xoo}/H/\psi_{xoo}\rangle = V_o\left[\frac{8}{\alpha} - \frac{11}{\alpha 2} - \frac{11C_6}{\alpha 2}\right]$$

$$\beta_o = \langle\psi_{yoo}/H/\psi_{xoo}\rangle = -V_o\exp(-\alpha\pi^2/16)\left[\frac{\pi^2}{4} - 1 + \frac{\pi^2}{8\alpha} - \frac{3}{\alpha} + \frac{11C_6}{2\alpha}\right]$$

$$\epsilon_o = \langle\psi_{yoo}/\psi_{xoo}\rangle = \exp(-\alpha\pi^2/16)$$

$$E_1^F 2g = \alpha_g - 2\beta_g + 2\epsilon_g\alpha_g$$

$$E_1^F 1g = \alpha_g + 2\beta_g - 2\epsilon_g\alpha_g$$

$$\alpha_g = \langle\psi_{xlo}/H/\psi_{xlo}\rangle = V_o\left[\frac{16}{\alpha} - \frac{29}{\alpha^2} - \frac{33C_6}{\alpha^2}\right]$$

$$\beta_g = \langle\psi_{ylo}/H/\psi_{xlo}\rangle = V_o\exp(-\alpha\pi^2/16)\left[\frac{\alpha\pi^4}{32} - \frac{\alpha\pi^2}{8} + \frac{\pi^4}{64} - \frac{\pi^2}{16}(26-11C_6)\right.$$
$$\left. + 1 + \frac{\pi^4}{128\alpha} - \frac{\pi^2}{32\alpha}(132C_6 + 31) - \frac{1}{2\alpha}(11C_6 - 6)\right]$$

$$\epsilon_g = -\exp(-\alpha\pi^2/16)\left[\frac{\alpha\pi^2}{8} - 1\right]$$

$$E_1^F 1u = \alpha_u + 2\beta_u - 2\epsilon_u\alpha_u$$

$$E_1^F 2u = \alpha_u - 2\beta_u + 2\epsilon_u\alpha_u$$

$$\alpha_u = \langle\psi_{xol}/H/\psi_{xol}\rangle = V_o\left[\frac{16}{\alpha} - \frac{29}{\alpha^2} - \frac{33C_6}{\alpha^2}\right]$$

$$\beta_u = \langle\psi_{yol}/H/\psi_{xol}\rangle = -V_o\exp(-\alpha\pi^2/16)\left[\frac{\pi^2}{4} - 1 + \frac{3\pi^2}{8\alpha} - \frac{2}{\alpha} + \frac{33C_6}{2\alpha}\right]$$

$$\epsilon_u = \exp(-\alpha\pi^2/16)$$

$$E_o^A 1g = V_o\left[\frac{8}{\alpha} - \frac{11}{\alpha^2}(1 + C_6)\right] - 4V_o\exp(-\alpha\pi^2/16)\left[\frac{\pi^2}{4} - 1 + \frac{\pi^2}{8\alpha} + \frac{5}{\alpha} + \frac{11C_6}{2\alpha}\right]$$

$$E_o^F 1u = V_o\left[\frac{8}{\alpha} - \frac{11}{\alpha^2}(1 + C_6)\right]$$

$$E_o^{E_g} = V_o\left[\frac{8}{\alpha} - \frac{11}{\alpha^2}(1 + C_6)\right] + 2V_o \exp(-\alpha\pi^2/16)\left[\frac{\pi^2}{4} - 1 + \frac{\pi^2}{8\alpha} + \frac{5}{\alpha} + \frac{11C_6}{2\alpha}\right]$$

$$E_1^{F_{2g}} = V_o\left[\frac{16}{\alpha} - \frac{29}{\alpha^2} - \frac{33C_6}{\alpha^2}\right] \mp 2V_o \exp(-\alpha\pi^2/16)\left[\left(\frac{\pi^4}{32} - \frac{\pi^2}{8}\right)\alpha + \frac{\pi^4}{64} + \frac{\pi^2}{16}\right.$$
$$\left.(6 + 11C_6) + 1 + \frac{\pi^4}{128\alpha} - \frac{\pi^2}{32\alpha}(264C_6 + 147) - \frac{1}{2\alpha}(26 + 11C_6)\right]$$

$$E_1^{F_{1u}} = V_o\left[\frac{16}{\alpha} - \frac{29}{\alpha^2} - \frac{33C_6}{\alpha^2}\right] \mp 2V_o \exp(-\alpha\pi^2/16)\left[\frac{\pi^2}{4} - 1 + \frac{3\pi^2}{8\alpha} + \frac{7}{\alpha} + \frac{33C_6}{2\alpha}\right]$$

The values of integrals which were needed for this problem are listed below.

$$I = \int_{-\infty}^{\infty} \exp(-ax^2) \cos bx\, dx = \left(\frac{\pi}{a}\right)^{\frac{1}{2}} \exp(-b^2/4a)$$

$$-\frac{\partial I}{\partial a} = \int_{-\infty}^{\infty} x^2 \exp(-ax^2) \cos bx\, dx = \left(\frac{\pi}{a}\right)^{\frac{1}{2}} \exp(-b^2/4a)\left(\frac{1}{2a} - \frac{b^2}{4a^2}\right)$$

$$\frac{\partial^2 I}{\partial a^2} = \int_{-\infty}^{\infty} x^4 \exp(-ax^2) \cos bx\, dx = \left(\frac{\pi}{a}\right)^{\frac{1}{2}} \exp(-b^2/4a)\left(\frac{3}{4a^2} - \frac{3b^2}{4a^3} + \frac{b^4}{16a^4}\right)$$

$$-\frac{\partial^3 I}{\partial a^3} = \int_{-\infty}^{\infty} x^6 \exp(-ax^2) \cos bx\, dx = \left(\frac{\pi}{a}\right)^{\frac{1}{2}} \exp(-b^2/4a)\left(\frac{15}{8a^3} - \right.$$
$$\left.\frac{45b^2}{16a^4} + \frac{15b^4}{32a^5} - \frac{b^6}{64a^6}\right)$$

$$-\frac{\partial I}{\partial b} = \int_{-\infty}^{\infty} x \exp(-ax^2) \sin bx\, dx = \left(\frac{\pi}{a}\right)^{\frac{1}{2}} \exp(-b^2/4a)\, \frac{b}{2a}$$

$$\frac{\partial^2 I}{\partial b \partial a} = \int_{-\infty}^{\infty} x^3 \exp(-ax^2) \sin bx\, dx = \left(\frac{\pi}{a}\right)^{\frac{1}{2}} \exp(-b^2/4a)\left(\frac{3b}{4a^2} - \frac{b^3}{8a^3}\right)$$

$$\int_{-\infty}^{\infty} x^{2n} \exp(-ax^2)\, dx = \frac{(2n-1)!!}{(2a)^n}\left(\frac{\pi}{a}\right)^{\frac{1}{2}}$$

B. Evaluation of Ground Librational Energies for $(O_h, \bar{D}_{3h})$ Near the $\bar{\bar{C}}_{3v}$ High Barrier Limit

An XY_3 molecule having the symmetry $\bar{D}_{3h}$ in a face-centered cubic lattice with a crystal field of symmetry O_h will be at a potential minimum with respect to rotation at the $\bar{\bar{C}}_{3v}$ high barrier limit, if there is repulsion between the crystal and the Y atoms. The number of equivalent minima is most easily determined from the orders of $(O_h, \bar{D}_{3h})$ and $\bar{\bar{C}}_{3v}$ and is 288/6 or 48. We will assume an oscillator type of wave function at each of the 48 minimum positions. The exact form of the wave functions is not important for the approximation to be used. Now, $G = (O_h, \bar{D}_{3h}) = 'O' \times '\bar{D}_{3h}'$ so we need to define the elements in the group G. The simplest groups to use are the symmetric groups S_4 and S_3. Let $O \cong S_4$ and $\bar{D}_{3h} \cong S_3 \times \{\bar{E}, \bar{E}^*\}$ define the elements in G. The approximation to be used is that only matrix elements between minima separated by the smallest rotations will be nonzero. The smallest rotations are 60° about the molecular threefold axis (the Q operation for S_3 is C_6) and 90° about the fourfold axis of the crystal. The diagonal element is E_o, the matrix element between minima separated by a 60° rotation is denoted by α, and the matrix element is β for minima separated by a 90° rotation.

In order to determine the energies it is necessary to divide the group $(O_h, \bar{D}_{3h})$ into 48 left cosets with all operations in any one coset representing the same rotation of the molecule relative to the crystal. The coset representing no relative rotation is the group $\bar{\bar{C}}_{3v} = \{E\bar{E}, (123)(\overline{123}), (132)(\overline{132}), (12)(\overline{12})^*, (13)(\overline{13}^*, (23)(\overline{23})^*\}$.

Representative operations of each of the 48 left cosets can easily be found for this group and are listed below by classes.

$E\bar{E}$, $8(123)\bar{E}$, $3(12)(34)\bar{E}$, $6(1234)\bar{E}$, $6(12)\bar{E}$, $E^*\bar{E}^*$,

$8(123)^*\bar{E}^*$, $3(12)(34)^*\bar{E}^*$, $6(1234)^*\bar{E}^*$, $6(12)^*\bar{E}^*$.

All the members in each left coset can be found by multiplying each operation in $\bar{C}_{3V}$ from the left by the representative operation. The cosets representing a 90° relative rotation are $6(1234)\bar{E}$ which is a rotation of the molecule about a fourfold crystal axis by 90°. The cosets representing a 60° relative rotation are $(123)^*\bar{E}^*$ and $(132)^*\bar{E}^*$ where a threefold crystal axis coincides with the threefold molecular axis. The operations $(123)^*$ and $(132)^*$ represent a rotation by 120° and the operation $\bar{E}^*$ a rotation of 180°, so the overall rotation is by 60°. All the operations of the cosets which are appropriate for 0°, 60°, and 90° relative rotations are listed below.

Coset	Matrix Element
$\|1\rangle = \{E\bar{E}, (123)(\overline{123}), (132)(\overline{132}), (12)^*(\overline{12})^*, (13)^*(\overline{13})^*, (23)^*(\overline{23})^*\}$	E_0
$\|2\rangle = \{(1234)\bar{E}, (1324)(\overline{123}), (14)(\overline{132}), (134)^*(\overline{12})^*, (14)(23)^*(\overline{13})^*, (124)^*(\overline{23})^*\}$	β
$\|3\rangle = \{(1432)\bar{E}, (34)(\overline{123}), (1243)(\overline{132}), (243)^*(\overline{12})^*, (12)(34)^*(\overline{13})^*, (143)^*(\overline{23})^*\}$	β
$\|4\rangle = \{(1324)\bar{E}, (14)(\overline{123}), (123)(\overline{132}), (14)(23)^*(\overline{12})^*, (124)^*(\overline{13})^*, (134)^*(\overline{23})^*\}$	β
$\|5\rangle = \{(1423)\bar{E}, (1342)(\overline{123}), (24)(\overline{132}), (13)(24)^*(\overline{12})^*, (234)^*(\overline{13})^*, (142)^*(\overline{23})^*\}$	β

$$|6\rangle = \{(1243)\bar{E},\ (1432)(\overline{123}),\ (34)(\overline{132}),\ (143)^*(\overline{12})^*,\ (243)^*(\overline{13})^*,\ (12)(34)^*(\overline{23})^*\} \qquad \beta$$

$$|7\rangle = \{(1342)\bar{E},\ (24)(\overline{123}),\ (1423)(\overline{132}),\ (234)^*(\overline{12})^*,\ (142)^*(\overline{13})^*,\ (13)(24)^*(\overline{23})^*\} \qquad \beta$$

$$|8\rangle = \{(123)^*\bar{E}^*,\ (132)^*(\overline{123})^*,\ E^*(\overline{132})^*,\ (13)(\overline{12}),\ (23)(\overline{13}),\ (12)(\overline{23})\} \qquad \alpha$$

$$|9\rangle = \{(132)^*\bar{E}^*,\ E^*(\overline{123})^*,\ (123)^*(\overline{132})^*,\ (23)(\overline{12}),\ (12)(\overline{13}),\ (13)(\overline{23})\} \qquad \alpha$$

The 14 different symmetry species in $(O_h, \bar{D}_{3h})$ which form the ground librator state in $\bar{\bar{C}}_{3V}$ are given in Table VII. The procedure for finding the energy for a particular symmetry species will be illustrated for $F_2\bar{A}_1'$. The character table appropriate for this symmetry and the first nine cosets is shown below.

	$\bar{E}\bar{E}$	$6(1234)\bar{E}$	$16(123)(\overline{123})$	$12(1234)(\overline{123})$	$12(12)(\overline{123})$	$18(12)(12)$	$8(123)^*\bar{E}^*$	$2E^*(\overline{123})^*$	$16(123)^*(\overline{123})^*$	$24(123)^*(\overline{12})^*$	$9(12)(34)^*(\overline{12})^*$	$18(12)(\overline{12})^*$
$F_2\bar{A}_1'$	3	-1	0	-1	1	1	0	3	0	0	-1	1

Each of the 48 cosets corresponds to one of the 48 minimum positions. Therefore, in this approximation the first row of the Hamiltonian matrix has the following form: $E_0\beta\beta\beta\beta\beta\beta\alpha\alpha 000\ldots0$. Since the only nonzero matrix elements in the first row correspond to the first nine cosets, then only the relative coefficients for these nine cosets need to be found for the symmetrized wave function and

then the methods in Section 6-6 of Molecular Vibrations (161) can be used to determine the energy. Therefore, from the Wigner method (159, 161) described in Section III.B.4, $\psi_{F_2\bar{A}_1'} \propto (6|1\rangle - 2|2\rangle - 2|3\rangle - 2|4\rangle - 2|5\rangle - 2|6\rangle - 2|7\rangle + 6|8\rangle + 6|9\rangle + 0 \ldots)$, so $E_{F_2\bar{A}_1'} \propto (6E_o - 12\beta + 12\alpha)$. It is clear from Section 6-6 (161) that the diagonal matrix element will have a coefficient of unity, therefore, the correct energy is $E_{F_2\bar{A}_1'} = \frac{1}{6}(6E_o - 12\beta + 12\alpha) = E_o - 2\beta + 2\alpha$. Actually the problem can be simplified further by noting the number of times the operations in a given class appear in the E_o, α, or β cosets and then summing through the group as before. This makes it unnecessary to distinguish between different α or β cosets. The energies of the other ground librational states are found in the same manner and the relative energies ($E_o = 0$) are shown in Table VIII. If this procedure is tried for a symmetry species which is not a part of the ground librator state, the resultant symmetrized wave function will be zero.

This method was used over and over in Chapter III. Once one becomes accustomed to using it, the ground librational energies can be found quite easily for any example.

C. Evaluation of Ground Librational Energies for $(O_h, \bar{T}_d)$ Near the $\bar{\bar{C}}_{3V}$ High Barrier Limit

The rotational states in $(O_h, \bar{T}_d)$ which make up the ground librational state in $\bar{\bar{C}}_{3V}$ can be found from Table X. The energies for symmetry species which appear once can be found using the method described in Appendix B, assuming only tunneling by 90° is important. The symmetry species $F_1\bar{F}_1$ and $F_2\bar{F}_2$ each appear twice and this method is not generally valid for a case like this.

The problem is set up in a very similar manner to that in Appendix B. $G = (O_h, \bar{T}_d) = 'O' \times '\bar{T}_d'$ so the simplest way to define the elements in G is to let $O \cong S_4$ and $\bar{T}_d \cong \bar{S}_4$ where S_4 is the symmetric group on four letters. There are 96 (576/6) equivalent potential minima and these can be represented by 96 left cosets where the coset representing no relative rotation is the subgroup $\bar{\bar{C}}_{3V} = \{E\bar{E}, (123)(\overline{123}), (132)(\overline{132}), (12)^*(\overline{12})^*, (13)^*(\overline{13})^*, (23)^*(\overline{23})^*\}$. The 96 left cosets are determined by systematically going through the group G until every element belongs to a coset. Representative operations for the cosets are listed below, this is done by classes whenever possible.

$E\bar{E}$, $8(123)\bar{E}$, $3(12)(34)\bar{E}$, $6(1234)\bar{E}$, $6(12)\bar{E}$, $3E(\overline{12})(\overline{34})$, $6E^*(\overline{1234})^*$, $E(\overline{124})$, $E(\overline{142})$, $E(\overline{134})$, $E(\overline{143})$, $E(\overline{234})$, $E(\overline{243})$, $E^*(\overline{14})^*$, $E^*(\overline{24})^*$, $E^*(\overline{34})^*$, $(124)(\overline{124})$, $(142)(\overline{142})$, $(143)(\overline{143})$, $(142)(\overline{124})$, $(124)(\overline{142})$, $(134)(\overline{143})$, $(143)(\overline{134})$, $(234)(\overline{243})$, $(243)(\overline{234})$, $(134)(\overline{124})$, $(143)(\overline{124})$, $(234)(\overline{124})$, $(243)(\overline{124})$, $(134)(\overline{142})$, $(143)(\overline{142})$, $(234)(\overline{142})$, $(243)(\overline{142})$, $(124)(\overline{143})$, $(142)(\overline{143})$, $(234)(\overline{143})$, $(243)(\overline{143})$, $(124)(\overline{134})$,

$(234)(\overline{134})$, $(134)(\overline{234})$, $(142)(\overline{234})$, $(124)(\overline{243})$, $(143)(\overline{243})$, $(1234)(\overline{124})$, $(1432)(\overline{124})$, $(1324)(\overline{124})$, $(1423)(\overline{124})$, $(1243)(\overline{124})$, $(1342)(\overline{124})$, $(1234)(\overline{142})$, $(1432)(\overline{142})$, $(1324)(\overline{142})$, $(1423)(\overline{142})$, $(1243)(\overline{142})$, $(1342)(\overline{142})$, $(1234)(\overline{143})$, $(1432)(\overline{143})$, $(1324)(\overline{143})$, $(1423)(\overline{143})$, $(1243)(\overline{143})$, $(1342)(\overline{143})$, $(1432)(\overline{134})$, $(1324)(\overline{134})$, $(1342)(\overline{134})$, $(1432)(\overline{243})$, $(1324)(\overline{243})$, $(1342)(\overline{243})$, $(1234)(\overline{234})$, $(1423)(\overline{234})$, $(1243)(\overline{234})$.

All the members in each left coset can be found by multiplying each operation in $\bar{C}_{3V}$ from the left by the representative operation. The cosets representing a 90° relative rotation are $6(1234)\bar{E}$ and $6E^{*}(\overline{1234})^{*}$ which are rotations about a fourfold crystal axis and a fourfold inversion axis of the molecule, respectively. These 12 cosets are used for the symmetry species which appear once.

The procedure to be followed now is to construct 18 symmetrized wave functions having $F_1\bar{F}_1$ symmetry. In general, these would not form an orthogonal set, but it is not necessary to use an orthogonalization procedure. The symmetrized wave functions are found as before and the first is given below.

$$\Psi_{F_1\bar{F}_1}(1) = \frac{1}{16\sqrt{3}}\,(12|1\rangle + 4|2\rangle + 4|3\rangle + 4|4\rangle + 4|5\rangle + 4|6\rangle + 4|7\rangle + 4|8\rangle + 4|9\rangle + 4|10\rangle + 4|11\rangle + 4|12\rangle + 4|13\rangle + 3|14\rangle + 3|15\rangle - |16\rangle - |17\rangle - |18\rangle - |19\rangle - |20\rangle - |21\rangle - |22\rangle - |23\rangle - |24\rangle - |25\rangle - |26\rangle - |27\rangle - 4|28\rangle - 4|29\rangle - 4|30\rangle - 4|31\rangle - 4|32\rangle - 4|33\rangle - 6|34\rangle - 6|35\rangle - 2|36\rangle - 6|37\rangle - 2|38\rangle - 2|39\rangle - 2|40\rangle - 2|41\rangle - 2|42\rangle + 4|43\rangle + 4|44\rangle + 4|45\rangle + 3|46\rangle + 3|47\rangle + 3|48\rangle + 3|49\rangle + 3|50\rangle + 3|51\rangle - |52\rangle - |55\rangle - |57\rangle - |58\rangle - |61\rangle - |63\rangle - |64\rangle - |65\rangle - |66\rangle - |67\rangle$$

$$- |68\rangle - |69\rangle - 2|70\rangle + 2|72\rangle - 2|74\rangle - 2|77\rangle + 2|79\rangle$$
$$- 2|81\rangle + 2|83\rangle - 2|85\rangle - 2|86\rangle - 2|89\rangle - 2|90\rangle - 2|91\rangle$$
$$- 2|92\rangle - 2|94\rangle - 2|95\rangle)$$

The numbering of the cosets is arbitrary so the wave function will depend on these choices. Here, $\bar{C}_{3v}$ is $|1\rangle$, the 12 cosets representing 90° relative rotations are numbered $|2\rangle$ to $|13\rangle$, and the others follow an orderly but arbitrary pattern. The other 17 wave functions have the same coefficients but they have undergone a permutation.

The 96 x 96 Hamiltonian matrix has the simplified form where the only nonzero entries are β for finding the relative energies ($E_o = 0$) for the ground librational states. Each of the 96 cosets is multiplied by a representative number of the 12 cosets representing a 90° relative rotation and 12 cosets related by a 90° rotation are found for each of the 96 cosets. In this approximation the matrix is real and symmetric so only the part above the diagonal will be given. The nonzero entries (β) above the diagonal are listed by the row ($\langle i|$) and columns ($|j, k, l, \ldots\rangle$) below.

$\langle 1|2, 3, 4, 5, 6, 7, 8, 9, 10, 11, 12, 13\rangle$,

$\langle 2|15, 17, 19, 21, 29, 43, 47, 48, 60, 64, 66\rangle$,

$\langle 3|14, 16, 18, 20, 29, 45, 49, 51, 53, 57, 63\rangle$,

$\langle 4|14, 17, 19, 20, 28, 43, 47, 48, 52, 56, 68\rangle$,

$\langle 5|15, 16, 18, 21, 28, 44, 46, 50, 54, 58, 61\rangle$,

$\langle 6|15, 17, 18, 20, 30, 45, 49, 51, 55, 59, 69\rangle$,

$\langle 7|14, 16, 19, 21, 30, 44, 46, 50, 62, 65, 67\rangle$,

$\langle 8|14, 23, 25, 27, 32, 43, 46, 49, 52, 53, 65\rangle$,

$\langle 9|15, 22, 24, 26, 32, 45, 48, 50, 60, 61, 69\rangle$,

⟨10|15, 23, 25, 26, 31, 43, 46, 49, 54, 55, 64⟩,

⟨11|14, 22, 24, 27, 31, 44, 47, 51, 56, 57, 67⟩,

⟨12|14, 23, 24, 26, 33, 45, 48, 50, 62, 63, 68⟩,

⟨13|15, 22, 25, 27, 33, 44, 47, 51, 58, 59, 66⟩,

⟨14|36, 38, 39, 40, 41, 42⟩, ⟨15|36, 38, 39, 40, 41, 42⟩,

⟨16|35, 37, 39, 70, 72, 76, 78, 82, 92⟩, ⟨17|35, 37, 39, 73, 75,

79, 81, 85, 93⟩ , ⟨18|34, 37, 38, 72, 78, 82, 84, 89, 94⟩,

⟨19|34, 37, 38, 71, 77, 83, 86, 88, 96⟩, ⟨20|34, 35, 36, 73, 79,

87, 90, 93, 95⟩, ⟨21|34, 35, 36, 74, 80, 83, 88, 91, 96⟩,

⟨22|35, 37, 42, 70, 71, 72, 73, 74, 75⟩, ⟨23|35, 37, 42, 76, 77,

78, 79, 80, 81⟩, ⟨24|34, 37, 41, 71, 72, 75, 88, 89, 90⟩,

⟨25|34, 37, 41, 82, 83, 84, 85, 86, 87⟩, ⟨26|34, 35, 40, 76, 79,

80, 94, 95, 96⟩, ⟨27|34, 35, 40, 83, 84, 87, 91, 92, 93⟩,

⟨28|35, 36, 37, 38, 71, 74, 77, 80, 86, 91⟩, ⟨29|34, 36, 37, 39,

75, 81, 85, 87, 90, 95⟩, ⟨30|34, 35, 38, 39, 70, 76, 84, 89, 92, 94⟩,

⟨31|35, 37, 40, 41, 82, 85, 86, 91, 92, 93⟩, ⟨32|34, 37, 40, 42,

77, 78, 81, 94, 95, 96⟩, ⟨33|34, 35, 41, 42, 70, 73, 74, 88, 89, 90⟩,

⟨36|52, 56, 60, 64, 66, 68⟩, ⟨38|54, 58, 61, 62, 65, 67⟩,

⟨39|53, 55, 57, 59, 63, 69⟩, ⟨40|52, 53, 54, 55, 64, 65⟩,

⟨41|56, 57, 58, 59, 66, 67⟩, ⟨42|60, 61, 62, 63, 68, 69⟩,

⟨43|71, 73, 75, 76, 78, 82, 84, 88⟩, ⟨44|73, 75, 76, 78, 80, 87,

93, 96⟩, ⟨45|71, 80, 82, 84, 87, 88, 93, 96⟩, ⟨46|70, 72, 74, 79,

81, 85, 87, 88⟩, ⟨47|70, 72, 77, 79, 81, 84, 92, 96⟩,

⟨48|72, 76, 83, 85, 86, 89, 93, 94⟩, ⟨49|72, 73, 77, 80, 83, 86,

89, 90⟩, ⟨50|75, 79, 82, 83, 90, 91, 92, 95⟩, ⟨51|71, 74, 78, 79,

83, 91, 94, 95⟩, ⟨52|71, 73, 74, 78, 84, 90, 92, 94⟩,

$\langle 53|70, 72, 75, 77, 83, 90, 91, 96\rangle$, $\langle 54|71, 72, 74, 79, 85, 89, 93, 95\rangle$, $\langle 55|70, 73, 75, 80, 86, 89, 91, 96\rangle$, $\langle 56|72, 77, 79, 80, 82, 89, 92, 95\rangle$, $\langle 57|71, 76, 78, 81, 86, 88, 91, 95\rangle$, $\langle 58|73, 77, 78, 80, 85, 87, 90, 94\rangle$, $\langle 59|74, 76, 79, 81, 83, 86, 88, 94\rangle$, $\langle 60|70, 72, 78, 83, 85, 87, 91, 94\rangle$, $\langle 61|73, 75, 81, 82, 84, 86, 91, 95\rangle$, $\langle 62|73, 79, 81, 83, 84, 86, 90, 92\rangle$, $\langle 63|74, 77, 80, 82, 85, 87, 88, 92\rangle$, $\langle 64|74, 75, 76, 82, 88, 90, 92, 94\rangle$, $\langle 65|70, 71, 81, 87, 88, 89, 93, 95\rangle$, $\langle 66|70, 80, 81, 82, 84, 89, 95, 96\rangle$, $\langle 67|75, 76, 77, 85, 90, 93, 94, 96\rangle$, $\langle 68|70, 76, 78, 86, 87, 89, 91, 93\rangle$, $\langle 69|71, 74, 77, 84, 85, 92, 93, 96\rangle$

Let us denote the 96 x 96 Hamiltonian matrix by H, and the 18 $F_1\bar{F}_1$ symmetrized wave functions by $|\bar{I}\rangle$. From the H matrix and the wave function $\Psi_{F_1\bar{F}_1}(1) = |\bar{I}\rangle$ written as a column vector it is straightforward to determine that

$$H|\bar{I}\rangle = \begin{pmatrix} 48\beta \\ 16\beta \\ 16\beta \\ 16\beta \\ \cdot \\ \cdot \\ \cdot \end{pmatrix} = 4\beta \begin{pmatrix} 12 \\ 4 \\ 4 \\ 4 \\ \cdot \\ \cdot \\ \cdot \end{pmatrix} = 4\beta|\bar{I}\rangle.$$

Similarly, $H|\bar{i}\rangle = 4\beta|\bar{i}\rangle$ for $\bar{i} = \bar{1}$ to $\bar{18}$. The Schmidt orthogonalization procedure (161) can be used to construct a set of 18 orthogonal eigenvectors but it is not necessary to do this. Let $\bar{\bar{i}}$ be the set of orthogonal eigenvectors where $\bar{\bar{i}} = \bar{\bar{1}}$ to $\bar{\bar{18}}$, then

$|\bar{\bar{i}}\rangle = \sum_{I=1}^{18} C_{\bar{\bar{i}}I} |I\rangle$, where the coefficients $C_{\bar{\bar{i}}I}$ are defined by the Schmidt procedure. Now, $H|\bar{\bar{i}}\rangle = H \sum_{I=1}^{18} C_{\bar{\bar{i}}I}|I\rangle = 4\beta \sum_{I=1}^{18} C_{\bar{\bar{i}}I}|I\rangle = 4\beta|\bar{\bar{i}}\rangle$. Therefore, $\langle \bar{\bar{j}}/H/\bar{\bar{i}}\rangle = 4\beta\langle \bar{\bar{j}}/\bar{\bar{i}}\rangle = 4\beta\delta_{ij}$. Therefore, all 18 eigenvalues for the $F_1\bar{F}_1$ symmetry species are 4β.

A simple way to find the eigenvalues for the two $F_2\bar{F}_2$ levels is to consider the traces. Let S be a similarity transformation which diagonalizes H, and λ be the diagonal matrix. Then $S^{-1}HS = \lambda$ and $tr(H) = tr(\lambda)$. Also, $(S^{-1}HS)(S^{-1}HS) = \lambda^2 = S^{-1}H^2S$, so $tr(H^2) = tr(\lambda^2)$. If we denote the two $F_2\bar{F}_2$ eigenvalues by λ_1 and λ_2 then since $tr(H) = 0$, from the other eigenvalues we have $\lambda_1 + \lambda_2 = -8\beta$. The diagonal elements in H^2 are clearly all $12\beta^2$ since a row and column of the same number are alike so $tr(H^2) = 1152\beta^2$. From the other eigenvalues we determine that $\lambda_1^2 + \lambda_2^2 = 32\beta^2$. From the equations $\lambda_1 + \lambda_2 = -8\beta$ and $\lambda_1^2 + \lambda_2^2 = 32\beta^2$, it is easy to find that $\lambda_1 = \lambda_2 = -4\beta$. Therefore all 18 eigenvalues for the $F_2\bar{F}_2$ symmetry species are -4β. All the eigenvalues for this problem are listed in Table XII.

The advantages of the Longuet-Higgins (93) approach to group theory are very evident from this section where the relationship between the permutation group $\{P\}$ and the rotation group $\{Q\}$ are most important in solving this problem.